

APPLIED SIMILARITY PROBLEMS USING FRÉCHET
DISTANCE

by
Kaveh Shahbaz

A thesis submitted to
the Faculty of Graduate Studies and Research
in partial fulfillment of
the requirements for the degree of
Doctor of Philosophy

Ottawa-Carleton Institute for Computer Science
School of Computer Science
Carleton University
Ottawa, Ontario

June 2013

© Copyright
2013, Kaveh Shahbaz

To my father, wish he was here ...

Abstract

The Fréchet distance is a well-known metric to measure similarity of polygonal curves. In the first part of this thesis, we introduce a new metric called Fréchet distance with speed limits and provide efficient algorithms for computing it. The classical Fréchet distance between two curves corresponds to the maximum distance between two point objects that traverse the curves with arbitrary non-negative speeds. We consider a problem instance in which the speed of traversal along each segment of the curves is restricted to be within a specified range. This setting is more realistic than the classical Fréchet distance setting, specially in GIS applications. We also study this problem in the setting where the polygonal curves are inside a simple polygon.

In the second part of this thesis, we present a data structure, called the free-space map, that enables us to solve several variants of the Fréchet distance problem efficiently. Back in 1995, a data structure was introduced by Alt and Godau, called the free space diagram, for computing Fréchet distance. That data structure is widely used in different applications involving the Fréchet distance. Our data structure encapsulates all the information available in the free-space diagram, yet it is capable of answering more general type of queries efficiently. Given that the free-space map has the same size and construction time as the standard free-space diagram, it can be viewed as a powerful alternative to it. As part of the results in Part II of the thesis, we exploit the free-space map to improve the long-standing bound for computing the partial Fréchet distance and obtain improved algorithms for computing the Fréchet distance between two closed curves, and the so-called minimum/maximum walk problem. We also improve the map matching algorithm for the case when the map is a directed acyclic graph.

As the last part of this thesis, given a point set S and a polygonal curve P in \mathbb{R}^d , we study the problem of finding a polygonal curve Q through S , which has a minimum Fréchet distance to P . Furthermore, if the problem requires that curve Q visits every point in S , we show it is NP-complete.

Acknowledgements

I would like to first thank my two supervisors, Prof. Jörg-Rüdiger Sack and Prof. Anil Maheshwari. I would like to give tremendous thanks to Prof. Sack for the support and insight that he has given me throughout my degree here at Carleton. Prof. Sack, I greatly appreciate your help both academically and financially. I am happy to have been a part of your research group.

I would like to give many thanks to Anil for the countless hours of time that he has made available to me throughout the development of this thesis. His many constructive comments and technical advice have helped me to complete this thesis. He has become more of a friend than a supervisor for me. Anil, I never forget your helps.

I would also like to thank my co-author and friend, Prof. Hamid Zarrabi-Zadeh, for his guidance and assistance in this thesis. It was my pleasure to work with an excellent fellow researcher such as Hamid. I learned a lot from him.

I thank the members of my thesis examinations committee for their helpful and encouraging comments. I would like to highly thank Prof. Helmut Alt for his valuable comments and also Prof. Michiel Smid for helpful discussions.

I would like to thank my parents, colleagues and friends for their love and encouragement for all these years.

This research was supported by National Sciences and Engineering Research Council of Canada and SUN Microsystems.

Table of Contents

Abstract	iii
List of Figures	viii
Chapter 1 Introduction and Motivation	1
1.1 Contributions of the Thesis	2
1.2 Organization of the Thesis	3
Chapter 2 Related Work	6
2.1 Classical Fréchet Distance Problem	6
2.2 Variants of Fréchet Distance	12
2.2.1 Weak Fréchet Distance	12
2.2.2 Fréchet Distance of a Set of Curves	14
2.2.3 Average Fréchet and Summed Fréchet Distance	15
2.2.4 Fréchet Distance of Specific Families of Curves	16
2.2.5 Fréchet Distance with no Leash Cross	17
2.2.6 Directional-based Fréchet Distance	18
2.2.7 Fréchet Distance of Closed Curves	18
2.3 Partial Curve Matching	20
2.3.1 Partial Curve Matching	20
2.3.2 Map Matching	22
2.3.3 Constrained Free-Space Diagram	25
2.4 Fréchet Distance in Different Metric Spaces	26
2.4.1 Geodesic Fréchet Distance	26
2.4.2 Homotopic Fréchet distance	27
2.5 Approximate Fréchet Distance	29
Chapter 3 Fréchet Distance with Speed Limits	31
3.1 Preliminaries	32

3.2	The Decision Problem	34
3.3	An Improved Algorithm	40
3.4	Optimization Problem	49
3.5	Conclusions	56
Chapter 4	Speed-constrained Geodesic Fréchet Distance	58
4.1	Introduction	58
4.2	Preliminaries	59
4.3	Computing the Free Space Inside a Cell	61
4.4	The Decision Problem	65
4.5	Conclusion	69
Chapter 5	Improved Algorithms for Partial Curve Matching	70
5.1	Introduction	70
5.2	Preliminaries	72
5.2.1	Vertical Ray Shooting	74
5.3	The Main Data Structure	78
5.3.1	Data Structure	81
5.3.2	Improved Query Time	84
5.4	Applications	85
5.4.1	Partial Curve Matching	85
5.4.2	Closed Curves	86
5.4.3	Maximum Walk	87
5.4.4	Minimum Walk	88
5.5	Matching a Curve in a DAG	88
5.6	Conclusions	91
Chapter 6	Curve-Pointset Matching Problem (CPM)	92
6.1	Introduction	92
6.2	Preliminaries	93
6.3	The Decision Algorithm	94

6.4	Conclusions	99
Chapter 7	All-Points CPM Problem is NP-complete	100
7.1	Introduction	100
7.2	General Case is NP-complete	100
7.2.1	Preliminaries	100
7.2.2	Reduction Algorithm	101
7.2.3	Implementation Results	112
7.3	Conclusions	113
	Bibliography	120

List of Figures

1.1	Hausdorff vs. Fréchet distance. Shows two curves P and Q with small Hausdorff distance h having a large Fréchet distance f . (a) The Fréchet distance is indicated by f . The Hausdorff distance is the distance from vertex q_4 to P_1 . A sample walk is also shown with a sequence of the locations of the moving objects. (b) The direction of P is reversed. The Fréchet distance is not same as before but the Hausdorff distance remains unchanged. Applet of Pelletier [55] is used to compute Fréchet distance.	3
2.1	(a) The free-space diagram for two polygonal curves P and Q ; (b) two segments P_i and Q_j and their corresponding free space. The diagram was generated using a Java applet developed by S. Pelletier [55].	8
2.2	The geometric situations corresponding to Type (B) and Type (C) critical distances. (a) a new passage opens between two neighboring cells in the free-space diagram (b) a horizontal passage opens in the free-space diagram.	11
2.3	The graph with grey nodes is built on top of $\mathcal{B}_{n \times m}$ to compute the weak Fréchet distance	13
2.4	$\delta_F(f_1, f_2) = \delta_F(f_2, f_3)$. But curve f_2 is more matched to curve f_3	15
2.5	Free-space surface consists of free-space diagrams glued together according to the topology of graph G . Grey dashed path is a monotone path in the free space.	23
2.6	Reachability pointers	24

2.7	The dashed lines show the leash between two objects while they are moving on their corresponding curves. The leash can not jump over the obstacles.	28
2.8	(a) The discrete Fréchet distance could be arbitrarily larger than the continuous distance, e.g., $\delta_F(P, Q) = \overline{dh} $, $\delta_{dF}(P, Q) = \overline{db} $. (b) If we put enough sample points on the two polygonal chains, then the resulting discrete Fréchet distance, that is, $ \overline{df} $, closely approximates $ \overline{dh} $	29
3.1	(a) A slope-constrained path \mathcal{P} in the free space of P and Q ; (b) Two speed-constrained parametrizations of P and Q , corresponding to the path \mathcal{P}	36
3.2	(a) Projecting a point p and an interval I onto the exit side of \mathcal{C}_{ij} ; (b) Computing reachable intervals on the exit side of a cell \mathcal{C}_{ij} . Dark gray areas represent infeasible (obstacles) regions. Reachable intervals are shown with bold line segments.	37
3.3	A lower bound example. The small gray diamonds represent obstacles in the free-space diagram. Reachable intervals are shown with bold black line segments. The numbers shown at each row and column represent speed limits on the corresponding segment.	40
3.4	I' is an iterated projection of I	42
3.5	An example of the execution of Algorithm 2 on a cell \mathcal{C}_{ij} . The intervals of $S \subseteq T$ are shown in gray. The black intervals in T represent the interior intervals. The intervals in $U(S) \cap \mathcal{F}_\varepsilon$ are boundary intervals which are inserted in Lines 12–13.	47
3.6	(a,c) Type (C) critical distances in the standard Fréchet distance problem vs. (b,d) type (C) critical distances in our instance of the problem.	50
3.7	Proof of Lemma 13	54

3.8	Transitivity of comparisons must be kept during stages of parallel sorting in parametric search	56
4.1	(a) An open hourglass (b) A closed hourglass (c) An intersecting hourglass.	61
4.2	An hourglass $\mathcal{H}_{\overline{ab}, \overline{cd}}$ with a butterfly $\mathcal{B}_{\overline{a'b'}, \overline{c'd'}}$	62
4.3	The free space inside a cell.	64
4.4	Projecting reachable intervals inside cells with convex and non-convex interior.	66
4.5	Proof of Theorem 20	67
5.1	(a) An example of a free-space diagram. (b) Proof of the crossing lemma.	73
5.2	An example of the execution of Algorithm 9. Segments in the queue at the end of each step are shown in bold.	75
5.3	A horizontal slab with vertical segments. The rightmost segment reachable from s_1 in this figure is t_i	78
5.4	Computing $\mathcal{R}(j)$ from $\mathcal{R}(j - 1)$	79
5.5	Proof of Lemma 29.	83
5.6	An example of a free-space surface.	89
6.1	A problem instance. The dashed curve is in ε -Fréchet distance to the solid curve. Point u is used multiple times in the dashed curve.	93
6.2	A cylinder of radius ε around segment L	94
6.3	Proof of Lemma 37	96
6.4	Point v is an entry point of C_i	98

7.1	Blue curve is an example of curve l_i which corresponds to variable x_i in formula ϕ . The formula has four clauses C_1, C_2, C_3 and C_4 , where the occurrence of variable x_i in those clauses is: $\neg x_i \in C_1, \neg x_i \in C_2, x_i \in C_3$ and $x_i \in C_4$. For each clause C_i , the reduction algorithm places three point s_i, g_i and c_i in the plane. (a) Red curve is curve A . (b) Red curve is curve B . . .	105
7.2	Base case of induction in the proof of Lemma 41	106
7.3	Proof of Lemma 41	107
7.4	Base case of induction in the proof of Lemma 42	108
7.5	Proof of Lemma 42	115
7.6	Proof of Lemma 43	118

Chapter 1

Introduction and Motivation

The problem of curve matching appears in a variety of different domains, like shape matching, GIS applications [7, 19, 24], pattern recognition [12, 43], computer vision [5], speech recognition [45], time series analysis [44], and signature verification [57, 58]. The main questions associated with curve matching in a specific domain are: What is a good measure of similarity between curves? How can we compute it (or some approximation of it) efficiently? Other questions that are often of interest include: given a database of curves and a candidate curve, can we find a nearest neighbor to this curve in the database? Can we cluster curves with respect to a given measure of similarity?

Curve matching has been studied extensively by computational geometers. The Hausdorff distance and the Fréchet distance are the most well-known distance measures to assess the resemblance of two curves (see [40] for some other metrics such as the bottleneck distance, the volume of symmetric difference). The Hausdorff distance between two curves P and Q is the smallest δ , such that P is completely contained in the δ -neighborhood of Q , and vice versa. Although the Hausdorff distance is arguably a natural distance measure between curves and/or compact sets, it is too static, in the sense that it neither considers direction nor any dynamics of the motion along the curves (see Figure 1.1). The Fréchet distance deals with this problem. It takes the order between points along the curves into consideration, making it a better measure of similarity for curves than alternatives such as the Hausdorff distance.

The Fréchet distance was first defined by Maurice Fréchet in 1906 [37]. While known as a famous distance measure in the field of mathematics (more specifically, abstract spaces), it was Alt and Godau [8] who first applied it in measuring the similarity of polygonal curves in early 1990s.

An intuitive way to understand the Fréchet metric is as follows: imagine a man is

walking his dog, he is walking on one curve, the dog on the other. Both are allowed to control their speeds, but are not allowed to go backwards. Then, the Fréchet distance of the curves is the minimal length of a leash that is necessary.

Alt and Godau [8] proposed an $O(n^2 \log n)$ time algorithm to compute the Fréchet distance, where n is the total complexity of the curves. Since that time, Fréchet metric has received much attention as a measure of curve similarity and many variants have been studied. These include minimizing the Fréchet distance under various classes of transformations [9, 54], extending it to graphs [7, 14], piecewise smooth curves [56], simple polygons [21], surfaces [6], and to more general metric spaces [28, 23, 29], in curve simplification [3], protein structure alignment [43, 12] and morphing [35].

1.1 Contributions of the Thesis

The main contributions of this thesis are summarized below:

- We introduce a generalization of the well-known Fréchet distance between two polygonal curves which incorporates speed limits. We provide efficient algorithms for computing that metric [46, 48].
- We present an algorithm which computes the speed-constrained Fréchet distance when the input curves are restricted to be inside a simple polygon [47].
- We introduce a new data structure called the *free-space map* which can be used to solve several variants of Fréchet distance problems efficiently. We improve algorithms for partial curve matching and closed curve matching using free-space map. We also obtain an improved algorithm for the map matching algorithm of Alt *et al.* [7] for the case when the map is a directed acyclic graph. We also solve *minimum/maximum walk* problem efficiently using our data structure [49, 51].
- We introduce the *curve-pointset matching* problem and present an efficient algorithm to solve it [50].
- We provide NP-completeness proof of *all-points curve-pointset matching* problem.

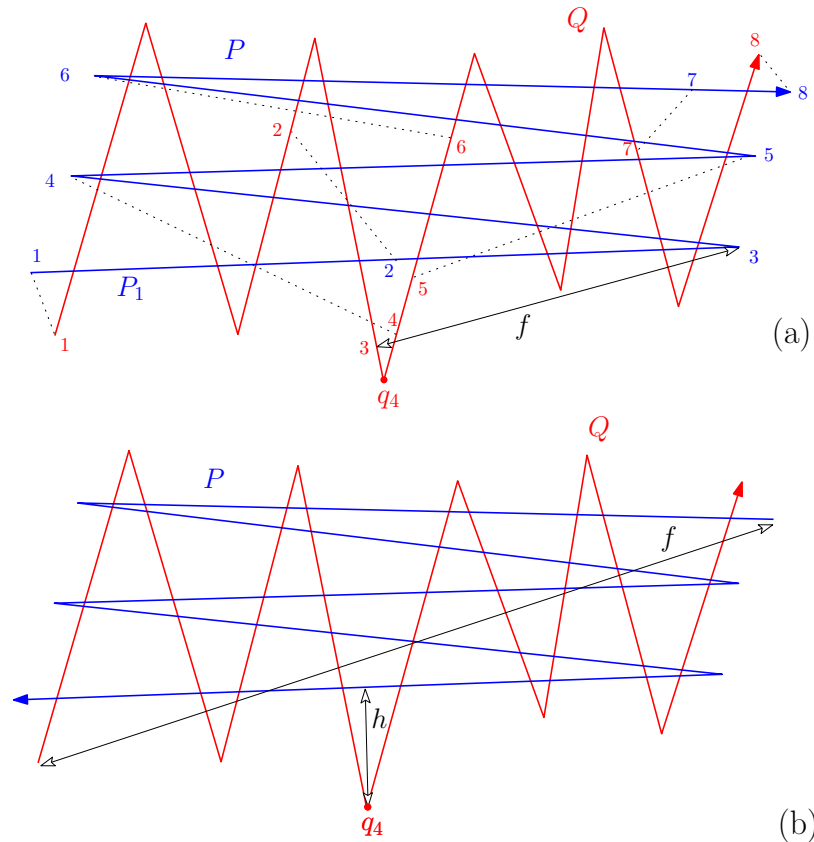


Figure 1.1. Hausdorff vs. Fréchet distance. Shows two curves P and Q with small Hausdorff distance h having a large Fréchet distance f . (a) The Fréchet distance is indicated by f . The Hausdorff distance is the distance from vertex q_4 to P_1 . A sample walk is also shown with a sequence of the locations of the moving objects. (b) The direction of P is reversed. The Fréchet distance is not same as before but the Hausdorff distance remains unchanged. Applet of Pelletier [55] is used to compute Fréchet distance.

1.2 Organization of the Thesis

This thesis is organized as follows. In the next chapter, we describe the algorithm due to Alt and Godau [8] for computing the Fréchet distance. In addition, we summarize different variants of Fréchet distance problem which have been studied and describe briefly the techniques for solving them.

Next, in Chapter 3, we introduce a new generalization of Fréchet distance and provide an efficient algorithm for computing it. The classical Fréchet distance between two polygonal curves corresponds to the maximum distance between two point objects that traverse the curves with arbitrary non-negative speeds. Here, we consider a

problem instance in which the speed of traversal along each segment of the curves is restricted to be within a specified range. We provide an efficient algorithm that decides in $O(n^2 \log n)$ time whether the Fréchet distance with speed limits between two polygonal curves is at most ε , where n is the number of segments in the curves, and $\varepsilon \geq 0$ is an input parameter. We then use our solution to this decision problem to find the exact Fréchet distance with speed limits in $O(n^3 \log n)$ time.

Given two polygonal curves inside a simple polygon, in Chapter 4, we study the problem of finding the Fréchet distance between the two curves under the following two conditions (i) the distance between two points on the curves is measured as the length of the shortest path between them lying inside the simple polygon, and (ii) the traversal along each segment of the polygonal curves is restricted to be between a minimum and a maximum permissible speed assigned to that segment. We provide an algorithm that decides in $O(n^2(k + n))$ time whether the speed-constrained geodesic Fréchet distance between two polygonal curves inside a simple polygon is within a given value ε , where n is the number of segments in the curves, and k is the complexity of the polygon.

In Chapter 5, we propose a new data structure, *free-space map*, that enables us to solve several variants of the Fréchet distance problem efficiently. Our data structure encapsulates all the information available in the free-space diagram of Alt and Godau [8] to compute the Fréchet distance. In addition, our data structure is capable of answering more general type of queries than the free-space diagram. Given that the free-space map has the same size and construction time ($O(n^2)$, n is the total complexity of the curves) as the standard free-space diagram, it can be viewed as a powerful alternative.

Using our new data structure, we present improved algorithms for several variants of the Fréchet distance problem. In particular, we improve the $O(n^2 \log^2 n)$ time algorithm for computing the partial Fréchet distance in [8], by a $\log n$ factor. Also, we obtain improved algorithms for computing Fréchet distance between two closed curves, and the so-called *minimum/maximum walk* problem. Our data structure leads to efficient algorithms for the map matching algorithm of Alt *et al.*[7] for the case

when the map is a directed acyclic graph.

In Chapter 6, we examine the following variant of the Fréchet distance problem, which we refer to as the *Curve-Pointset Matching (CPM)* problem. Given a pointset S of size k and a polygonal curve P of size n in \mathbb{R}^d , we study the problem of finding a polygonal curve Q whose vertices are from S , and has a minimum Fréchet distance to P . In the decision version of that problem, given a distance $\varepsilon \geq 0$, we present an $O(nk^2)$ time algorithm to decide if exists a curve Q through some points of S in ε -Fréchet distance to curve P , where vertices of Q are from S , and curve Q need not contain all points of S and may use a point of S multiple times. Also, we show that the curve of minimum Fréchet distance can be computed in time $O(nk^2 \log(nk))$. As a by-product of our result, we improve the map matching algorithm of Alt *et al.* [7] by a $\log k$ factor for the case when the map is a complete graph. Finally, in Chapter 7, we study the same problem as in the previous chapter, under the new condition that curve Q must visit every point in the pointset S . We refer to this problem as All-Points CPM problem and we show that it is NP-complete.

Chapter 2

Related Work

2.1 Classical Fréchet Distance Problem

The Fréchet distance is a metric to measure the similarity of polygonal curves. It was first defined by a French mathematician, Maurice Fréchet [37]. The Fréchet distance between two curves is often referred to as a dog-leash distance because it can be interpreted as the minimum-length leash required for a person to walk a dog, if the person and the dog, each travels from its respective starting position to its ending position, without ever letting go off the leash or backtracking. The length of the leash determines how similar the two curves are to each other: a short leash means the curves are similar, and a long leash means that the curves are different from each other.

Two problem instances naturally arise: decision and optimization. In the *decision problem*, one wants to decide whether two polygonal curves P and Q are within ε Fréchet distance from each other, i.e., if a leash of given length ε suffices. In the *optimization problem*, one wants to determine the minimum such ε . In [8], Alt and Godau gave an $O(n^2)$ time algorithm for the decision problem, where n is the total number of segments in the curves. They also solved the corresponding optimization problem in $O(n^2 \log n)$ time. Here, we first describe their decision algorithm:

Polygonal Curve (or Polyline). A *polygonal curve* in \mathbb{R}^d is a continuous function $P : [0, n] \rightarrow \mathbb{R}^d$ with $n \in \mathbb{N}$, such that for each $i \in \{0, \dots, n-1\}$, the restriction of P to the interval $[i, i+1]$ is affine (i.e., forms a line segment). The integer n is called the *length* of P . Moreover, the sequence $P(0), \dots, P(n)$ represents the set of *vertices* of P . For each $i \in \{1, \dots, n\}$, we denote the line segment $P(i-1)P(i)$ by P_i .

Fréchet Distance. A *monotone parametrization* of $[0, n]$ is a continuous non-decreasing function $\alpha : [0, 1] \rightarrow [0, n]$ with $\alpha(0) = 0$ and $\alpha(1) = n$. Given two polygonal curves P and Q of lengths n and m respectively, the *Fréchet distance* between P and Q is defined as

$$\delta_F(P, Q) = \inf_{\alpha, \beta} \max_{t \in [0, 1]} d(P(\alpha(t)), Q(\beta(t))),$$

where d is the Euclidean distance, and α and β range over all monotone parameterizations of $[0, n]$ and $[0, m]$, respectively.

Free-Space Diagram. To compute the Fréchet distance, a way of representing all possible person and dog walks is needed. Let $\mathcal{B}_{n \times m} = [0, n] \times [0, m]$ be an n by m rectangle in the plane. Each point $(s, t) \in \mathcal{B}_{n \times m}$ uniquely represents a pair of points $(P(s), Q(t))$ on the polygonal curves P and Q . We decompose $\mathcal{B}_{n \times m}$ into $n \cdot m$ unit grid cells $\mathcal{C}_{ij} = [i - 1, i] \times [j - 1, j]$ for $(i, j) \in \{1, \dots, n\} \times \{1, \dots, m\}$, where each cell \mathcal{C}_{ij} corresponds to a segment P_i on P and a segment Q_j on Q . Given a parameter $\varepsilon \geq 0$, the *free space* \mathcal{F}_ε is defined as

$$\mathcal{F}_\varepsilon = \{(s, t) \in \mathcal{B}_{n \times m} \mid d(P(s), Q(t)) \leq \varepsilon\}.$$

We call any point $p \in \mathcal{F}_\varepsilon$ a *feasible* point. An example of the free-space diagram for two curves P and Q is illustrated in Figure 2.1.a. The free-space diagram was first used in [8] to find the standard Fréchet distance in near quadratic time. Consider any segment P_i and Q_j from polygonal curves P and Q , respectively. Then, the free space inside cell \mathcal{C}_{ij} is convex and can be determined in $O(1)$ time by computing the intersection of a unit square and an ellipse [8].

Here, we show how the function of such an ellipse is computed: Let the coordinates of the endpoints of P_i be: $(p_{1a}; p_{1b}); (p_{2a}; p_{2b})$ and the coordinates of the endpoints of Q_j be: $(q_{1a}; q_{1b}); (q_{2a}; q_{2b})$. Let P_i be defined by the function: $y = a_1x + b_1$ and Q_j be defined by the function: $y = a_2x + b_2$. Then:

$$a_1 = \frac{p_{2b} - p_{1b}}{p_{2a} - p_{1a}}, b_1 = \frac{p_{2a}p_{1b} - p_{1a}p_{2b}}{p_{2a} - p_{1a}}$$

$$a_2 = \frac{q_{2b} - q_{1b}}{q_{2a} - q_{1a}}, b_2 = \frac{q_{2a}q_{1b} - q_{1a}q_{2b}}{q_{2a} - q_{1a}}$$

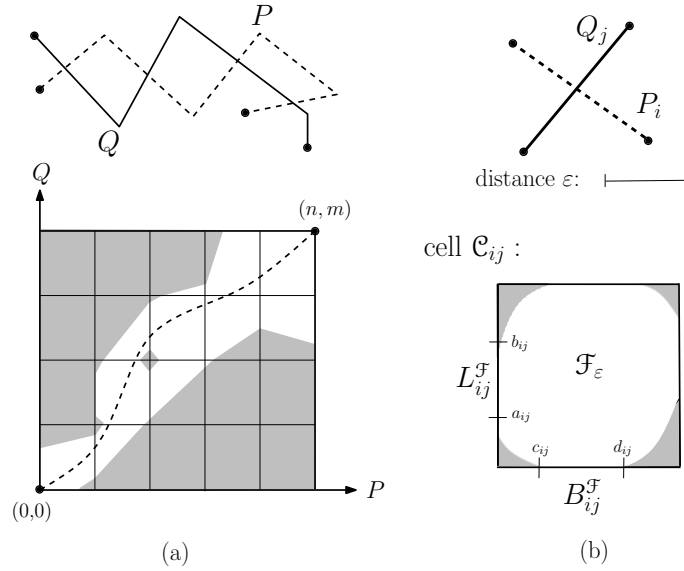


Figure 2.1. (a) The free-space diagram for two polygonal curves P and Q ; (b) two segments P_i and Q_j and their corresponding free space. The diagram was generated using a Java applet developed by S. Pelletier [55].

The points located in the 2-dimensional coordinate system of the parametrization of P_i and Q_j satisfy: $x' \in [0, 1], y' \in [0, 1]$, thus the coordinate of points in P_i are :

$$((p_{2a} - p_{1a})x' + p_{1a}, (p_{2b} - p_{1b})x' + p_{1b}).$$

The coordinates of the points in Q are:

$$((q_{2a} - q_{1a})y' + q_{1a}, (q_{2b} - q_{1b})y' + q_{1b}).$$

Every point in the free space inside $\mathcal{C}_{i,j}$, corresponds to exactly two points, one from P_i the other from Q_j where their distance is less than or equal parameter ϵ . Therefore,

$$[(p_{2a} - p_{1a})x' + p_{1a} - (q_{2a} - q_{1a})y']^2 + [(p_{2b} - p_{1b})x' + p_{1b} - (q_{2b} - q_{1b})y' - q_{1b}]^2 \leq \epsilon^2$$

by expanding the above inequality and considering the fact that :

$$(p_{2a} - p_{1a})^2 + (p_{2b} - p_{1b})^2 = |P_i|^2; (q_{2a} - q_{1a})^2 + (q_{2b} - q_{1b})^2 = |Q_i|^2.$$

We derive the function of the ellipse as follows:

$$\begin{aligned}
& |P_i|^2 x'^2 + |Q_j|^2 y'^2 - 2[(p_{2a} - p_{1a})(q_{2a} - q_{1a}) + (p_{2b} - p_{1b})(q_{2b} - q_{1b})]x'y' \\
& + 2[(p_{1a} - q_{1a})(p_{2a} - p_{1a}) + (p_{1b} - q_{1b})(p_{2b} - p_{1b})]x' \\
& - 2[(p_{1a} - q_{1a})(q_{2a} - q_{1a}) + (p_{1b} - q_{1b})(q_{2b} - q_{1b})]y' \\
& + (p_{1a} - q_{1a})^2 + (p_{1b} - q_{1b})^2 \leq \epsilon^2
\end{aligned}$$

Since an ellipse is a convex shape and the unit square in the free-space diagram is convex too, the intersection of two convex objects is convex and therefore, the free space inside each cell is convex. In addition, Alt and Godau [8] observed that any xy -monotone path from $(0, 0)$ to (n, m) in the free space corresponds to traversals of P and Q , where the traversing objects remain at a distance of at most ϵ from each other.

Based on the above observations, Alt and Godau [8] provided an algorithm to solve the decision problem (i.e., decide if $\delta_F(P, Q) \leq \epsilon$ for a given $\epsilon \geq 0$) in quadratic time as follows:

Let L_{ij} (resp., B_{ij}) denote the left (bottom, resp.) line segment bounding \mathcal{C}_{ij} (see Figure 2.1.b). As a preprocessing step, the free space, \mathcal{F}_ϵ , is computed by the algorithm. Let $L_{ij}^\mathcal{F} = L_{ij} \cap \mathcal{F}_\epsilon$ and $B_{ij}^\mathcal{F} = B_{ij} \cap \mathcal{F}_\epsilon$ (see Figure 2.1.b). Since \mathcal{F}_ϵ is convex within \mathcal{C}_{ij} , each of $L_{ij}^\mathcal{F}$ and $B_{ij}^\mathcal{F}$ is a line segment. The preprocessing step therefore involves computing line segments $L_{ij}^\mathcal{F}$ and $B_{ij}^\mathcal{F}$ for all feasible pairs (i, j) , which can be done in $O(n^2)$ time. A point $(s, t) \in \mathcal{F}_\epsilon$ is called *reachable* if there is a monotone path from $(0, 0)$ to (s, t) in \mathcal{F}_ϵ . Let $L_{ij}^\mathcal{R}$ be the set of reachable points in L_{ij} , and $B_{ij}^\mathcal{R}$ be the set of reachable points in B_{ij} . Observe that all non-empty sets $L_{ij}^\mathcal{R}$ and $B_{ij}^\mathcal{R}$ for each cell \mathcal{C}_{ij} forms line segment [8]. The algorithm processes the cells in the row-wise order, from $\mathcal{C}_{0,0}$ to \mathcal{C}_{nm} , and at each cell \mathcal{C}_{ij} , $L_{ij}^\mathcal{R}$ and $B_{ij}^\mathcal{R}$ are computed. Finally, at the last cell, if the top-right corner of $\mathcal{B}_{n \times m}$ is reachable, “YES” is returned as the answer to the decision problem, otherwise “NO” is returned. Details are shown in Algorithm 1. Given polygonal curves P and Q with total complexity n , Algorithm 1 decides in $O(n^2)$ time if $\delta_F(P, Q) \leq \epsilon$ [8].

The algorithm proposed by Alt and Godau for actually computing the Fréchet

Algorithm 1 STANDARD FRÉCHET DECISION ALGORITHM [8]

- 1: **for** each cell \mathcal{C}_{ij} **do**
 - 2: Compute $L_{ij}^{\mathcal{F}}$ and $B_{ij}^{\mathcal{F}}$
 - 3: Set $L_{0,0}^{\mathcal{R}} = B_{0,0}^{\mathcal{R}} = \{(0,0)\}$, $L_{i,0}^{\mathcal{R}} = \emptyset$ for $i \in \{1, \dots, n\}$, $B_{0,j}^{\mathcal{R}} = \emptyset$ for $j \in \{1, \dots, m\}$

 - 4: **for** $i = 0$ to n **do**
 - 5: **for** $j = 0$ to m **do**
 - 6: Compute $L_{i+1,j}^{\mathcal{R}}$ and $B_{i,j+1}^{\mathcal{R}}$ from $L_{i,j}^{\mathcal{R}}$, $B_{i,j}^{\mathcal{R}}$, $L_{i+1,j}^{\mathcal{F}}$ and $B_{i,j+1}^{\mathcal{F}}$.
 - 7: Return “YES” if $(n, m) \in L_{n+1,m}^{\mathcal{R}}$, “NO” otherwise.
-

distance δ_F makes use of Algorithm 1, and the technique of parametric search of Megiddo [53], accompanied by a speedup technique due to Cole [27]. The resulting algorithm has time complexity $O(n^2 \log n)$.

Let $L_{ij}^{\mathcal{F}} = [a_{ij}, b_{ij}]$ and $B_{ij}^{\mathcal{F}} = [c_{ij}, d_{ij}]$ (see Figure 2.1.b). Notice that the free space, \mathcal{F}_ε , is an increasing function of ε , that is, for $\varepsilon_1 \leq \varepsilon_2$, we have $\mathcal{F}_{\varepsilon_1} \subseteq \mathcal{F}_{\varepsilon_2}$. Therefore, to find the exact value of $\delta_F(P, Q)$, we can start from $\varepsilon = 0$, and continuously increase ε until we reach the first point at which \mathcal{F}_ε contains a monotone path from $(0, 0)$ to (n, m) . This occurs at only one of the following “critical values” [8]:

- (A) smallest ε for which $(0, 0) \in \mathcal{F}_\varepsilon$ or $(n, m) \in \mathcal{F}_\varepsilon$. These are the distances between starting point and endpoints of P and Q .
- (B) smallest ε at which $L_{ij}^{\mathcal{F}}$ or $B_{ij}^{\mathcal{F}}$ becomes non-empty for some pair (i, j) (when a new passage opens between two adjacent cells in the diagram). These are the distances between vertices of one curve and edges of the other (see Figure 2.2a).
- (C) smallest ε at which $a_{ij} = b_{k\ell}$, or $d_{ij} = c_{k\ell}$, for some i, j, k , and ℓ , (when a new horizontal or vertical passage opens within the diagram). A critical distance of type (C) corresponds to the common distance of two vertices of one curve to the intersection point of their bisector with an edge of the other curve [8] (see Figure 2.2b).

There are two critical values of type (A), $O(n^2)$ critical values of type (B), and

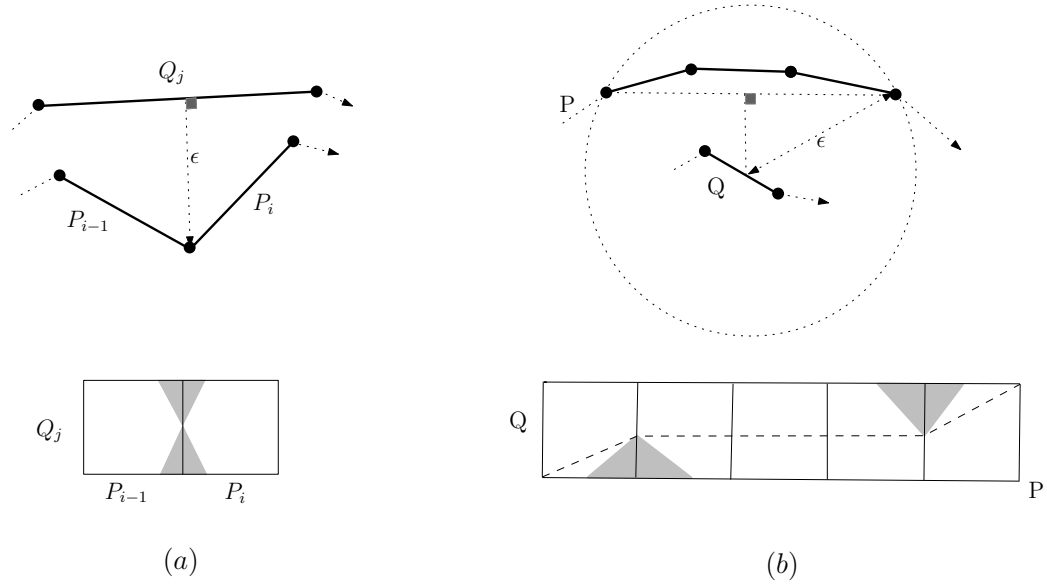


Figure 2.2. The geometric situations corresponding to Type (B) and Type (C) critical distances. (a) a new passage opens between two neighboring cells in the free-space diagram (b) a horizontal passage opens in the free-space diagram.

$O(n^3)$ critical values of type (C), each computable in $O(1)$ time. Therefore, to find the exact value of $\delta_{\bar{F}}(P, Q)$, one can compute all these $O(n^3)$ values, sort them, and do a binary search (equipped with Algorithm 1) to find the smallest ϵ for which $\delta_F(P, Q) \leq \epsilon$, in $O(n^3 \log n)$ total time. However, as mentioned in [8], a parametric search method [53, 27] can be applied to the critical values of type (C) to get a faster algorithm.

The crucial observation made in [8] is that any comparison-based sorting algorithm that sorts a_{ij} , b_{ij} , c_{ij} , and d_{ij} (defined as functions of ϵ) has critical values that include those of type (C). This is because the critical values of type (C) occur if $a_{ij} = b_{k\ell}$ or $d_{ij} = c_{k\ell}$, for some i, j, k , and ℓ . Thus, Algorithm 2, uses parametric search to find the exact value of Fréchet distance.

Steps 1 and 2 together take $O(n^2 \log n)$ time. The parametric search in Step 3 takes $O((k + T) \log k)$ time, where k is the number of values to be sorted, and T is the time needed by the decision algorithm. In case of the standard Fréchet distance problem, $k = |S| = O(n^2)$, and $T = O(n^2)$. We conclude that the exact Fréchet distance between two polygonal curves can be computed in $O(n^2 \log n)$ time [8].

Algorithm 2 STANDARD FRÉCHET COMPUTATION ALGORITHM [8]

- 1: Compute all critical values of types (A) and (B), and sort them.
 - 2: Binary search to find two consecutive values ε_1 and ε_2 in the sorted list such that $\delta_F \in [\varepsilon_1, \varepsilon_2]$.
 - 3: Let S be the set of endpoints $a_{ij}, b_{ij}, c_{ij}, d_{ij}$ of intervals $L_{ij}^{\mathcal{F}}$ and $B_{ij}^{\mathcal{F}}$ that are nonempty for $\varepsilon \in [\varepsilon_1, \varepsilon_2]$. Use Cole's parametric search method [27] based on sorting the values in S to find the exact value of δ_F .
-

2.2 Variants of Fréchet Distance

In this section, we summarize different variants of Fréchet distance metric which have been studied in the literature.

2.2.1 Weak Fréchet Distance

One of the variants of the Fréchet metric studied in [8] is the weak Fréchet distance or non-monotone Fréchet distance. Coming back to the man-dog illustration of the Fréchet metric, in this instance, both the man and the dog are allowed to backtrack on their respective curves.

Let $\delta_{\bar{N}}(P, Q)$ denote the weak Fréchet distance between two polygonal curves P and Q . In order to solve the decision and optimization problems, the same $m \times n$ -diagram $\mathcal{B}_{n \times m}$ can be used as in the previous section. Now the decision problem has a yes answer iff there exists a path from $(0, 0)$ to (m, n) in \mathcal{F}_ε which is not necessarily monotone [8]. To solve the decision problem, an undirected labeled graph, $G = (V, E)$, is constructed on top of $\mathcal{B}_{n \times m}$ as follows:

For each cell in the diagram, one node is added to V ; two additional nodes s and t are added to the graph, where node s represents point $(0, 0)$ and node t represents point (m, n) . Two nodes are connected via an edge in the graph if their corresponding cells are adjacent in the diagram. Furthermore, one edge connects node s (resp., node t) to the node which corresponds to cell \mathcal{C}_{11} (resp., cell \mathcal{C}_{mn}) as depicted in Figure 2.3. The edge between two neighboring cells is labeled with a minimal ε for which there is a possible direct transition between the two cells within \mathcal{F}_ε . The edge $\{s, \mathcal{C}_{11}\}$ is

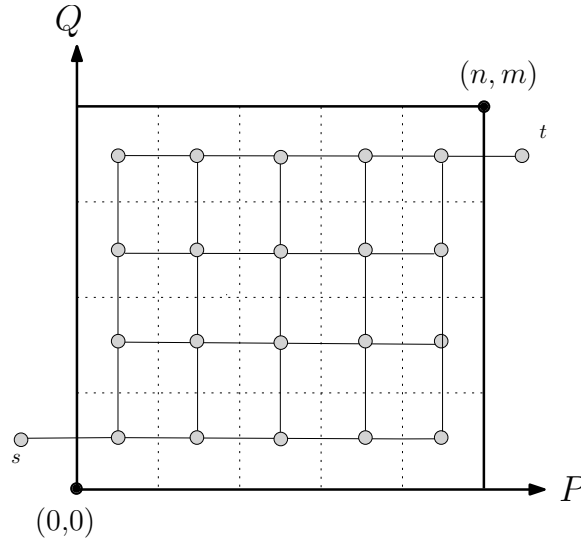


Figure 2.3. The graph with grey nodes is built on top of $\mathcal{B}_{n \times m}$ to compute the weak Fréchet distance

labeled with the distance between starting points of the curves and the edge $\{s, \mathcal{C}_{11}\}$ is labeled with the distance between ending points of the curves. Let the weight of a path within G be the largest weight of its edges. After constructing graph G , the decision problem has a positive answer iff there exists a path of weight ϵ between s and t within graph G . This can be done by removing all edges of weight greater than ϵ , and checking if s and t are in the same connected component, for example, by running BFS algorithm [8].

The computation of the exact value of $\delta_{\bar{N}}(P, Q)$ consists of determining the minimum weight path within graph G from s to t . This can be computed by using Prim's minimum spanning tree algorithm starting from s and running it until the minimum spanning tree containing s and t is found. After finding the MST, one can run breadth first search algorithm to find a path from s to t in MST. We conclude that given two polygonal curves P and Q with total length n and a distance ϵ , one can decide in $O(n^2)$ time if $\delta_{\bar{N}}(P, Q) \leq \epsilon$ and the exact value of $\delta_{\bar{N}}(P, Q)$ can be found in $O(n^2 \log n)$ [8].

2.2.2 Fréchet Distance of a Set of Curves

Dumitrescu *et al.* [33] have extended the Fréchet distance notion between two curves to a set of curves and showed how to compute and approximate it. The corresponding intuitive illustration is as follows. Suppose that points are moving, one on each of given curves. The speed of each point may vary but no point is allowed to move backwards. Assume that all pairs of points are connected by strings of the same length. Then, the Fréchet distance of the set of curves is the minimum length of a connecting string that is necessary.

To compute the Fréchet distance of a set of m curves f_1, f_2, \dots, f_m (with complexity n_1, n_2, \dots, n_m , respectively), the approach of [8] can be adapted. First, a free-space diagram corresponding to each pair of curves is built. To answer the decision problem, one would check whether there exists a path from $(0, \dots, 0)$ to (n_1, \dots, n_m) in free-space diagram in \mathbb{R}^m which is monotone in all m coordinates. This takes $O(n_1 \dots n_m)$ time and using parametric search, the resulting final algorithm has time complexity $O(n_1 \dots n_m \log(n_1 \dots n_m))$. In [33], a simple algorithm is proposed which computes the Fréchet distance of set of curves (i.e., $\delta_{\mathcal{F}}$) approximately. Let $d_{ij} = \delta_F(f_i, f_j)$. Observe that $\delta_{\mathcal{F}} \leq \min_{1 \leq i \leq m} \max_{1 \leq j < k \leq m} (d_{ij} + d_{ik})$ [33]. Thus, one can compute all pairwise Fréchet distances and output $\min_{1 \leq i \leq m} \max_{1 \leq j < k \leq m} (d_{ij} + d_{ik})$ as the Fréchet distance of a set of curves with the approximation ratio 2 [33]. The running time of this approach is $O(\sum_{1 \leq i < j \leq m} n_i n_j \log(n_i n_j))$ which is much better than that of the exact algorithm previously mentioned.

Alt *et al.* [9] consider the problem of minimizing the Fréchet distance under translations: Given two polygonal curves, search for a translation which, when applied to the first curve, minimizes the Fréchet distance to the second one. The decision algorithm decides whether there is a transformation that, when applied to the first curve, results in a Fréchet distance less or equal than some given parameter ϵ . The runtime of the decision algorithm is $O((mn)^3(m+n)^2)$. The parametric search adds only a logarithmic overhead, since Cole's technique for parametric search based on sorting [27] can be applied, so the optimization problem can be solved in $O((mn)^3(m+n)^2 \log(m+n))$

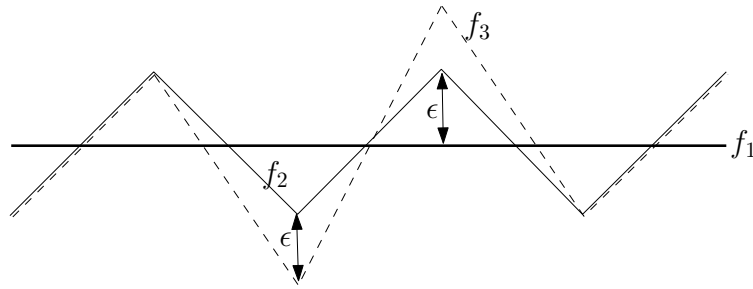


Figure 2.4. $\delta_F(f_1, f_2) = \delta_F(f_2, f_3)$. But curve f_2 is more matched to curve f_3 .

time. In [43], the authors present algorithms for matching two polygonal chains in two dimensions to minimize their discrete Fréchet distance under translation and rotation.

2.2.3 Average Fréchet and Summed Fréchet Distance

Notice that the Fréchet metric is a max measure; it is defined as the maximum pointwise distance minimized over all parametrizations. This dependence on the maximum value can often lead to non-robust behavior, where small variations in the input can distort the distance function by a large amount. Consider for example the curves shown in Figure 2.4. Assume one wants to match the curve f_2 either to the curve f_1 or f_3 . Intuitively, it seems that f_3 is the better match. This is however not reflected by the Fréchet distance which is equal for both pairs of curves (f_1, f_2) and (f_2, f_3). An average Fréchet distance was suggested in [14] which averages over certain distances instead of taking the maximum. Efrat *et al.* [34] has combined *dynamic time warping* to compute an integral version of the Fréchet distance, which can smooth out the impact of some outliers. Dynamic time warping measure (DTW) is a measure which was first proposed in the 60s as a measure of speech signal similarity. In the dog-man setting, the DTW distance between two curves (defined as sequences of points) is the sum of the leash lengths measured at each (discrete) position (minimized over all trajectories).

2.2.4 Fréchet Distance of Specific Families of Curves

It has been an open problem to find a sub-quadratic algorithm for computing the Fréchet distance. A lower bound of $\Omega(n \log n)$ is given by [16] for the problem of deciding whether the Fréchet distance between two curves is smaller or equal a given value. In [5], Alt conjectured that the decision problem may be 3SUM-hard [38]. In a very recent work [17], Buchin *et al.* present an algorithm with total expected time $O(n^2 \sqrt{\log n} (\log \log n)^{3/2})$ which is the first algorithm to achieve a running time of $o(n^2 \log n)$ for computing Fréchet distance. Furthermore, they show that there exists an algebraic decision tree for the decision problem of depth $O(n^{2-\gamma})$, for some $\gamma > 0$. This provides some insights that might suggest that the decision problem may not be 3SUM-hard.

The only subquadratic algorithms known are for quite restricted classes of curves such as for closed convex curves and for k -bounded curves [10], or discrete version of Fréchet distance [2]. For a curve to be k -bounded means that for any two points on the curve the portion of the curve in between them cannot be further away from either point than $\frac{k}{2}$ times the distance between the two points. For closed convex curves the Fréchet distance equals the Hausdorff distance and for k -bounded curves the Fréchet distance is at most $(1 + k)$ times the Hausdorff distance, and hence the $O(n \log n)$ algorithm for the Hausdorff distance applies.

The Fréchet distance of another family of curves, c -packed curves, is studied in a recent work by Driemel *et al.* [32]. A curve P is called c -packed if the total length of P inside any circle is bounded by c times the radius of the circle. Intuitively, the constant c measures how unrealistic the input curves are.

A k -bounded curve might have arbitrary length while maintaining a finite diameter, and as such may not be c -packed. Unlike k -bounded curves, the Fréchet distance between two c -packed curves might be arbitrarily larger than their Hausdorff distance. Indeed, c -packed curves are considerably more general and a more natural family of curves. For example, a c -packed curve might self cross and revisit the same location several times, and the class of c -packed curves is closed under concatenation, none of

which is true for k -bounded curves. Given two c -packed curves P and Q with total complexity n , a $(1 + \epsilon)$ -approximation of the Fréchet distance between them can be computed in $O(\frac{n}{\epsilon} + cn \log n)$ time [32].

In standard Fréchet metric, the objects are piecewise linear. Rote [56] explores the Fréchet distance between more general curves where each input curve is given as a sequence of smooth curve pieces that are sufficiently well-behaved, such as circular arcs, parabolic arcs, or some class of spline curves. He has shown that the combinatorial complexity, i.e., the number of steps, for solving the decision problem is not larger than for polygonal paths, $O(n^2)$ (n is the total size of two given curves). Furthermore, under the assumption that the curves consist of algebraic pieces whose degree is bounded by a constant, the optimization problem can be solved in $O(n^2 \log n)$ time, which matches the running time for the polygonal case.

2.2.5 Fréchet Distance with no Leash Cross

In the Fréchet metric, the leash is allowed to cross the two polylines. A natural restriction to apply is to require that the leash not cross the polylines. Efrat *et al.* [35] has introduced two new metrics for measuring the distance between non-intersecting (not self-intersecting) polygonal curves: Given two polylines with total complexity n , they present algorithms to compute the geodesic width of the two polylines in $O(n^2 \log^2 n)$ time using $O(n^2)$ space and the link width in $O(n^3 \log n)$ time using $O(n^2)$ working space where n is the total number of edges of the polylines. Their computation of these metrics relies on two closely-related combinatorial structures: the shortest-path diagram and the link diagram of a simple polygon. The shortest-path (resp., link) diagram encodes the Euclidean (resp., link) shortest path distance between all pairs of points on the boundary of the polygon. Later, Bespamyatnikh [13] obtained a faster algorithm for computing the geodesic width in $O(n^2)$ time, using $O(n)$ space.

2.2.6 Directional-based Fréchet Distance

Notice that small deviations in one curve can disproportionately influence the similarity of two curves. Furthermore, translations and scalings can affect the result, and it is very difficult to make the Fréchet distance invariant under these types of transformations. To address these issues, [30] has proposed the *direction-based* Fréchet distance. Like the standard Fréchet distance, this measure optimizes over all parametrizations for a pair of curves. Unlike the Fréchet distance, it is based on differences between the directions of movement along the curves, rather than on positional differences. Therefore, the directional-based Fréchet distance is invariant under translations and scalings. It measures the similarity of polygonal curves by integrating over the angular differences between pairs of vectors. The direction-based Fréchet distance of two polygonal curves with m and n vertices can be computed in $O(mn)$ time, using $O(m + n)$ space [30]. Furthermore, the direction-based integral Fréchet distance is proposed in [30] to ensure that small variations in one path do not disproportionately affect the similarity measure.

The measure most closely related to the direction-based Fréchet distance is the turning angle distance [11]. This distance measure is essentially the same as the direction-based integral Fréchet distance, but with the following important difference: the turning angle distance does not optimize over all possible one-to-one mappings between the two curves. Rather, the direction-based Fréchet distance optimizes over all possible one-to-one mappings between the two curves. The turning angle distance is easily computed in $O(m + n)$ time for two polygonal curves with m and n vertices [11].

2.2.7 Fréchet Distance of Closed Curves

Closed polygonal curves are curves with common starting and ending points. The man-dog illustration of Fréchet metric in this variant is as follows: the man and the dog are not only allowed to control their speeds, but also to choose optimal starting points on the closed curves to minimize the length of the leash.

Let $\delta_{\bar{C}}(P, Q)$ denote the Fréchet distance between two closed curves. Alt *et al.* [8] proposed a polynomial time algorithm to solve the decision problem of $\delta_{\bar{C}}(P, Q)$ as follows. First, a new diagram $\mathcal{B}_{2n \times m}$ is constructed by concatenating two copies of $\mathcal{B}_{n \times m}$ [8]. Then, a data structure is built on top of $\mathcal{B}_{2n \times m}$ to check the following property in constant time: $\delta_{\bar{C}}(P, Q) \leq \epsilon$ iff there exists a $t \in [0, n]$ and a monotone curve from $(t, 0)$ to $(t + n, m)$ in the free space \mathcal{F}_ϵ of $\mathcal{B}_{2n \times m}$ [8]. Suppose diagram $D = \mathcal{B}_{2n \times m}$ is given and B, T, L , and R are its bottom, top, left and right sides, respectively. In the data structure, these sides are partitioned into some intervals where each interval is a connected subset of white points on the boundary of D . There are three types of intervals:

- I is n -interval iff from no point on $I \subseteq B \cup L$, a point on $T \cup R$ can be reached by a monotone path in \mathcal{F}_ϵ of $\mathcal{B}_{2n \times m}$.
- I is r -interval iff from any two points in $I \subseteq B \cup L$, the same set of points on $R \cup T$ can be reached.
- I is s -interval iff from any point in $I \subseteq L$ (resp., $I \subseteq B$), the horizontal (resp., the vertical) line segment connecting that point with R (resp., T) lies completely within \mathcal{F}_ϵ .

Two pointers h and ℓ are attached to each r -interval I : pointer h points to the highest point in $T \cup R$ that can be reached from I and pointer ℓ points to the lowest point in $T \cup R$ which is reachable from I . In addition, an h pointer is assigned to each s -interval on L , and an ℓ pointer is assigned to each s -interval on B . Analogously, $T \cup R$ is partitioned into n -, s -, and r intervals depending on their reachability from $L \cup B$ and h and ℓ pointers are attached to them.

The data structure is constructed recursively by starting from diagram D and splitting the diagram in half at its longer side into two diagrams D_1 and D_2 . The recursion continues until a 1×1 - diagram, which is a cell, is reached. For one cell, the partitioning and the pointers can be found in $O(1)$ time.

In order to merge the two solutions D_1 and D_2 into one for D , first the intervals on the right side R_1 of D_1 are merged with the ones of the left side L_2 of D_2 . This

causes a refinement of the partitions of R_1 and L_2 . Each new interval inherits the type and pointers from the old interval of which it is subset. Then, the types and pointers of the intervals on $L_1 \cup B_1$ and $T_2 \cup R_2$ are updated and the intervals and pointers on T_1 and B_2 remain unchanged. Details of how intervals on $L_1 \cup B_1$ (or intervals on $T_2 \cup R_2$) are updated, can be found in [8]. It is shown that the total time for merging is proportional to the number of intervals in the partitioning of D_1 and D_2 ; in the worst case, this number is $O(nm)$. Thus, the runtime of the merging step is $O(nm)$ and consequently, the whole divide-and-conquer algorithm has $O(nm \log nm)$ running time.

Observe that given two points $u \in I \subseteq B$ and $v \in J \subseteq T$, there exists a monotone path from u to v in \mathcal{F}_ϵ iff one of the following conditions (a) or (b) holds: (a) I is an r -interval and v lies between $h(I)$ and $\ell(I)$ (b) I is type-s and v lies to the right of u and to the left of $\ell(I)$ [8]. Having constructed the data structure on $\mathcal{B}_{2n \times m}$, one can determine in $O(n)$ time by scanning intervals on the bottom and top side of $\mathcal{B}_{2n \times m}$ simultaneously, if there exists $t \in [0, n]$ and a monotone curve from $(t, 0)$ to $(t + n, m)$ in \mathcal{F}_ϵ of $\mathcal{B}_{2n \times m}$. Given two closed curves P and Q with total length n , whether $\delta_{\bar{C}}(P, Q) \leq \epsilon$ can be decided in $O(n^2 \log n)$ time. The exact value of $\delta_{\bar{C}}(P, Q)$ can be computed in $O(n^2 \log^2 n)$ time using parametric search.

2.3 Partial Curve Matching

In this section, we discuss the problem of measuring partial similarity between curves.

2.3.1 Partial Curve Matching

Alt and Godau [8] considered one natural partial similarity measure by computing the Fréchet distance between a single consecutive piece of subcurve of P and another curve Q . Let $\delta_{\bar{P}}(P, Q) = \inf \{\delta_F(R, Q) \mid \text{where } R \text{ is a subcurve of } P\}$. The same technique for two closed curves can be applied to solve the decision problem, i.e., to decide if $\delta_{\bar{P}}(P, Q) \leq \epsilon$. Let P and Q be two curves with length n and m , respectively and a parameter $\epsilon \geq 0$ is given. Once we have constructed the data structure on

top of $\mathcal{B}_{n \times m}$, we only have to check the type of the intervals on the bottom side of $\mathcal{B}_{n \times m}$. If all are of type n , then the answer is “NO”, otherwise the answer is “YES”. Therefore, the decision problem can be solved in $O(n^2 \log n)$ time and the exact value of $\delta_{\bar{P}}(P, Q)$ can be computed in $O(n^2 \log^2 n)$ time using the parametric search [8].

The partial similarity measure introduced in [8] only allows to have outliers in one of the input curve, and more importantly, it does not allow outliers appearing in different (non-consecutive) locations along the input curve. In addition, the summed versions introduced in [34] do not fully resolve the issue of partial similarity, especially when significant parts of the curves are dissimilar.

Recently, Buchin *et al.* [20] have proposed a natural extension of the Fréchet distance to measure the partial similarity between curves. They introduce a continuous partial curve similarity measure that allows general types of outliers, and develop an exact algorithm to compute it. The goal here is to maximize the total length of subcurves that are close to each other, where closeness is measured by the Fréchet distance.

Specifically, given a distance threshold ϵ and two polygonal curves P and Q , the partial Fréchet similarity between P and Q is the total length of longest subcurves of P and Q that are matched with Fréchet distance at most ϵ . The Fréchet distance can be measured under any L_p norm, and they consider the L_1 and L_∞ norms in [20]. The partial Fréchet similarity can be considered as the length of the longest monotone path in a certain polygonal domain with weighted regions, where the weight is either 0 or 1. Hence computing that measure bears similarity with the standard shortest path queries in weighted regions. The algorithm in [20] computes the partial Fréchet similarity measure in $O(mn(m+n) \log(mn))$ time, by constructing a “shortest-path map” type decomposition.

In another recent work [18], Buchin *et al.* introduce locally correct Fréchet matchings. They introduce the local correctness criterion for Fréchet matchings and prove that there always exists at least one locally correct Fréchet matching between any two polygonal curves. They provide an $O(n^3 \log n)$ algorithm to compute such matching, where n is the total complexity of the two curves.

Although the Fréchet distance is considered to be a high quality metric to measure the similarity between polygonal curves, it is very sensitive to the presence of outliers. In [31], Driemel and Har-Peled discuss a new notion of robust Fréchet distance, where they allow k shortcuts between vertices of one of the two curves, where k is a constant given as an input parameter. They provide a constant factor approximation algorithm for finding the minimum Fréchet distance among all possible k -shortcuts. However, their approach has this drawback that a shortcut is selected without considering the length of the ignored part. Therefore, such shortcuts may remove a significant portion of a curve. Recently, in another work [22], authors propose an alternative Fréchet distance measure to tolerate outliers, considering the length of portion of the curves that must be discarded. Roughly, their goal is to minimize the length of subcurves of two polygonal curves that need to be ignored to achieve a given Fréchet distance.

2.3.2 Map Matching

In GIS applications, the method of sampling the movements of vehicles using GPS is affected by errors and consequently produces inaccurate trajectory data. To become useful, the data has to be related to the underlying road network by using map matching algorithms. A quality map matching algorithm utilizing the Fréchet distance is introduced in [7].

Given a planar graph G as a road network and a polygonal curve P as a trajectory of a vehicle, the objective is to find a path π in graph G with minimum Fréchet distance to curve P . To find such a path, Alt *et al.* [7] generalized the definition of free space between two curves to the free space between a graph and a curve as follows.

The free space of graph $G = (V, E)$ and curve P is the union of all free spaces of edges of G with the polygonal curve P . Observe that the free space of one node v with curve P is a one-dimensional free space (denoted by FD_v), and the individual free spaces of all edges incident to node v with curve P share a one-dimensional free space at v . Thus, we can glue together the two-dimensional free-space diagrams along the one-dimensional free space they have in common, according to the adjacency

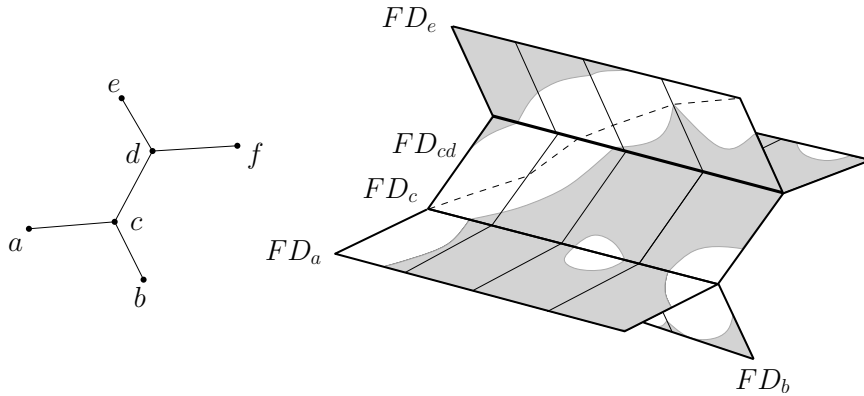


Figure 2.5. Free-space surface consists of free-space diagrams glued together according to the topology of graph G . Gray dashed path is a monotone path in the free space.

information of the graph. The resulting three-dimensional structure is called *free-space surface* of graph G and curve P in [7] (see Figure 2.5).

Let $(i, j) \in E$ be an edge of graph G . Furthermore, let FD_{ij} be an edge-curve free-space diagram corresponding to edge (i, j) , curve P , and distance ϵ . FD_{ij} consists of one dimensional free-space FD_i , then m (size of curve P) cells in a row, and another one dimensional free-space FD_j (see Figure 2.5 and Figure 2.6).

In [7] it has been shown that, after constructing a free surface corresponding to a planar graph G and a polygonal curve P , there exists a path π in G s.t. $\delta_F(\pi, P) \leq \epsilon$ iff there is a monotone path in the free-space surface from a lower left corner of some individual edge-curve free-space diagram to an upper right corner of some other individual edge-trajectory free-space diagram (e.g., see the gray dashed path in Figure 2.5).

For I a continuous interval of white points in FD_i , let the reachability pointers $\ell_{i,j}(I)$ and $r_{i,j}(I)$ be the leftmost and the rightmost white points, respectively, of FD_j that can be reached from some point in I by a monotonic path in FD_{ij} (see Figure 2.6). As a first step of the decision algorithm in [7], all one-dimensional free-spaces FD_i (for every vertex $i \in V$), and also reachability pointers are computed. Next, the algorithm sweeps a line from left to right (in direction of P) over all free spaces at the same time while maintaining the points on the sweepline that are reachable by some monotone path in the free space from some lower left corner. It then updates

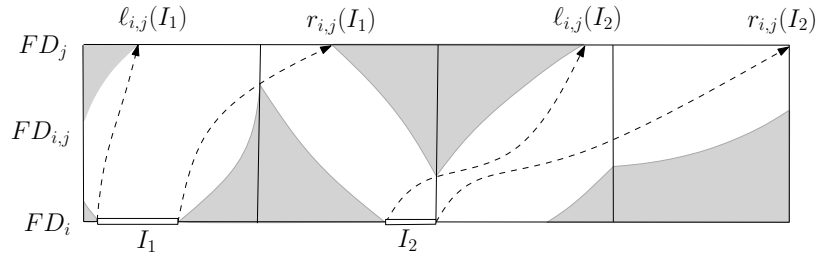


Figure 2.6. Reachability pointers

this reachability information (using the reachability pointers) Dijkstra-style while advancing the sweepline.

Given a planar graph G with n vertices, a polygonal curve P with length m and a distance ϵ , the algorithm decides in $O(mn \log n)$ time whether there exists a path π in G such that $\delta_F(P, \pi) \leq \epsilon$. One can use parametric search equipped with the decision algorithm, to find a path π in G which minimizes $\delta_F(\pi, P)$, by spending $O(mn \log(mn) \log n)$ time and using $O(mn)$ space. The decision algorithm in [7] is only a log-factor slower than the standard Fréchet distance decision problem, although it accomplishes a more complicated task of comparing curve P to all possible curves in graph G .

Map Matching based on the weak Fréchet distance has been also studied by Brakatsoulas *et al.* [14], who give an $O(mn \log(mn))$ algorithm, where m is the size of the curve and n is the size of the graph. As explained before, the decision problem for the weak Fréchet distance between two curves can be solved by testing if there exists any path in the free space of the two curves from lower left corner to upper right corner. This can be done using any graph traversal algorithm such as depth-first search in $O(mn)$ time. In [14], this approach is generalized to the map matching problem by applying depth first search to the free-space surface. They initialize the search with all white lower left corners of individual edge-trajectory free spaces, and stop the search if some upper right white corner is found. Since the free-space surface consists of mn edge-segment cells, this algorithm runs in $O(mn)$ time, which is a log-factor faster than the algorithm based on the normal Fréchet distance. Applying parametric search for optimization, in the same way as in [8], adds an additional log-factor to

the runtime for a total of $O(mn \log(mn))$ to solve the optimization problem. A new result [25] improves this running time to $O(mn)$. The method provided in that paper does not involve parametric search, and hence is also easier to implement. Their algorithm also yields an $O(mn)$ algorithm for computing the weak Fréchet distance between polygonal curves, where one curve has size m and the other has size n (which improves the $O(mn \log mn)$ result given by [8]).

2.3.3 Constrained Free-Space Diagram

Spatio-temporal data is any information relating space and time. Recently, there has been considerable research in the area of analyzing and modeling spatio-temporal data [15]. Movement patterns in such data refer to events and episodes expressed by a set of entities. The problem of detecting movement patterns in spatio-temporal data has recently received considerable attention from several research communities, e.g., geographic information science, data mining, data bases and algorithms.

Buchin *et al.* [15] propose a new and powerful tool, called constrained free space, for the analysis of trajectories, which, in particular, allows for more temporally aware analyses.

Their new tool provides an algorithm for detecting single file movement. A single file is a set of moving entities, which are following each other, one behind the other.

Let a spatio-temporal trajectory \mathcal{T} of a moving entity a be given by n time-space positions. That is, $\mathcal{T} = ((t_1, p_1), \dots, (t_n, p_n))$, where $p_i \in \mathbb{R}^2$ gives the position of entity a at time t_i for $i = 1, \dots, n$. Assume that in between time stamps t_i and t_{i+1} the entity e moves with constant speed along a straight line from p_i to p_{i+1} for $i = 1, \dots, n$ [15].

For detecting a single file behavior, we are given m spatio-temporal trajectories $\mathcal{T}_1, \dots, \mathcal{T}_m$ of entities a_1, \dots, a_m . The entities a_1, \dots, a_m are moving in single file for a given time interval if during this time each entity a_{j+1} is following behind entity a_j for $j = 1, \dots, m - 1$. For the definition of following, fix three parameters T_{min}, T_{max} , and $\delta \in \mathbb{R}$ with $T_{min} < T_{max}$. The parameters T_{min} and T_{max} specify minimum and maximum offsets in time, respectively, and δ specifies a maximum offset in space. One can detect whether one trajectory is following behind another during a fixed time

interval by searching for a monotone path in the $[T_{min}, T_{max}]$ -strip of the free-space diagram of the trajectories. Let k_{avg} and k_{max} denote the average and maximum number of cells intersected by the $[T_{min}, T_{max}]$ -strip per row or column of the free-space diagram. Then, for two trajectories of complexity n each, it can be determined in $O(nk_{avg}^2)$ time and $O(n + k_{max}^2)$ space during which time intervals one trajectory is following behind the other. Furthermore, for m trajectories of complexity n each, one can detect in $O(m^2nk_{avg})$ time and $O(nm + m^2 + k_{max})$ space all single file behaviors for a given time interval [15] .

2.4 Fréchet Distance in Different Metric Spaces

In the Fréchet distance problem, when the two curves are embedded in a general metric space, the distance between two points on the curves (i.e., the length of the shortest leash joining them) is not necessarily the Euclidean distance, but sometimes it is a geodesic distance due to existence of obstacles in the space.

2.4.1 Geodesic Fréchet Distance

In [28], Cook and Wenk described an algorithm for the geodesic Fréchet distance between two polygonal curves P and Q inside a simple polygon K . To solve the decision version, they used the free-space diagram structure introduced by Alt and Godau [8]. The main observation here is that when two curves are located inside a simple polygon, the free space inside a cell is x -monotone, y -monotone, and connected [28]. As such, only the boundaries of a cell need to be computed to propagate reachability in the free-space diagram. There are $O(n^2)$ cells in the free-space diagram. Computing the boundary of each cell takes $O(\log k)$ time by the algorithm of Guibas and Hershberger [39]. Then, the reachability information is propagated through all cells in a dynamic programming manner as [8]. Since the free space inside each cell is monotone, propagating reachability through each cell takes constant time. Therefore, if P and Q have total complexity n and polygon K has complexity k , after a one-time preprocessing step of $O(k)$ time, the geodesic Fréchet decision problem can

be solved for any $\epsilon \geq 0$ in $O(n^2 \log k)$ time and $O(k + n)$ space. The space bounds follow because $O(1)$ space is needed per cell and dynamic programming only requires that two rows of cells reside in memory at any one time. The $O(k)$ term comes from storing the preprocessing structures of [39] throughout the algorithm's execution. Using parametric search, the exact geodesic Fréchet distance can be computed in $O(n^2 \log k \log n)$. Cook and Wenk [28] proposed a randomized algorithm using a *red-blue* intersection approach which finds the exact geodesic Fréchet distance in $O(k + n^2 \log kn \log n)$ expected time and $O(k + n^3 \log kn)$ worst case time.

Although the exact standard Fréchet distance is normally found in $O(n^2 \log n)$ time using parametric search, parametric search is often regarded as impractical because it is difficult to implement and involves large constant factors [27]. The randomized algorithm in [28] is the first practical alternative to parametric search for solving the exact Fréchet optimization problem. Using the red-blue intersection approach as [28], one can compute the exact Fréchet distance in $O(n^2 \log^2 n)$ expected time and $O(n^2)$ space, where n is the larger of the complexities of P and Q [28].

2.4.2 Homotopic Fréchet distance

The definition of the classical Fréchet distance allows the leash to switch discontinuously, without penalty, from one side of an obstacle or a mountain to another. Chambers *et al.* [23] study the Fréchet distance between two polygonal curves P and Q , located in the punctuated plane consisting of k points. They introduce a continuity requirement on the motion of the leash, i.e. the leash cannot switch, discontinuously, from one geodesic to another; in particular, the leash can not jump over obstacles and can sweep over a mountain only if it is long enough (see Figure 2.7). This new similarity metric is called *homotopic* Fréchet distance. It finds applications in morphing and robotics. In spaces where shortest paths vary continuously as their endpoints move, such as the Euclidean plane, the Fréchet distance and homotopic Fréchet distance are identical. In general, however, homotopic Fréchet distance could be larger (but never smaller) than the classical Fréchet distance. Given two polygonal curves P and Q with complexity n and m , respectively and k points in the plane,

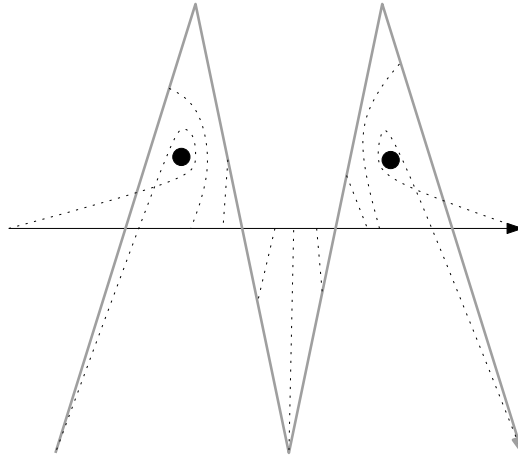


Figure 2.7. The dashed lines show the leash between two objects while they are moving on their corresponding curves. The leash can not jump over the obstacles.

the homotopic Fréchet distance between P and Q in the plane can be computed in $O(m^2n^2k^3 \log(mnk))$ time [23].

The algorithm for computing the geodesic Fréchet distance between two curves within a simple polygon due to Cook and Wenk [28], is faster than the homotopic Fréchet computation algorithm in [23] by roughly a factor of n . This is because they use a randomized strategy in place of parametric search.

Cook *et al.* [29] develop algorithms to compute the Fréchet distance of two curves on convex and non-convex polyhedral surface. Let M be the total complexity of a problem space that contains a polyhedral surface and auxiliary objects on the surface such as points, line segments, and polygonal curves. Then, Fréchet distance can be computed in $O(M^6 \log^2 M)$ time and $O(M^2)$ space in a convex polyhedral surface and $O(M^7 \log^2 M)$ time and $O(M^3)$ space in a non-convex polyhedral surface.

Cheung *et al.* [26] consider two versions of the Fréchet distance problem in weighted planar subdivisions. In the first one, the distance between two points is the weighted length of the line segment joining the points. In the second one, the distance between two points is the length of the shortest path between the points. In both cases they give algorithms for finding a $(1 + \epsilon)$ -factor approximation of the Fréchet distance between two polygonal curves.

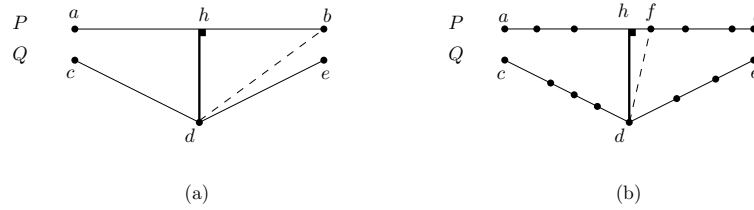


Figure 2.8. (a) The discrete Fréchet distance could be arbitrarily larger than the continuous distance, e.g., $\delta_F(P, Q) = |\overline{dh}|$, $\delta_{dF}(P, Q) = |\overline{db}|$. (b) If we put enough sample points on the two polygonal chains, then the resulting discrete Fréchet distance, that is, $|\overline{df}|$, closely approximates $|\overline{dh}|$.

2.5 Approximate Fréchet Distance

A considerable amount of work has been done to improve running time of computing Fréchet distance. Since improving the quadratic-time solution for general curves seems to be hard, many researchers investigated Fréchet distance in restricted class of curves, rather than general curves. Also many works have been done to compute approximate Fréchet distance.

In [36], Eiter and Mannila introduced a close approximation and slightly simpler version of the Fréchet distance, called *discrete Fréchet distance*, which only considers vertices of polygonal curves. They showed that given two polygonal curves of n and m vertices, their discrete Fréchet distance can be computed in $O(mn)$ time by a dynamic programming algorithm. Figure 2.8 demonstrated the relationship between discrete and continuous Fréchet distance. It has been shown in [36] that the discrete Fréchet distance is an upper bound for the Fréchet distance and the difference between these measures is bounded by the length of the longest edge of the polygonal curves.

In a very recent work, Agarwal *et al.* [2] show how to break the quadratic barrier for the discrete Fréchet distance. They propose sub-quadratic $O(\frac{mn \log \log n}{\log n})$ time algorithm for computing discrete Fréchet distance using $O(n + m)$ space, where n and m are the complexity of two polygonal curves.

In [16], Buchin *et al.* gave a lower bound of $\Omega(n \log n)$ time for the decision version of the Fréchet problem. They also showed that this bound holds for the discrete version of the problem as well. The only subquadratic algorithms known are for restricted classes of curves such as for closed convex curves and for k -bounded curves [10]. A

curve is called k -bounded when for any two points on the curve, the portion of the curve in between them cannot be further away from either point than $k/2$ times the distance between the two points. For closed convex curves the Fréchet distance equals the Hausdorff distance and for k -bounded curves the Fréchet distance is at most $(1 + k)$ times the Hausdorff distance, and hence the $O(n \log n)$ algorithm for the Hausdorff distance applies [10]. Aronov et al. [12] proposed a near linear time $(1 + \varepsilon)$ -approximation algorithm for the discrete Fréchet distance, which only considers distances between vertices of the curves. Their algorithm works for backbone curves, which are used to model protein backbones in molecular biology. Backbone curves are required to have, unit edge length and a minimal distance between any pair of vertices.

In [3], Agarwal *et al.* consider the problem of approximating a polygonal curve P under a given error criterion by another polygonal curve P' whose vertices are a subset of the vertices of P . The goal is to minimize the number of vertices of P' while ensuring that the error between P' and P is below a certain threshold.

In another recent work [32], the Fréchet distance has been studied between c -packed curves. A curve P is c -packed if the total length of P inside any ball is bounded by c times the radius of the ball. While not all curves are c -packed, the most real life curves are c -packed [32]. Given two polygonal c -packed curves P and Q with a total of n vertices, and a parameter $0 < \epsilon < 1$, they show that one can $(1 + \epsilon)$ -approximate the Fréchet distance between P and Q in $O(\frac{cn}{\epsilon} + cn \log n)$ time.

Chapter 3

Fréchet Distance with Speed Limits

In the classical Fréchet distance problem, the speed of motion on the two polygonal curves is unbounded. In which motion speeds are bounded, both from below and from above. More precisely, associated to each segment of the curves, is a speed range that specifies the minimum and the maximum speed allowed for travelling along that segment. We say that a point object traverses a curve with *permissible speed*, if it traverses the polygonal curve from start to end so that the speed used on each segment falls within its permissible range.

The decision version of the Fréchet distance problem with speed limits is formulated as follows: Let P and Q be two polygonal curves with minimum and maximum permissible speeds assigned to each segment of P and Q . For a given $\varepsilon \geq 0$, is there an assignment of speeds so that two point objects can traverse P and Q with permissible speed and, throughout the entire traversal, remain at distance at most ε from each other? The objective in the optimization problem is to find the smallest such ε .

In this chapter, we present a new algorithm that solves the decision version of the Fréchet distance problem with speed limits in $O(n^2 \log n)$ time. Our main approach is to compute a free-space diagram similar to the one used in the standard Fréchet distance algorithm (Section 2.1). However, since the complexity of the free-space diagram in our problem is cubic, in contrast to the standard free-space diagram that has quadratic complexity, we use a “lazy computation” technique to avoid computing unneeded portions of the free space, and still be able to solve the decision problem correctly. We then use our algorithm for the decision problem to solve the optimization problem exactly in $O(n^3 \log n)$ time.

The Fréchet distance with speed limits we consider here is a natural generalization of the classical Fréchet distance. It has potential applications in GIS, when the speed

of moving objects is considered in addition to the geometric structure of the trajectories. For a practical application of this metric, consider the case where trajectory of a vehicle is given to us, and we want to find the closest path in the road network to that trajectory. The good thing about the standard Fréchet metric is that we can use it here and find the closest path in the road network to the trajectory. Using our metric however, we can consider speed limits in the road network as well, and find a path in the road network which is more realistic.

This chapter is organized as follows. The problem is formally defined in the next section. In Section 3.2, we describe a simple algorithm that solves the decision problem in $O(n^3)$ time. In Section 3.3, we provide an improved algorithm for the decision problem that runs in $O(n^2 \log n)$ time. Section 3.4 describes how the optimization problem can be solved efficiently. Finally, we summarize in Section 3.5 and outline directions for future work.

3.1 Preliminaries

Fréchet Distance with Speed Limits. Consider two point objects \mathcal{O}_P and \mathcal{O}_Q that traverse P and Q , respectively from start to end. If we think of the parameter t in the parametrizations α and β as “time”, then $P(\alpha(t))$ and $Q(\beta(t))$ specify the positions of \mathcal{O}_P and \mathcal{O}_Q on P and Q respectively at time t . The preimages of \mathcal{O}_P and \mathcal{O}_Q can be viewed as two point objects $\bar{\mathcal{O}}_P$ and $\bar{\mathcal{O}}_Q$ traversing $[0, n]$ and $[0, m]$, respectively, with their positions at time t being specified by $\alpha(t)$ and $\beta(t)$ (n is the length of P , m is the length of Q).

In the classical definition of Fréchet distance, the parametrizations α and β are arbitrary non-decreasing functions, meaning that $\bar{\mathcal{O}}_P$ and $\bar{\mathcal{O}}_Q$ (and therefore, \mathcal{O}_P and \mathcal{O}_Q) can move with arbitrary speeds in the range $[0, \infty]$. In our variant of the Fréchet distance with speed limits, each segment S of the curves P and Q is assigned a pair of non-negative real numbers $(v_{\min}(S), v_{\max}(S))$ that specify the minimum and the maximum permissible speed for moving along S . The speed limits on each segment is independent of the limits of other segments. When \mathcal{O}_P moves along a segment S

with speed v , $\bar{\mathcal{O}}_P$ moves along the preimage of S (which is a unit segment) with speed $v/\|S\|$. Therefore, the speed limit $(v_{\min}(S), v_{\max}(S))$ on a segment S , forces a speed limit on the preimage of S which is bounded by the following two values:

$$\bar{v}_{\min}(S) = \frac{v_{\min}(S)}{\|S\|} \quad \text{and} \quad \bar{v}_{\max}(S) = \frac{v_{\max}(S)}{\|S\|}.$$

We define a *speed-constrained parametrization of P* to be a continuous surjective function $f : [0, T] \rightarrow [0, n]$ with $T > 0$ such that for any $i \in \{1, \dots, n\}$, the slope of f at all points $t \in [f^{-1}(i-1), f^{-1}(i)]$ is within $[\bar{v}_{\min}(P_i), \bar{v}_{\max}(P_i)]$. Here, we define the slope of a function f at a point t to be $\lim_{h \rightarrow 0^+} f(t+h)/h$, where h approaches 0 only from above (right). By this definition, if f is a continuous function, then the slope of f at any point t in its domain is well-defined, even if f is not differentiable at t .

Given two polygonal curves P and Q of lengths n and m , respectively with speed limits on their segments, the *speed-constrained Fréchet distance* between P and Q is defined as:

$$\delta_{\bar{F}}(P, Q) = \inf_{\alpha, \beta} \max_{t \in [0, T]} d(P(\alpha(t)), Q(\beta(t))),$$

where $\alpha : [0, T] \rightarrow [0, n]$ ranges over all speed-constrained parametrizations of P and $\beta : [0, T] \rightarrow [0, m]$ ranges over all speed-constrained parametrizations of Q . Note that this new formulation of Fréchet distance is similar to the classical one, with the only difference that the parametrizations here are restricted to have limited slopes, reflecting the speed limits on the segments of the input polygonal curves.

Notation. We introduce some notation used throughout this chapter.

Let $\mathcal{B}_{n \times m} = [0, n] \times [0, m]$ be an n by m rectangle in the plane. Each point $(s, t) \in \mathcal{B}_{n \times m}$ uniquely represents a pair of points $(P(s), Q(t))$ on the polygonal curves P and Q . We decompose $\mathcal{B}_{n \times m}$ into $n \cdot m$ unit grid cells $\mathcal{C}_{ij} = [i-1, i] \times [j-1, j]$ for $(i, j) \in \{1, \dots, n\} \times \{1, \dots, m\}$, where each cell \mathcal{C}_{ij} corresponds to a segment P_i on P and a segment Q_j on Q . Given a parameter $\varepsilon \geq 0$, the *free space* \mathcal{F}_ε is defined as

$$\mathcal{F}_\varepsilon = \{(s, t) \in \mathcal{B}_{n \times m} \mid d(P(s), Q(t)) \leq \varepsilon\}.$$

We call any point $p \in \mathcal{F}_\varepsilon$ a *feasible* point. An example of the free-space diagram for two curves P and Q is given in Figure 2.1.a.

Each line segment bounding a cell in $\mathcal{B}_{n \times m}$ is called an *edge* of $\mathcal{B}_{n \times m}$. We denote by L_{ij} (resp., by B_{ij}) the left (resp., bottom) line segment bounding \mathcal{C}_{ij} . For a cell \mathcal{C}_{ij} , we define the *entry side* of \mathcal{C}_{ij} to be $\text{entry}(\mathcal{C}_{ij}) = L_{ij} \cup B_{ij}$, and its *exit side* to be $\text{exit}(\mathcal{C}_{ij}) = B_{i,j+1} \cup L_{i+1,j}$. Throughout this chapter, we process the cells in a *cell-wise* order, in which a cell \mathcal{C}_{ij} precedes a cell $\mathcal{C}_{k\ell}$ if either $i < k$ or ($i = k$ and $j < \ell$) (this corresponds to the row-wise order of the cells, from the first cell, $\mathcal{C}_{0,0}$, to the last cell, \mathcal{C}_{nm}).

For an easier manipulation of the points and intervals on the boundary of the cells, we define the following orders: Given two points p and q in the plane, we say that p is *before* q , and denote it by $p \prec q$, if either $p_x < q_x$ or ($p_x = q_x$ and $p_y > q_y$). For an interval I of points in the plane, the *left endpoint* of I , denoted by $\text{left}(I)$, is a point p such that $p \prec q$ for all $q \in I$, $q \neq p$. The *right endpoint* of I , denoted by $\text{right}(I)$, is defined analogously. Given two intervals I_1 and I_2 in the plane, we say that I_1 is *before* I_2 , and denote it by $I_1 \prec I_2$, if $\text{left}(I_1) \prec \text{left}(I_2)$ and $\text{right}(I_1) \prec \text{right}(I_2)$. Note that $I_1 \prec I_2$ implies that none of the intervals I_1 and I_2 can be properly contained in the other.

3.2 The Decision Problem

In this section, we provide an algorithm for solving the following decision problem: Given two polygonal curves P and Q of lengths n and m respectively ($n \geq m$) with speed limits on their segments, and a parameter $\varepsilon \geq 0$, decide whether $\delta_{\bar{F}}(P, Q) \leq \varepsilon$. We use a free-space diagram approach, similar to the one used in the standard Fréchet distance problem (Section 2.1). However, the complexity of the “reachable portion” on the cell boundaries is different in our problem; namely, each cell boundary in our problem has a complexity of $O(n^2)$, while in the original problem cell boundaries have $O(1)$ complexity. This calls for a more detailed construction of the free space.

Consider two point objects, \mathcal{O}_P and \mathcal{O}_Q , traversing P and Q , with their preimages, $\bar{\mathcal{O}}_P$ and $\bar{\mathcal{O}}_Q$, traversing $[0, n]$ and $[0, m]$, respectively. When \mathcal{O}_P and \mathcal{O}_Q traverse P and Q from beginning to the end, the trajectories of $\bar{\mathcal{O}}_P$ and $\bar{\mathcal{O}}_Q$ on $[0, n]$ and $[0, m]$

specify a path \mathcal{P} in $\mathcal{B}_{n \times m}$ from $(0, 0)$ to (n, m) . Suppose that \mathcal{P} passes through a point $(s, t) \in \mathcal{C}_{ij}$. The slope of \mathcal{P} at point (s, t) is equal to the ratio of the speed of $\bar{\mathcal{O}}_Q$ at point t to the speed of $\bar{\mathcal{O}}_P$ at point s . Therefore, the minimum slope at (s, t) is obtained when $\bar{\mathcal{O}}_Q$ moves with its minimum speed at point t , and $\bar{\mathcal{O}}_P$ moves with its maximum speed at point s . Similarly, the maximum slope is obtained when $\bar{\mathcal{O}}_Q$ moves with its maximum speed, and $\bar{\mathcal{O}}_P$ moves with its minimum speed. We define

$$\text{minSlope}_{ij} = \frac{\bar{v}_{\min}(Q_j)}{\bar{v}_{\max}(P_i)} \quad \text{and} \quad \text{maxSlope}_{ij} = \frac{\bar{v}_{\max}(Q_j)}{\bar{v}_{\min}(P_i)},$$

where $\bar{v}_{\min}(\cdot)$ and $\bar{v}_{\max}(\cdot)$ are the speed limits for $\bar{\mathcal{O}}_P$ and $\bar{\mathcal{O}}_Q$ as defined in Section 3.1. Indeed, minSlope_{ij} and maxSlope_{ij} specify the minimum and the maximum “permissible” slopes for \mathcal{P} at any point inside \mathcal{C}_{ij} . A path $\mathcal{P} \subset \mathcal{B}_{n \times m}$ is called *slope-constrained* if for any point $(s, t) \in \mathcal{P} \cap \mathcal{C}_{ij}$, the slope of \mathcal{P} at (s, t) is within $[\text{minSlope}_{ij}, \text{maxSlope}_{ij}]$. A point $(s, t) \in \mathcal{F}_\varepsilon$ is called *reachable* if there is a slope-constrained path from $(0, 0)$ to (s, t) in \mathcal{F}_ε .

Lemma 1 $\delta_{\bar{F}}(P, Q) \leq \varepsilon$ iff (n, m) is reachable.

Proof: The (\Rightarrow) part is straightforward. For (\Leftarrow) , we need to show that if (n, m) is reachable, then there exist a speed-constrained parametrization $\alpha : [0, T] \rightarrow [0, n]$ of P (for some $T > 0$), and a speed-constrained parametrization $\beta : [0, T] \rightarrow [0, m]$ of Q such that $d(P(\alpha(t)), Q(\beta(t))) \leq \varepsilon$ for all $t \in [0, T]$. If (n, m) is reachable, then by definition there is a slope-constrained path \mathcal{P} from $(0, 0)$ to (s, t) in \mathcal{F}_ε . We construct two parametrizations α and β from \mathcal{P} as follows. Let $\mathcal{C}_{i_1 j_1}, \mathcal{C}_{i_2 j_2}, \dots, \mathcal{C}_{i_N j_N}$ be the sequence of cells that \mathcal{P} passes through, where $(i_1, j_1) = (0, 0)$ and $(i_N, j_N) = (n, m)$. We can assume w.l.o.g. that for any k ($1 \leq k \leq N$), the path portion $\mathcal{P}_k = \mathcal{P} \cap \mathcal{C}_{i_k j_k}$ is a line segment. Otherwise, we could replace \mathcal{P}_k by a line segment connecting the two endpoints of \mathcal{P}_k which lies completely inside \mathcal{F}_ε (because $\mathcal{F}_\varepsilon \cap \mathcal{C}_{i_k j_k}$ is convex), and whose slope remains within $[\text{minSlope}_{i_k j_k}, \text{maxSlope}_{i_k j_k}]$.

Let (p_{k-1}, q_{k-1}) and (p_k, q_k) be the two endpoints of \mathcal{P}_k . The sequence $\sigma = (p_0, q_0), \dots, (p_N, q_N)$ uniquely represents \mathcal{P} (see Figure 3.1.a). We incrementally construct two point sequences A and B from σ to represent α and β , respectively. Let $t_0 = 0$, $a_0 = 0$, and $b_0 = 0$. We start with $A = \{(t_0, a_0)\}$, and $B = \{(t_0, b_0)\}$. At each

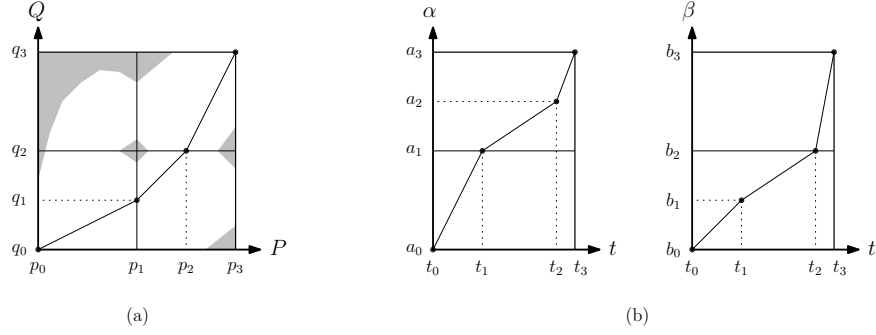


Figure 3.1. (a) A slope-constrained path \mathcal{P} in the free space of P and Q ; (b) Two speed-constrained parametrizations of P and Q , corresponding to the path \mathcal{P} .

subsequent step k from 1 to N , we update A and B as follows. Let s be the slope of \mathcal{P}_k . Since $s \in [\text{minSlope}_{i_k j_k}, \text{maxSlope}_{i_k j_k}]$, there exist a $v_P \in [\bar{v}_{\min}(P_{i_k}), \bar{v}_{\max}(P_{i_k})]$ and a $v_Q \in [\bar{v}_{\min}(Q_{j_k}), \bar{v}_{\max}(Q_{j_k})]$ such that $s = v_Q/v_P$. Let $t = (p_k - p_{k-1})/v_P = (q_k - q_{k-1})/v_Q$, and set $t_k = t_{k-1} + t$. We add to A the point (t_k, p_k) , and to B the point (t_k, q_k) (see Figure 3.1.b). The slope of segment $(t_{k-1}, a_{k-1})(t_k, a_k)$ is v_P , and the slope of segment $(t_{k-1}, b_{k-1})(t_k, b_k)$ is v_Q . Therefore, both these newly created segments satisfy the corresponding speed constraints in α and β . Therefore, after the N th step, we obtain two point sets A and B of size $N + 1$ that fully define the speed-constrained parametrizations α and β , respectively. \square

A Simple Algorithm. We now describe a simple algorithm for the decision problem. As a preprocessing step, the free space, \mathcal{F}_ε , is computed by the algorithm. Let $L_{ij}^\mathcal{F} = L_{ij} \cap \mathcal{F}_\varepsilon$ and $B_{ij}^\mathcal{F} = B_{ij} \cap \mathcal{F}_\varepsilon$. Since F_ε is convex within \mathcal{C}_{ij} (Section 2.1), each of $L_{ij}^\mathcal{F}$ and $B_{ij}^\mathcal{F}$ is a line segment. The preprocessing step therefore involves computing line segments $L_{ij}^\mathcal{F}$ and $B_{ij}^\mathcal{F}$ for all feasible pairs (i, j) , which can be done in $O(n^2)$ time. We then compute the reachability information on the boundary of each cell. Let $L_{ij}^\mathcal{R}$ be the set of reachable points in L_{ij} , and $B_{ij}^\mathcal{R}$ be the set of reachable points in B_{ij} . We process the cells in cell-wise order, from $\mathcal{C}_{0,0}$ to \mathcal{C}_{nm} , and at each cell \mathcal{C}_{ij} , we propagate the reachability information from the entry side of the cell to its exit side, using the following projection function. Given a point $p \in \text{entry}(\mathcal{C}_{ij})$, the *projection*

Lemma 2 *After the execution of Algorithm 3, a point $q \in \text{exit}(\mathcal{C}_{ij})$ is reachable iff $q \in B_{i,j+1}^{\mathcal{R}} \cup L_{i+1,j}^{\mathcal{R}}$.*

Proof: We prove the lemma by induction on the cells in cell-wise order. (\Leftarrow) Let $q \in B_{i,j+1}^{\mathcal{R}} \cup L_{i+1,j}^{\mathcal{R}}$. Then, by our construction, there is a point $p \in L_{ij}^{\mathcal{R}} \cup B_{ij}^{\mathcal{R}}$ such that $q \in \pi_{ij}(p)$. By induction hypothesis, p is reachable, and therefore, there is a slope-constrained path \mathcal{P} in \mathcal{F}_ε connecting $(0,0)$ to p . Now, \mathcal{P} concatenated with \overline{pq} is a slope-constrained path from $(0,0)$ to q , implying that q is reachable. (\Rightarrow) We show that any point $q \in \text{exit}(\mathcal{C}_{ij})$ which is not in $B_{i,j+1}^{\mathcal{R}} \cup L_{i+1,j}^{\mathcal{R}}$ is unreachable. Suppose the contrary, i.e., q is reachable. Then, there exists a slope-constrained path \mathcal{P} in \mathcal{F}_ε that connects $(0,0)$ to q . Because the slope of \mathcal{P} cannot be negative, \mathcal{P} must cross $\text{entry}(\mathcal{C}_{ij})$ at some point p . Now, p is reachable from $(0,0)$, because it is on a slope-constrained path from $(0,0)$ to p . Therefore, $p \in L_{ij}^{\mathcal{R}} \cup B_{ij}^{\mathcal{R}}$ by induction. Consider two line segments s_1 and s_2 that connect p to $\text{exit}(\mathcal{C}_{ij})$ with slopes minSlope_{ij} and maxSlope_{ij} , respectively. Since $q \notin \pi_{ij}(p)$, the portion of \mathcal{P} that lies between p and q must cross either s_1 or s_2 . But, it implies that the slope of \mathcal{P} at the cross point falls out of the permissible range $[\text{minSlope}_{ij}, \text{maxSlope}_{ij}]$, and thus, \mathcal{P} cannot be slope-constrained: a contradiction. \square

Corollary 3 *Algorithm 3 returns “YES” iff $\delta_{\overline{F}}(P, Q) \leq \varepsilon$.*

Proof: This follows immediately from Lemmas 1 and 2. \square

We now show how Algorithm 1 can be implemented efficiently. Let a *reachable interval* be a maximal contiguous subset of reachable points on the entry side (or the exit side) of a cell. Therefore, each of $L_{ij}^{\mathcal{R}}$ and $B_{ij}^{\mathcal{R}}$ can be represented as a sequence of reachable intervals. We make two observations:

Observation 1 *For each cell \mathcal{C}_{ij} , the number of reachable intervals on $\text{exit}(\mathcal{C}_{ij})$ is at most one more than the number of reachable intervals on $\text{entry}(\mathcal{C}_{ij})$.*

Proof: Let $\sigma = L_{ij}^{\mathcal{R}} \cup B_{ij}^{\mathcal{R}}$ be the set of reachable points on $\text{entry}(\mathcal{C}_{ij})$, and let $\lambda = \pi_{ij}(\sigma)$ be the projection of σ onto $\text{exit}(\mathcal{C}_{ij})$. Since the projection on each reachable

interval on the exit side is contiguous, no reachable interval in σ can contribute to more than one reachable interval in λ . Therefore, the number of intervals in λ is at most equal to the number of intervals in σ . (Note that projected intervals can merge.) However, after splitting λ between $L_{i+1,j}$ and $B_{i,j+1}$, at most one of the intervals in λ (the one containing $L_{i+1,j} \cap B_{i,j+1}$) may split into two, which increases the number of intervals by at most one. \square

Corollary 4 *The number of reachable intervals on the entry side of each cell is $O(n^2)$.*

The above upper bound of $O(n^2)$ is indeed tight as proved in Section 3.3.

Observation 2 *Let $\langle I_1, I_2, \dots, I_k \rangle$ be a sequence of intervals on the entry side of a cell \mathcal{C}_{ij} . If $I_1 \prec I_2 \prec \dots \prec I_k$ then $\pi_{ij}(I_1) \prec \pi_{ij}(I_2) \prec \dots \prec \pi_{ij}(I_k)$.*

Proof: For all $t \in \{1, \dots, k\}$, let ℓ_t be the line segment connecting $\text{left}(I_t)$ to $\text{left}(\pi_{ij}(I_t))$, and r_t be the line segment connecting $\text{right}(I_t)$ to $\text{right}(\pi_{ij}(I_t))$. The observation immediately follows from the fact that all segments in the set $\{\ell_t\}_{1 \leq t \leq k}$ have slope maxSlope_{ij} (and thus are parallel), and all segments in $\{r_t\}_{1 \leq t \leq k}$ have slope minSlope_{ij} . Note that this proof holds even if the intervals in the original sequence and/or intervals in the projected sequence overlap each other. \square

Theorem 5 *Algorithm 3 solves the decision problem in $O(n^3)$ time.*

Proof: The correctness of the algorithm follows from Corollary 3. For the running time, we first compute the time needed for processing a cell \mathcal{C}_{ij} . Let r_{ij} be the number of reachable intervals on the entry side of \mathcal{C}_{ij} . We use a simple data structure, like a linked list, to store each $L_{ij}^{\mathcal{R}}$ and $B_{ij}^{\mathcal{R}}$ as a sequence of its reachable intervals (sorted in \prec order). We show that Lines 5–8 can be performed in $O(r_{ij})$ time. In particular, Line 5 can be performed by a simple concatenation of two lists in $O(1)$ time; and Lines 7 and 8 involve an easy intersection test for each of the intervals in λ , which takes $O(r_{ij})$ time. The crucial part is Line 6 at which reachable intervals are projected. Computing the projection of each interval takes constant time. However, we need

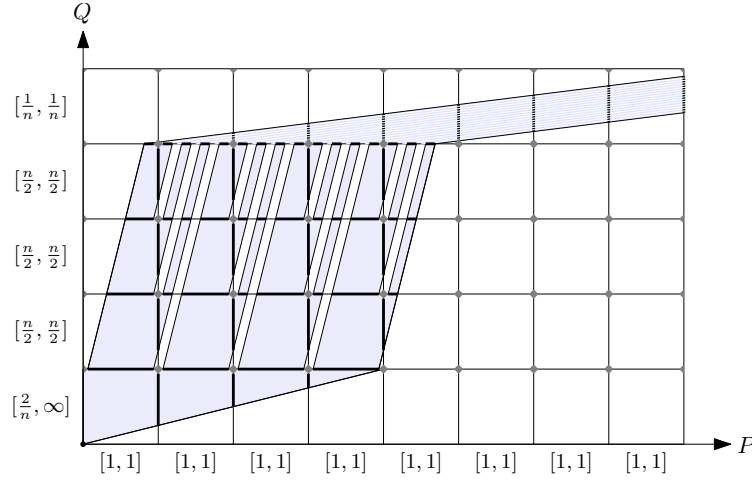


Figure 3.3. A lower bound example. The small gray diamonds represent obstacles in the free-space diagram. Reachable intervals are shown with bold black line segments. The numbers shown at each row and column represent speed limits on the corresponding segment.

to merge intersecting intervals afterwards. By Observation 2, the merge step can be performed via a linear scan, which takes $O(r_{ij})$ time. The overall running time of the algorithm is therefore $O(\sum_{i,j} r_{ij})$.

Since $r_{ij} = O(n^2)$ by Corollary 4, and there are $O(n^2)$ cells, a running time of $O(n^4)$ is immediately implied. We can obtain a tighter bound by computing $\sum_{i,j} r_{ij}$ explicitly. Define $R_k = \sum_{i+j=k} r_{ij}$, for $0 \leq k \leq 2n$. R_k denotes the number of reachable intervals on the entry side of all cells \mathcal{C}_{ij} with $i + j = k$. By Observation 1, each of the $k + 1$ cells contributing to R_k can produce at most 1 new interval. Therefore, $R_{k+1} \leq R_k + k + 1$. Starting with $R_0 = 1$, we get $R_k \leq \sum_{\ell=0}^k (\ell + 1) = O(k^2)$. Thus,

$$\sum_{0 \leq i,j \leq n} r_{ij} \leq \sum_{0 \leq k \leq 2n} R_k = \sum_{0 \leq k \leq 2n} O(k^2) = O(n^3).$$

□

3.3 An Improved Algorithm

In the previous section, we provided an algorithm that solves the decision problem in $O(n^3)$ time. It is not difficult to see that any algorithm which is based on computing the reachability information on all cells cannot be better than $O(n^3)$ time. This is proved in the following lemma.

Lemma 6 *For any $n > 0$, there exist two polygonal curves P and Q of size $O(n)$ such that in the free-space diagram corresponding to P and Q , there are $\Theta(n)$ cells each having $\Theta(n^2)$ reachable intervals on its entry side.*

Proof: Let P be a polygonal curve consisting of n horizontal segments of unit length centered at $(0,0)$, and let Q be a polygonal curve consisting of $n/2 + 1$ vertical segments, where each segment Q_2 to $Q_{n/2+1}$ has unit length centered at the origin, and Q_1 has length $1 - \delta$, for a sufficiently small $\delta \ll 1/n$. Let $\varepsilon = \sqrt{1/2 - \delta + \delta^2}$. The free-space diagram \mathcal{F}_ε for the two curves has a shape like Figure 3.3 (the gray diamond-shape regions show obstacles in the free space each having a width of 2δ in x direction). We assign the following speed limits to the segments of P and Q . All segments of P have speed limits $[1, 1]$, Q_1 has speed limits $[2/n, \infty]$, Q_2 to $Q_{n/2}$ have limits $[n/2, n/2]$, and $Q_{n/2+1}$ has limits $[1/n, 1/n]$. The number of reachable intervals on each horizontal line $y = i$ is increased by $n/2$ at each row i , for i from 1 to $n/2$, yielding a total number of $\Theta(n^2)$ reachable intervals on the line $y = n/2$. Since all these reachable intervals are projected to the right side in the last row, each cell $\mathcal{C}_{i,n/2+1}$ for $i \in \{n/2 + 1, \dots, n\}$ has $\Theta(n^2)$ reachable intervals on its entry side. \square

While the complexity of the free space is cubic by the previous lemma, we show in this section that it is possible to eliminate some of the unneeded computations, and obtain an improved algorithm that solves the decision problem in $O(n^2 \log n)$ time. The key idea behind our faster algorithm is to use a “lazy computation” technique: we delay the computation of reachable intervals until they are actually required. In our new algorithm, instead of computing the projection of all reachable intervals one by one from the entry side of each cell to its exit side, we only keep a sorted order of projected intervals, along with some minimal information that enables us to compute the exact location of the intervals whenever necessary.

To this end, we distinguish between two types of reachable intervals. Given a reachable interval I in $\text{exit}(\mathcal{C}_{ij})$, we call I an *interior interval* if there is a reachable interval I' in $\text{entry}(\mathcal{C}_{ij})$ such that $I = \pi_{ij}(I')$, and we call I a *boundary interval* otherwise. The main gain, as we see later in this section, is that the exact location of

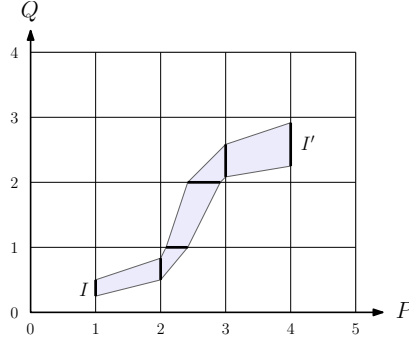


Figure 3.4. I' is an iterated projection of I .

interior intervals can be computed efficiently based on the location of the boundary intervals. The following iterated projection is a main tool that we will use.

Iterated Projections. Let I_1 be a reachable interval on the entry side of a cell $\mathcal{C}_{i_1j_1}$, and I_k be an interval on the exit side of a cell $\mathcal{C}_{i_kj_k}$. We say that I_k is an *iterated projection* of I_1 , if there is a sequence of cells $\mathcal{C}_{i_2j_2}, \dots, \mathcal{C}_{i_{k-1}j_{k-1}}$ and a sequence of intervals I_2, \dots, I_{k-1} such that for all $1 \leq t \leq k-1$, $I_t \subseteq \text{entry}(\mathcal{C}_{i_tj_t})$ and $I_{t+1} = \pi_{i_tj_t}(I_t)$ (see Figure 3.4). In the following, we show that I_k can be computed efficiently from I_1 .

Given two points $p \in \mathcal{C}_{ij}$ and $q \in \mathcal{C}_{i'j'}$, we say that q is the *min projection* of p , if there is a polygonal path \mathcal{P} from p to q passing through a sequence of cells $\mathcal{C}_{i_1j_1}, \mathcal{C}_{i_2j_2}, \dots, \mathcal{C}_{i_kj_k}$ ($k \geq 1$), such that $(i_1, j_1) = (i, j)$, $(i_k, j_k) = (i', j')$, and $\mathcal{P} \cap \mathcal{C}_{i_tj_t}$ is a line segment whose slope is $\text{minSlope}_{i_tj_t}$, for all $1 \leq t \leq k$. The *max projection* of a point p is defined analogously.

Lemma 7 *Using $O(n)$ preprocessing time and space, we can build a data structure that for any point $p \in \mathcal{B}_{n \times m}$ and any edge e of $\mathcal{B}_{n \times m}$, determines in $O(1)$ time if the min (or the max) projection of p onto the line containing e lies before, after, or on e ; and in the latter case, computes the exact projection of p onto e in constant time.*

Proof: Suppose, w.l.o.g., that e is a vertical edge of $\mathcal{B}_{n \times m}$, corresponding to a vertex $P(i)$ of P and a segment $Q(j-1)Q(j)$ of Q . Then $e = \{i\} \times [j-1, j]$. Let q be the min projection of p on the line $x = i$. Let $p = (p_x, p_y)$ and $q = (q_x, q_y)$. The path

connecting p to q in the definition of the min projection has slope minSlope_{ij} in each cell \mathcal{C}_{ij} it passes through. Such a path corresponds to the traversals of two point objects $\bar{\mathcal{O}}_P$ and $\bar{\mathcal{O}}_Q$, where $\bar{\mathcal{O}}_P$ traverses $[p_x, q_x]$ with its maximum permissible speed, and $\bar{\mathcal{O}}_Q$ traverses $[p_y, q_y]$ with its minimum permissible speed. Since each of the point objects $\bar{\mathcal{O}}_P$ and $\bar{\mathcal{O}}_Q$ can traverse $O(n)$ segments, computing the min projection can be easily done in $O(n)$ time. However, we can speedup the computation using a simple table lookup technique. For $\bar{\mathcal{O}}_P$, we keep two arrays T_{\min}^P and T_{\max}^P of size n , where for each $i \in \{1, \dots, n\}$, $T_{\min}^P[i]$ (resp., $T_{\max}^P[i]$) represents the minimum (resp., maximum) time needed for $\bar{\mathcal{O}}_P$ to traverse the interval $[0, i]$. Similarly, we keep two arrays T_{\min}^Q and T_{\max}^Q for $\bar{\mathcal{O}}_Q$. These four tables can be easily constructed in $O(n)$ time. To find time t needed for $\bar{\mathcal{O}}_P$ to traverse $[p_x, q_x]$ with its maximum speed, we do the following: we first lookup $a = T_{\max}^P[\lceil p_x \rceil]$ and $b = T_{\max}^P[q_x]$ in $O(1)$ time. Clearly, $b - a$ is equal to the time needed for $\bar{\mathcal{O}}_P$ to traverse $[\lceil p_x \rceil, q_x]$ (note that q_x is an integer). We also compute the time t' needed for $\bar{\mathcal{O}}_P$ to traverse $[p_x, \lceil p_x \rceil]$ directly from the length of the interval, and the maximum speed of $\bar{\mathcal{O}}_P$ in interval $[\lceil p_x \rceil - 1, \lceil p_x \rceil]$. Therefore, $t = t' + b - a$ can be computed in $O(1)$ time total. By similar table lookups, we compute the times t_1 and t_2 needed for $\bar{\mathcal{O}}_Q$ to traverse $[p_y, j - 1]$ and $[p_y, j]$, respectively, with its minimum speed. If $t_1 \leq t \leq t_2$, then we conclude that q_y lies in e , and we can easily compute its exact location on e by computing the distance that $\bar{\mathcal{O}}_Q$ traverses in $t - t_1$ time using its minimum speed on interval $[j - 1, j]$. Otherwise, we output that q is before or after e , depending on whether $t < t_1$ or $t > t_2$, all in $O(1)$ time. \square

Corollary 8 *If I' is an iterated projection of I , then I' can be computed from I in $O(1)$ time, after $O(n)$ preprocessing time.*

Proof: This is a direct corollary of Lemma 7 and the fact that if $I' = [a', b']$ is an iterated projection of $I = [a, b]$, then a' is the max projection of a , and b' is the min projection of b . \square

The Data Structure. The main data structure that we need in our algorithm is a dictionary for storing a sorted sequence of intervals. A balanced binary search

tree can be used for this purpose. Let T be the data structure that stores a sequence $\langle I_1, I_2, \dots, I_k \rangle$ of intervals in \prec order. We need the following operations to be supported by T .

SEARCH: Given a point x , find the leftmost interval I in T such that $x \leq \text{left}(I)$.

INSERT: Insert a new interval I into T , right before $T.\text{SEARCH}(\text{left}(I))$, or at the end of T if I is to the right of all existing intervals in T . In our algorithm, inserted intervals are not properly contained in any existing interval of T , and therefore, the resulting sequence is always sorted.

DELETE: Delete an existing interval I from T .

SPLIT: Given an interval $I = I_j$, $1 < j \leq k$, split T into two data structures T_1 and T_2 , containing $\langle I_1, \dots, I_{j-1} \rangle$ and $\langle I_j, \dots, I_k \rangle$, respectively.

JOIN: Given two data structures with interval sequences J_1 and J_2 , where each interval in J_1 is before any interval in J_2 , join the two structures to obtain a single structure T containing the concatenated sequence $J_1 \cdot J_2$.

It is straightforward to modify a standard balanced binary search tree to perform all the above operations in $O(\log |T|)$ time (for example, see Chapter 4 in [59]). Note that the exact coordinates of the interior intervals are not explicitly stored in the data structure. Rather, we compute the coordinates on the fly whenever a comparison is made, in $O(1)$ time per comparison, using Corollary 10.

The Algorithm. Let L_{ij}^T (resp., B_{ij}^T) denote the balanced search tree storing the sequence of reachable intervals on L_{ij} (resp., on B_{ij}). The reachable intervals stored in the trees are not necessarily disjoint. In particular, we allow interior intervals to have overlaps with each other, but not with boundary intervals. Moreover, the exact locations of the interior intervals are not explicitly stored. However, we maintain the invariant that each interior interval can be computed in $O(1)$ time, and that the

union of the reachable intervals stored in L_{ij}^T (resp., in B_{ij}^T) at each time is equal to $L_{ij}^{\mathcal{R}}$ (resp., $B_{ij}^{\mathcal{R}}$).

The overall structure of the algorithm is similar to that of Algorithm 1. We process the cells in cell-wise order, and propagate the reachability information through each cell by projecting the reachable intervals from the entry side to the exit side. However, to get a better performance, cells are processed in a slightly different manner, as presented in Algorithm 2. In this algorithm, $\text{exit}(\mathcal{C}_{ij})$ is considered as a single line segment whose points are ordered by \prec relation. For a set S of intervals, we define $U(S) = \bigcup_{I \in S} I$. Given a data structure T as defined in the previous subsection, we use T to refer to both the data structure and the set of intervals stored in T . Given a point set S on a line, by an interval (or a segment) of S we mean a maximal continuous subset of points contained in S .

Algorithm 4 IMPROVED DECISION ALGORITHM

- 1: Compute the free space, \mathcal{F}_ε
 - 2: **for** $i \in \{0, \dots, n\}$ **do** $L_{i,0}^T = \emptyset$
 - 3: **for** $j \in \{0, \dots, m\}$ **do** $B_{0,j}^T = \emptyset$
 - 4: $L_{0,0}^T.\text{INSERT}([o, o])$ where $o = (0, 0)$
 - 5: **for** $i = 0$ to n **do**
 - 6: **for** $j = 0$ to m **do**
 - 7: $T = \text{JOIN}(L_{ij}^T, B_{ij}^T)$
 - 8: Project T to the exit side of \mathcal{C}_{ij}
 - 9: $S = \{I \in T \mid I \not\subseteq B_{i,j+1}^{\mathcal{F}}$ and $I \not\subseteq L_{i+1,j}^{\mathcal{F}}\}$
 - 10: **for each** $I \in S$ **do** $T.\text{DELETE}(I)$
 - 11: $(B_{i,j+1}^T, L_{i+1,j}^T) = T.\text{SPLIT}(T.\text{SEARCH}((i, j)))$
 - 12: **for each** $I \subseteq (U(S) \cap B_{i,j+1}^{\mathcal{F}})$ **do** $B_{i,j+1}^T.\text{INSERT}(I)$
 - 13: **for each** $I \subseteq (U(S) \cap L_{i+1,j}^{\mathcal{F}})$ **do** $L_{i+1,j}^T.\text{INSERT}(I)$
 - 14: Return YES if $(n, m) \in L_{n+1,m}^T$, NO otherwise.
-

The algorithm works as follows. We first compute \mathcal{F}_ε in Line 5. Lines 2–4 initializes

the data structures for the first row and the first column of $\mathcal{B}_{n \times m}$. Lines 5–13 process the cells in cell-wise order. For each cell \mathcal{C}_{ij} , Lines 7–13 propagate the reachability information through \mathcal{C}_{ij} by creating data structures $B_{i,j+1}^T$ and $L_{i+1,j}^T$ on the exit side of \mathcal{C}_{ij} , based on B_{ij}^T and L_{ij}^T , and the feasible intervals $B_{i,j+1}^{\mathcal{F}}$ and $L_{i+1,j}^{\mathcal{F}}$. In Line 7, a data structure T is obtained by joining the interval sequences in B_{ij}^T and L_{ij}^T . We then project T to the exit side of \mathcal{C}_{ij} in Line 8 by (virtually) transforming each interval $I \in T$ to an interval $\pi_{ij}(I)$ on $\text{exit}(\mathcal{C}_{ij})$. Since the projection preserves the relative order of intervals, by Observation 2, and we do not need to explicitly update the location of interior intervals on the exit side, the projection is simply done by copying T to the exit side of \mathcal{C}_{ij} (boundary intervals will be fixed later in Lines 12–13). Furthermore, since B_{ij}^T and L_{ij}^T are not needed afterwards in the algorithm, we do not actually duplicate T . Instead, we simply assign T to the exit side, without making a new copy. In Line 9, we determine a set S of intervals that are not completely contained in $B_{i,j+1}^{\mathcal{F}}$ or in $L_{i+1,j}^{\mathcal{F}}$. All such intervals are deleted from T in Line 10 (see Figure 3.5 for an illustration). The remaining intervals in T have no intersection with the corner point (i, j) . Therefore, we can easily split T in Line 11 into two disjoint data structures, $B_{i,j+1}^T$ and $L_{i+1,j}^T$, each corresponding to one edge of the exit side. In Lines 12–13 we insert the boundary intervals to $B_{i,j+1}^T$ and $L_{i+1,j}^T$, which are computed as those portions of $U(S)$ that lie inside \mathcal{F}_ε . Note that whenever a boundary interval I is inserted into a data structure, its coordinates are stored along with the interval. After processing all cells, the decision problem is easily answered in Line 14 of the algorithm by checking if the target point (n, m) is reachable.

Lemma 9 *After processing each cell \mathcal{C}_{ij} , the following statements hold true:*

- (i) *any interval inserted into $\text{exit}(\mathcal{C}_{ij})$ in Lines 12–13 is a boundary interval,*
- (ii) *each interior interval on $\text{exit}(\mathcal{C}_{ij})$ can be expressed as an iterated projection of a boundary interval.*

Proof: (i) This is easily shown by observing that no interior interval is added to S in Line 9, and therefore, $U(S)$ cannot completely contain any interior interval. (ii)

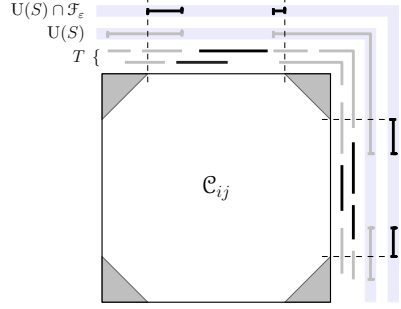


Figure 3.5. An example of the execution of Algorithm 2 on a cell \mathcal{C}_{ij} . The intervals of $S \subseteq T$ are shown in gray. The black intervals in T represent the interior intervals. The intervals in $U(S) \cap \mathcal{F}_\varepsilon$ are boundary intervals which are inserted in Lines 12–13.

The proof is by induction on the cells in cell-wise order. Let I be an interior interval on $\text{exit}(\mathcal{C}_{ij})$. Then, I is a direct projection of an interval $I' \subseteq \text{entry}(\mathcal{C}_{ij})$ obtained in Line 8. If I' is a boundary interval, then we are done. Otherwise, I' is an interior interval, and therefore, it is by induction an iterated projection of another boundary interval I'' . Since $I = \pi_{ij}(I')$ and $I' \subseteq \text{entry}(\mathcal{C}_{ij})$, I is in turn an iterated projection of I'' . \square

Corollary 10 *After processing each cell \mathcal{C}_{ij} , the exact location of each reachable interval on $\text{exit}(\mathcal{C}_{ij})$ is accessible in $O(1)$ time.*

Proof: Fix a reachable interval I on $\text{exit}(\mathcal{C}_{ij})$. If I is a boundary interval, then by Lemma 9(i), it is inserted into a data structure by Lines 12–13, and hence, its coordinates are stored in the data structure upon insertion. If I is an interior interval, then by Lemma 9(ii), it is an iterated projection of a boundary interval, and hence, its location can be computed in $O(1)$ time using Corollary 8. \square

Lemma 11 *After processing each cell \mathcal{C}_{ij} , $B_{i,j+1}^{\mathcal{R}} \cup L_{i+1,j}^{\mathcal{R}} = U(B_{i,j+1}^{\mathcal{T}} \cup L_{i+1,j}^{\mathcal{T}})$.*

Proof: We prove the statement by induction on the cells in cell-wise order. Recall from Section 3.2 (Algorithm 1) that $B_{i,j+1}^{\mathcal{R}} \cup L_{i+1,j}^{\mathcal{R}} = \pi_{ij}(L_{ij}^{\mathcal{R}} \cup B_{ij}^{\mathcal{R}}) \cap (B_{i,j+1}^{\mathcal{F}} \cup L_{i+1,j}^{\mathcal{F}})$. Therefore, it satisfies to show that $U(B_{i,j+1}^{\mathcal{T}} \cup L_{i+1,j}^{\mathcal{T}}) = \pi_{ij}(L_{ij}^{\mathcal{R}} \cup B_{ij}^{\mathcal{R}}) \cap (B_{i,j+1}^{\mathcal{F}} \cup L_{i+1,j}^{\mathcal{F}})$. By Line 7, $U(T) = U(L_{ij}^{\mathcal{T}} \cup B_{ij}^{\mathcal{T}})$. Let T_1 be the set of intervals in T right after the execution of Line 8, S be the set of intervals deleted in Line 10, N be the set of new

intervals inserted in Lines 12–13, and $T_2 = (T_1 \setminus S) \cup N$. Fix a point $p \in U(T_1)$, and let K be the set of intervals in T_1 containing p . We distinguish between two cases:

- $p \in \mathcal{F}_\varepsilon$: There are two possibilities: (1) $K \not\subseteq S$: Here, there is an interval in K that remains in T_1 after deletion of S in Line 10. Therefore, $p \in U(T_2)$. (2) $K \subseteq S$: Here, all intervals of K are removed in Line 10. However, since $p \in \mathcal{F}_\varepsilon$, there is an interval $I \in N$ such that $p \in I$. Therefore, after insertion of I in Lines 12–13, we have $p \in U(T_2)$.
- $p \notin \mathcal{F}_\varepsilon$: In this case, $K \subseteq S$, and hence $p \notin U(T_1 \setminus S)$. Moreover, no interval in N can contain p . Therefore, $p \notin U(T_2)$.

The above two cases together show that $U(T_2) = U(T_1) \cap \mathcal{F}_\varepsilon$. Note that, $U(T_1) = \pi_{ij}(U(L_{ij}^T \cup B_{ij}^T))$ (by Lines 7 and 8), and $T_2 = B_{i,j+1}^T \cup L_{i+1,j}^T$. Therefore, $U(B_{i,j+1}^T \cup L_{i+1,j}^T) = \pi_{ij}(U(L_{ij}^T \cup B_{ij}^T)) \cap (B_{i,j+1}^{\mathcal{F}} \cup L_{i+1,j}^{\mathcal{F}})$, which completes the proof, because $L_{ij}^{\mathcal{R}} \cup B_{ij}^{\mathcal{R}} = U(L_{ij}^T \cup B_{ij}^T)$ by induction. \square

Theorem 12 *Algorithm 4 solves the decision problem in $O(n^2 \log n)$ time.*

Proof: The correctness of the algorithm follows from Lemma 11, combined with Lemma 2. For the running time, we compute the number of operations needed to process each cell \mathcal{C}_{ij} in Lines 7–13. Let \mathcal{T} denote the time needed for each data structure operation. Line 7 needs one join operation that takes $O(\mathcal{T})$ time. Line 8 consists of a simple assignment taking only $O(1)$ time. To compute the subset S in Line 9, we start walking from the two sides of T , and add intervals to S until we reach the first intervals from both sides that do not belong to S . Moreover, we find the interval $I = T.\text{SEARCH}((i, j))$, and start walking around I in both directions until we find all consecutive intervals around I that lie in S (see Figure 3.5). To check if an interval lies in S or not, we need to compute the coordinates of the interval that can be done in $O(1)$ time. Therefore, computing S takes $O(|S| + \mathcal{T})$ time in total. Line 10 requires $|S|$ delete operation that takes $O(|S| \times \mathcal{T})$ time. Line 11 consists of a split operation taking $O(\mathcal{T})$ time. The set $U(S)$ used in Lines 12–13 can be

computed in $O(|S|)$ time by a linear scan over the set S . Since $U(S)$ consists of at most three segments (see Figure 3.5), computing $U(S) \cap \mathcal{F}_\varepsilon$ in Lines 12–13 takes constant time. Moreover, there are at most four insertion operations in Lines 12–13 to insert boundary intervals. Therefore, Lines 12–13 takes $O(|S| + \mathcal{T})$ time. Thus, letting $s_{ij} = |S|$, processing each cell \mathcal{C}_{ij} takes $O((s_{ij} + 1) \times \mathcal{T})$ time in total. Since at most four new intervals are created at each cell, the total number of intervals created over all cells is $O(n^2)$. Note that any of these $O(n^2)$ intervals can be deleted at most once, meaning that $\sum_{i,j} s_{ij} = O(n^2)$. Moreover, each comparison made in the data structures takes $O(1)$ time by Corollary 10, and hence, $\mathcal{T} = O(\log n)$. Therefore, the total running time of the algorithm is $O(\sum_{i,j} (s_{ij} + 1) \log n) = O(n^2 \log n)$. \square

3.4 Optimization Problem

In this section, we describe how our decision algorithm can be used to compute the exact value of the Fréchet distance with speed limits between two polygonal curves. Let $L_{ij}^{\mathcal{F}} = [a_{ij}, b_{ij}]$ and $B_{ij}^{\mathcal{F}} = [c_{ij}, d_{ij}]$. Notice that the free space, \mathcal{F}_ε , is an increasing function of ε . That is, for $\varepsilon_1 \leq \varepsilon_2$, we have $\mathcal{F}_{\varepsilon_1} \subseteq \mathcal{F}_{\varepsilon_2}$. It is not hard to see that:

Observation 3 *To find the exact value of $\delta = \delta_{\bar{F}}(P, Q)$, we can start from $\varepsilon = 0$, and continuously increase ε until we reach the first point at which \mathcal{F}_ε contains a slope-constrained path from $(0, 0)$ to (n, m) . This occurs at only one of the following “critical values”:*

- (A) *smallest ε for which $(0, 0) \in \mathcal{F}_\varepsilon$ or $(n, m) \in \mathcal{F}_\varepsilon$,*
- (B) *smallest ε at which $L_{ij}^{\mathcal{F}}$ or $B_{ij}^{\mathcal{F}}$ becomes non-empty for some pair (i, j) ,*
- (C) *smallest ε at which $b_{k\ell}$ is the min projection of a_{ij} , or d_{ij} is the max projection of $c_{k\ell}$, for some i, j, k , and ℓ .*

Notice that here type (A) and (B) of critical values are similar to the type (A) and (B) critical values in the standard Fréchet distance problem (see Section 2.1 on

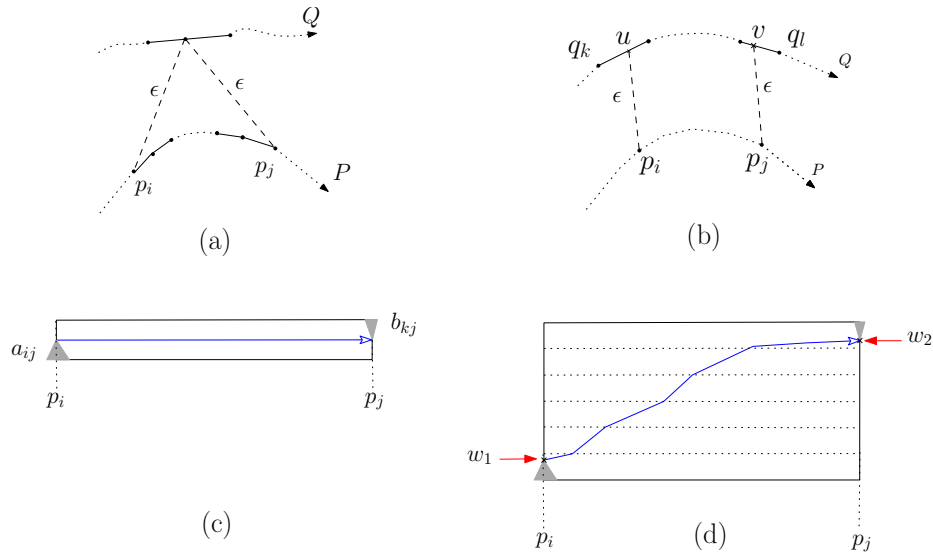


Figure 3.6. (a,c) Type (C) critical distances in the standard Fréchet distance problem vs. (b,d) type (C) critical distances in our instance of the problem.

Page 10). There are two critical distances of type (A) and $O(n^2)$ critical distance of type (B). All of these critical values can be computed in $O(n^2)$ time.

Here, type (C) critical distances are slightly different from those distances in the standard Fréchet distance problem. Figure 3.6 illustrates that difference. In the standard Fréchet problem, a type (C) critical distance corresponds to the common distance of two vertices of one curve to the intersection point of their bisector with an edge of the other curve (see Figure 3.6a). This happens when a new horizontal or vertical passage opens within the diagram (see Figure 3.6c). All type (C) critical values in the standard Fréchet distance problem can be computed in $O(n^3)$ time.

In our instance of the problem, computing type (C) critical distances has further complications. Those distances arise when a new slope-constrained path opens within \mathcal{F}_ϵ which consists of a sequence of min-slopes (or max-slopes) of the cells through which the path goes. If ϵ is reduced, this path will cease to exist (for an instance, see Figure 3.6d).

The geometric meaning of type (C) critical distances is as follows (see Figure 3.6b for an illustration). Consider two vertices p_i and p_j from P and let $t_{p_i p_j}$ denote the time it takes for \mathcal{O}_p to travel from p_i to p_j on P when the speed of \mathcal{O}_p on each

segment is its corresponding maximum allowed speed. Furthermore, let q_k and q_ℓ be two vertices of Q where q_ℓ is the first vertex after q_k where $t_{p_i p_j} \leq t_{q_\ell q_k}$ (\mathcal{O}_Q walks always with minimum allowed speed assigned to the segments of Q). Now, let u and v be two points on Q , where:

- (a) u is before v on Q ,
- (b) both are located between q_k and q_ℓ ,
- (c) $\|u p_i\| = \|v p_j\|$,
- (d) and the time of travel from u to v is equal to $t_{p_i p_j}$.

Then, among all such pairs of points (u, v) , let (u_0, v_0) be the one which has the smallest distance. Since we are looking for the smallest distance where slope-constrained path opens up in the free-space diagram, $\|u_0 p_i\|$ is a critical distance of type (C).

Next, we show how to compute all type (C) critical distances. We first introduce a function, called COMPUTE-POTENTIAL-CHAINS(R, t) provided in Algorithm 5. Input to that function consists of a curve R and a fixed time $t \neq 0$. The function computes a set A which includes all the subcurves of R from vertex r_i to vertex r_j , $i < j$, where r_j is the first vertex after r_i such that $t \leq t_{r_i r_j}$. Algorithm 5 accomplishes this by using two pointers, called μ_1 and μ_2 . At the start of the algorithm, μ_1 points to the first vertex and μ_2 points to the second vertex of R . Then R is scanned once to report the set A as described in Algorithm 5. In this algorithm, $chain_Q(\mu_1, \mu_2)$ means the polygonal chain of Q which starts at μ_1 and ends at μ_2 .

In Algorithm 6, we use the function stated in Algorithm 5 to compute all the critical distances of type (C), for two curves P and Q . For every pair of vertices p_i and p_j of P , we call function COMPUTE-POTENTIAL-CHAINS($Q, t_{p_i p_j}$) to compute subcurves α of Q which start at some vertex q_k and end at some vertex q_ℓ , $k < \ell$, such that q_ℓ is the first vertex after q_k where $t_{p_i p_j} \leq t_{q_k q_\ell}$. Then, for each curve α , we do the calculation in Line 4 to compute critical distances of type (C). We repeat the above for each pair of vertices q_i and q_j of Q and curve P , in Line 7. See Algorithm 6 for more details.

Lemma 13 *Algorithm 6 computes all critical values of type (C) in $O(n^3)$ total time.*

Algorithm 5 COMPUTE-POTENTIAL-CHAINS(R, t)

```

1:  $A = \emptyset$ 
2: Let  $(r_1, r_2, \dots, r_m)$  be the vertices of  $R$ 
3: if  $t \leq t_{r_1 r_m}$  then
4:    $i = 1, j = 2$ 
5:    $\mu_1 = r_i, \mu_2 = r_j$ 
6:   while  $\mu_1 \neq r_m$  do
7:     if  $t \leq t_{\mu_1 \mu_2}$  then
8:        $A = A \cup \text{chain}_Q(\mu_1, \mu_2)$ 
9:        $i = i + 1, \mu_1 = r_i$ 
10:    else
11:       $j = j + 1, \mu_2 = r_j$ 
12:  return  $A$ 

```

Proof: The correctness of Algorithm 6 follows from Observation 3 and the geometric nature of type (C) critical distances as described above.

Algorithm 6 calls the function stated as Algorithm 5, $O(n^2)$ times in Line 2. Thus, to prove the lemma, it is sufficient to show that the running time of Algorithm 5 is linear in the size of curve R .

Notice that the speed of travel on curve R in Algorithm 5 is equal to the minimum allowed speed assigned to each segment of R . Thus, using the same approach as in Lemma 7, after linear time preprocessing, we can compute, in constant time, the time of travel from a vertex to another one.

The loop in Line 6 terminates when pointer μ_1 reaches the last vertex of R . Notice that pointer μ_1 always moves forward in direction R and points to vertices of R one by one, in order. Also, pointer μ_2 always moves forward in direction R and is never before μ_1 . Therefore, with one linear scan, Algorithm 5 computes and returns set A .

Next, we show that the computation in Line 4 of Algorithm 6 can be done in $O(1)$ time. Let $e_1 = ab$ and $e_k = cd$ be the first and last edges of α (see Figure 3.7).

Algorithm 6 COMPUTE TYPE(C) CRITICAL DISTANCES

-
- 1: **for** each pair (p_i, p_j) , $0 \leq i < j \leq n$ **do**
 - 2: $A = \text{COMPUTE-POTENTIAL-CHAINS}(Q, t_{p_i p_j})$
 - 3: **for** each curve α in A **do**
 - 4: let (e_1, e_2, \dots, e_k) be the list of edges of α ,
 determine if there exists pairs of points $u \in e_1, v \in e_k$,
 such that $\|up_i\| = \|vp_j\|$ and $t_{uv} = t_{p_i p_j}$
 among all such pairs,
 add minimum of the distances $\|up_i\|$ to the critical distances of type (C).
 - 5: **for** each pair (q_i, q_j) , $0 \leq i < j \leq m$ **do**
 - 6: $A = \text{COMPUTE-POTENTIAL-CHAINS}(P, t_{q_i q_j})$
 - 7: Repeat Lines 3 and 4 for each curve α in A
-

Suppose that the coordinate of the points in that figure are:

$$a = (a_x, a_y), b = (b_x, b_y), c = (c_x, c_y), d = (d_x, d_y), p_i = (p_x, p_y), p_j = (q_x, q_y)$$

Then, any point u on segment \overline{ab} can be written as:

$$u = (b_x, b_y) + \frac{\|ub\|}{\|ab\|}(a_x - b_x, a_y - b_y)$$

and any point v on segment \overline{cd} can be written as:

$$v = (c_x, c_y) + \frac{\|cv\|}{\|cd\|}(d_x - c_x, d_y - c_y)$$

We are looking for pairs of points u and v such that:

$$\frac{\|p_i u\|^2}{v_{e_1}} + \frac{\|cv\|^2}{v_{e_k}} = t_{p_i p_j} - t_{bc}$$

Thus,

$$\begin{aligned} & (b_x - p_x + \frac{\|ub\|}{\|ab\|}(a_x - b_x))^2 + (b_y - p_y + \frac{\|ub\|}{\|ab\|}(a_y - b_y))^2 \\ & = \\ & (c_x - q_x + \frac{\|cv\|}{\|cd\|}(d_x - c_x))^2 + (c_y - q_y + \frac{\|cv\|}{\|cd\|}(d_y - c_y))^2 \end{aligned}$$

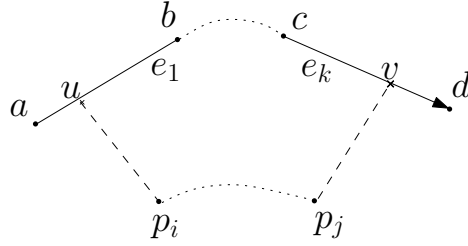


Figure 3.7. Proof of Lemma 13

$$\frac{\|ub\|}{v_{e_1}} + \frac{\|cv\|}{v_{e_k}} = t_{p_i p_j} - t_{bc}$$

Note that above equations can be solved in constant time. The following cases arise: (I) no such pair (u, v) is found, or (II) only one pair (u, v) is found. In this case, $\|up_i\|$ is a critical distance, or (III) more than one pairs of point (u, v) are found. In this case, we determine, in constant time, the pair (u_0, v_0) which has the minimum distance $\|u_0 p_i\| = \|v_0 p_j\|$ and then, $\|u_0 p_i\|$ is a critical distance of type (C). Hence, the running time of Algorithm 6 is $O(n^3)$.

□

Theorem 14 *The exact Fréchet distance with speed limits can be computed in $O(n^3 \log n)$ time.*

Proof: To find the exact value of $\delta_{\bar{F}}(P, Q)$, we first compute all $O(n^3)$ critical distances of type (A), (B) and (C), and then we sort them. After sorting these values, we do a binary search (equipped with our decision algorithm) to find the smallest ε for which $\delta_{\bar{F}}(P, Q) \leq \varepsilon$. In each search step, we solve the decision problem, if it has a positive answer, we continue with the half which contains smaller values. Otherwise, we continue with the half containing larger values. The running time is dominated by the time of sorting $O(n^3)$ values, which is $O(n^3 \log n)$. □

In the standard Fréchet distance problem, parametric search based approach is used to compute the exact value of Fréchet distance. Next, we outline that approach and show that we cannot apply it to our instance of the problem.

Alt and Godau [8] observed that any comparison-based sorting algorithm that sorts a_{ij} , b_{ij} , c_{ij} , and d_{ij} (defined as functions of ε) has critical values that include those of type (C). This is because the critical values of type (C) in the standard Fréchet distance problem occur if $a_{ij} = b_{kj}$ or $c_{ij} = d_{ik}$, for some i, j , and k . Therefore, to compute type (C) critical values, they used parametric search technique as follows. First, compute all critical values of types (A) and (B), sort them and then, perform binary search, and find two consecutive values ε_1 and ε_2 such that $\delta_F \in [\varepsilon_1, \varepsilon_2]$. Let S be the set of endpoints $a_{ij}, b_{ij}, c_{ij}, d_{ij}$ of intervals $L_{ij}^{\mathcal{F}}$ and $B_{ij}^{\mathcal{F}}$ that are nonempty for $\varepsilon \in [\varepsilon_1, \varepsilon_2]$. Then, Alt and Godau [8] used Cole's parametric search method [27] based on sorting the values in S to find the exact value of δ_F . Set S consists of $O(n^2)$ polynomial functions $f_1(\varepsilon) = a_{ij}, f_2(\varepsilon) = b_{kj}, f_3(\varepsilon) = c_{ij}, \dots$ of ε . The values of these functions at δ will be given to a sorting network consists of parallel processors to get sorted (see Figure 3.8). The crucial requirement here is that at each stage, the transitivity of comparisons must hold, i.e., $f_1(\delta) \leq f_2(\delta)$ and $f_2(\delta) \leq f_4(\delta)$, implies that $f_1(\delta) \leq f_4(\delta)$.

That is not the case in our instance of the problem because of the speed limit constraints. Here, the critical values of type (C) occur if $b_{kl} = a_{ij} + K_{ijkl}$ or $d_{ij} = c_{kl} + K'_{ijkl}$, for some i, j, k , and ℓ . Although K_{ijkl} or K'_{ijkl} can be computed in $O(1)$ time using Lemma 7, their value depends on i, j, k and ℓ .

Suppose that we use parametric search here. Assume that in the first stage of parallel sorting, a processor compares e.g. $f_{kl}(\delta)$ with $f_{ij}(\delta) + K_{ijkl}$. Let $f_{ij}(\delta) + K_{ijkl} < f_{kl}(\delta)$. Furthermore, assume that another processor compares e.g. $f_{gh}(\delta)$ with $f_{ef}(\delta) + K'_{efgh}$. Let $f_{gh}(\delta) < f_{ef}(\delta) + K'_{efgh}$. Then, assume in the next stage, $f_{kl}(\delta)$ is compared with $f_{ef}(\delta) + K''_{klef}$ and let $f_{ef}(\delta) + K''_{klef} < f_{kl}(\delta)$. Unlike in the case of standard Fréchet distance problem, we cannot conclude that $f_{gh}(\delta) < f_{kl}(\delta)$ by transitivity since another K'''_{ghkl} affects the comparison. Therefore, it seems unlikely that we can apply the parametric search technique to compute $\delta_{\bar{F}}(P, Q)$, as pointed out by Alt [4].

Recently, in [41], a randomized algorithm is introduced that computes the Fréchet distance between two polygonal curves in $O(n^2 \log n)$ time with high probability,

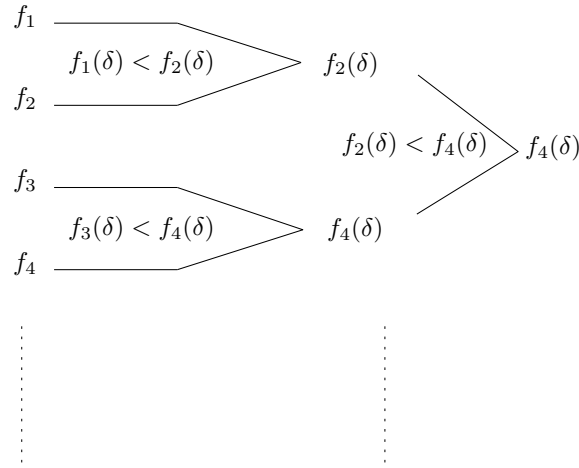


Figure 3.8. Transitivity of comparisons must be kept during stages of parallel sorting in parametric search

without using parametric search. The key observation used in their algorithm is that given a distance interval $I = [a, b]$, one can find all type (C) critical distances in I in $O((n^2 + k) \log n)$ time, where k is number of these distances in range I . They use a sweep line algorithm to achieve that running time. In our instance of the problem, we have additional speed constraints, which makes it hard to adopt the approach in [41] to get a faster running time. To be more precise, consider the following sub-problem:

Suppose a curve Q , a time t , a distance interval $I = [a, b]$ and two vertices p_i and p_j from curve P are given. Also assume that the object on Q always walks with minimum speed associated to each edge. Now find all pairs of points u and v on Q which satisfy the conditions:

(I) $\|p_i, u\| = \|p_j, v\| = d$, (II) $a \leq d \leq b$, and (III) time of travel from u to v on Q is t . It is unclear how to find such pairs efficiently.

3.5 Conclusions

In this chapter, we introduced a variant of the Fréchet distance between two polygonal curves in which the speed of traversal along each segment of the curves is restricted to be within a specified range. We presented an efficient algorithm to solve the decision problem in $O(n^2 \log n)$ time. This led to a $O(n^3 \log n)$ time algorithm for finding the

exact value of the Fréchet distance with speed limits.

Several open problems arise from our work. In particular, it is interesting to consider speed limits in other variants of the Fréchet distance studied in the literature. In the next chapter, we will study the same problem in the case where two curves lie inside a simple polygon. Our result can be also useful in matching planar maps, where the objective is to find a curve in a road network that is as close as possible to a vehicle trajectory. In [7], the traditional Fréchet metric is used to match a trajectory to a road network. If the road network is very congested, the Fréchet distance with speed limits introduced here seems to find a more realistic path in the road network, close to the trajectory of the vehicle. It is also interesting to extend our variant of the Fréchet distance to the setting where the speed limits on the segments of the curves change as functions over time.

Preliminary results of this chapter are presented in the 21st Canadian Conference on Computational Geometry [46]. The full version of the paper is published in the special issue of Computational Geometry - Theory and Application [48]. Alt [4] pointed out that due to the restrictions imposed by speed constraints, parametric search is not applicable. It remains open whether there exists an algorithm that can solve the optimization problem faster than $O(n^3 \log n)$ time.

Chapter 4

Speed-constrained Geodesic Fréchet Distance

4.1 Introduction

Several variants of the Fréchet distance have been studied in the literature. Cook and Wenk [28] studied the geodesic Fréchet distance inside a simple polygon. In this variant, the leash is constrained to the interior of a simple polygon. Therefore, a *geodesic* distance is used to measure the length of the leash, which is the length of the shortest path inside the polygon connecting the two endpoints of the leash. In [28], it is shown that the geodesic Fréchet distance between two polygonal curves of size n inside a simple polygon of size k can be computed in $O(n^2 \log(kn) \log n + k)$ expected time and $O(n^2 + k)$ space.

In Chapter 3, we introduced a generalization of the Fréchet distance, in which users are allowed to set speed limits on each segment. We showed that for two polygonal curves of size n with speed limits assigned to their segments, the speed-constrained Fréchet distance can be computed in $O(n^2 \log^2 n)$ time and $O(n^2)$ space. Note that in the problem instance of that chapter, there is no restriction for the leash to stay inside a simple polygon and thus, the leash lengths are measured using the Euclidean distance.

In this chapter, we study the speed-constrained geodesic Fréchet distance inside a simple polygon which is a simultaneous generalization of both Fréchet distances studied in [28] and in the previous chapter. The decision version of the problem is formulated as follows: Let P and Q be two polygonal curves inside a simple polygon, with minimum and maximum permissible speeds assigned to each segment of P and Q . For a given $\varepsilon \geq 0$, can two point objects traverse P and Q with permissible speeds (without backtracking) and, throughout the entire traversal, remain at geodesic distance at most ε from each other? The objective in the optimization problem is to find the smallest such ε .

We show that the decision version of the speed-constrained geodesic Fréchet distance problem can be solved in $O(n^2(k+n))$ time and $O(n^2+k)$ space, where n is the number of segments in the curves, and k is the complexity of the simple polygon. This leads to a solution to the optimization problem in $O(kn^3)$ time.

Algorithms for computing various variants of the Fréchet distance are typically based on computing a free-space diagram consisting of $O(n^2)$ cells, as we have seen in Chapters 2 and 3, and then propagating the reachability information one by one through the cells. While we adopt this general approach, the construction of the free-space diagram is more challenging in our problem as we need to compute the whole free space inside each cell. This is in contrast to other variants that only need to compute the free space on the boundaries of the cells. A main contribution of our work is thus to fully describe the structure of the free space inside a cell, establish its complexity, and show how it can be computed efficiently. Propagating the reachability information through the cells is also more challenging in our problem compared to the previous ones in previous chapters, as here, the shape of the free space inside a cell can substantially affect the projection of the reachable intervals on its boundaries.

4.2 Preliminaries

A *polygonal curve* in \mathbb{R}^d is a continuous function $P : [0, n] \rightarrow \mathbb{R}^d$ with $n \in \mathbb{N}$, such that for each $i \in \{0, \dots, n-1\}$, the restriction of P to the interval $[i, i+1]$ is affine (i.e., forms a line segment). The integer n is called the *length* of P . Moreover, the sequence $P(0), \dots, P(n)$ represents the set of *vertices* of P . For each $i \in \{1, \dots, n\}$, we denote the line segment $P(i-1)P(i)$ by P_i . Given a simple polygon K and two points $p, q \in K$, the *geodesic distance* of p and q with respect to K , denoted by $d_K(p, q)$, is defined as the length of the shortest path between p and q that lies completely inside K .

Speed-constrained geodesic Fréchet distance. Let P be a polygonal curve such that assigned to each segment S of P , there is a pair of non-negative real numbers $(v_{\min}(S), v_{\max}(S))$ specifying the minimum and the maximum permissible speed for

moving along S . We define a *speed-constrained parametrization* of P to be a continuous surjective function $f : [0, T] \rightarrow [0, n]$ with $T > 0$ such that for any $i \in \{1, \dots, n\}$, the slope of f at all points $t \in [f^{-1}(i-1), f^{-1}(i)]$ is within $[\bar{v}_{\min}(P_i), \bar{v}_{\max}(P_i)]$, where $\bar{v}_{\min}(S) = v_{\min}(S)/\|S\|$ and $\bar{v}_{\max}(S) = v_{\max}(S)/\|S\|$.

Given a simple polygon K and two polygonal curves P and Q inside K of lengths n and m respectively with speed limits assigned to their segments, the *speed-constrained geodesic Fréchet distance* of P and Q inside K is defined as

$$\delta_{\bar{F}}(P, Q) = \inf_{\alpha, \beta} \max_{t \in [0, T]} d_K(P(\alpha(t)), Q(\beta(t))),$$

where $\alpha : [0, T] \rightarrow [0, n]$ ranges over all speed-constrained parametrizations of P and $\beta : [0, T] \rightarrow [0, m]$ ranges over all speed-constrained parametrizations of Q .

Free-space diagram. Let $\mathcal{B}_{n \times m} = [0, n] \times [0, m]$ be a n by m rectangle in the plane. Each point $(s, t) \in \mathcal{B}_{n \times m}$ uniquely represents a pair of points $(P(s), Q(t))$ on the polygonal curves P and Q . We decompose $\mathcal{B}_{n \times m}$ into $n \times m$ unit grid cells $\mathcal{C}_{ij} = [i-1, i] \times [j-1, j]$ for $(i, j) \in \{1, \dots, n\} \times \{1, \dots, m\}$, where each cell \mathcal{C}_{ij} corresponds to a segment P_i on P and a segment Q_j on Q . Given two polygonal curves P and Q inside a simple polygon K and a parameter $\varepsilon \geq 0$, the *free space* \mathcal{F}_ε is defined as $\mathcal{F}_\varepsilon = \{(s, t) \in \mathcal{B}_{n \times m} \mid d_K(P(s), Q(t)) \leq \varepsilon\}$. We denote by L_{ij} (resp., by B_{ij}) the left (resp., bottom) line segment bounding \mathcal{C}_{ij} . The *entry side* of \mathcal{C}_{ij} is defined as $\text{entry}(\mathcal{C}_{ij}) = L_{ij} \cup B_{ij}$, and its *exit side* as $\text{exit}(\mathcal{C}_{ij}) = B_{i,j+1} \cup L_{i+1,j}$. Given two points p and q on the boundary of a cell, we say that p is *before* q , denoted by $p \prec q$, if either $p_x < q_x$ or $(p_x = q_x \text{ and } p_y > q_y)$.

Hourglass data structure. Fix a simple polygon K . Given two points $p, q \in K$, we denote by $\pi(p, q)$ the shortest path between p and q that lies inside K , and denote its length by $\|\pi(p, q)\|$. Let \overline{ab} and \overline{cd} be two line segments inside K . The *hourglass* $\mathcal{H}_{\overline{ab}, \overline{cd}}$ is defined as the maximal region bounded by the segments \overline{ab} and \overline{cd} , and the shortest path chains $\pi(a, c)$, $\pi(a, d)$, $\pi(b, c)$ and $\pi(b, d)$. Three examples of hourglasses are illustrated in Figure 4.1. (See [39] for applications of the hourglass.) Note that for any two points $p \in \overline{ab}$ and $q \in \overline{cd}$, the shortest path $\pi(p, q)$ is contained in $\mathcal{H}_{\overline{ab}, \overline{cd}}$.

The intersection of $\mathcal{H}_{\overline{ab},\overline{cd}}$ and the boundary of K consists of at most four polygonal curves, each of which is called a *chain* of $\mathcal{H}_{\overline{ab},\overline{cd}}$.

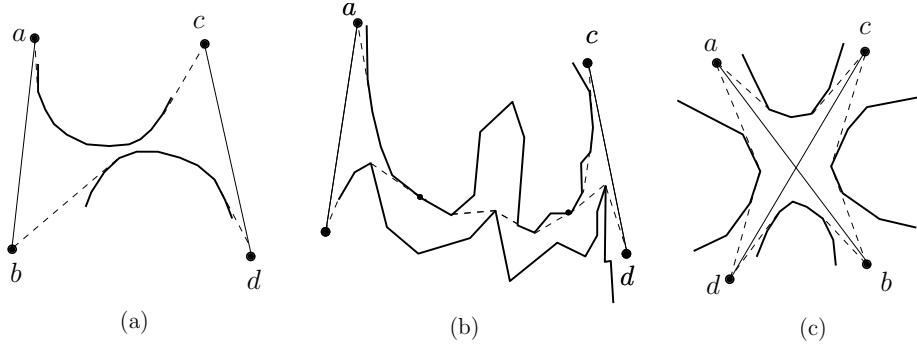


Figure 4.1. (a) An open hourglass (b) A closed hourglass (c) An intersecting hourglass.

4.3 Computing the Free Space Inside a Cell

In the classical Fréchet distance problem (Section 2.1), the free space inside each cell is convex and can be determined in $O(1)$ time. When distances are geodesic, the free space is not necessarily convex, but it is still connected and xy -monotone (see [28] for the proof).

Therefore, to solve the geodesic Fréchet distance (without speed limits), one only needs to compute the free space on the boundaries of the cells. In [28], A. Cook *et al.* show how to compute the boundary of a cell in $O(\log k)$ time after $O(k)$ time preprocessing, based on the algorithm of Guibas and Hershberger [39]. Also, one could use Chambers *et al.*'s approach in [23], to compute the boundary of the cells in $O(\log k)$ time. In contrast to above works, in our generalized version where motion speeds are limited, we need to compute the full description of the free space in the interior of the cells as well in order to propagate the reachability information correctly.

We use the hourglass data structure to compute the boundary of the free space inside a cell. Consider an hourglass $\mathcal{H}_{\overline{ab},\overline{cd}}$ and two points $p \in \overline{ab}$ and $q \in \overline{cd}$. The shortest path $\pi(p, q)$ is either a straight segment (in case p and q see each other), or consists of two tangents from p and q to the chains of $\mathcal{H}_{\overline{ab},\overline{cd}}$ plus a subpath between

the two tangent points. We denote this subpath by $\sigma(p, q)$. Note that $\sigma(p, q)$ consists of a sequence of vertices of K , lying on at most two chains of the hourglass.

Definition 1 Consider an hourglass $\mathcal{H}_{\overline{ab}, \overline{cd}}$ and two intervals $\overline{a'b'} \subseteq \overline{ab}$ and $\overline{c'd'} \subseteq \overline{cd}$, so that for any $p \in \overline{a'b'}$ and any $q \in \overline{c'd'}$, $\sigma(p, q)$ is the same. The region bounded by the intervals $\overline{a'b'}$ and $\overline{c'd'}$ and the paths $\pi(a', c')$ and $\pi(b', d')$ is called a butterfly, and is denoted by $\mathcal{B}_{\overline{a'b'}, \overline{c'd'}}$ (see Figure 4.2).

Lemma 15 Given a butterfly $\mathcal{B}_{\overline{a'b'}, \overline{c'd'}}$, the function $f(p, q) = \|\pi(p, q)\|$ over the domain $[a', b'] \times [c', d']$ is a hyperbolic surface.

Proof: Fix a point $p \in \overline{a'b'}$ and a point $q \in \overline{c'd'}$. Let k_1 and k_2 be the two endpoints of $\sigma(p, q)$. Then $\|\pi(p, q)\| = \|pk_1\| + \|\sigma(p, q)\| + \|k_2q\|$. By the butterfly property, k_1 , k_2 , and $\|\sigma(p, q)\|$ are fixed for all p and q in the domain. Therefore, $\|\pi(p, q)\|$ is the sum of two L_2 distances plus a constant, which forms a hyperbolic surface. \square

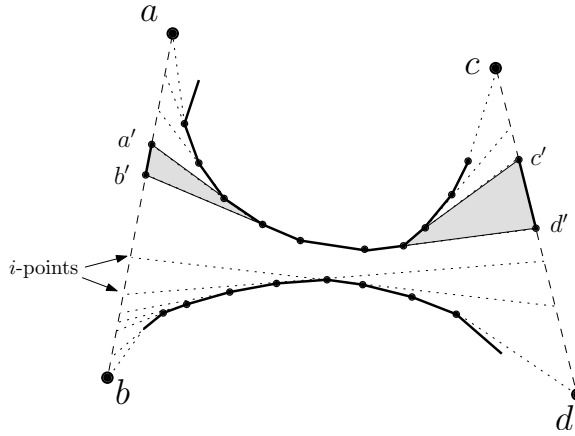


Figure 4.2. An hourglass $\mathcal{H}_{\overline{ab}, \overline{cd}}$ with a butterfly $\mathcal{B}_{\overline{a'b'}, \overline{c'd'}}$.

Consider an edge e on a chain of the hourglass $\mathcal{H}_{\overline{ab}, \overline{cd}}$. Extend e to a line and find its intersection with \overline{ab} and \overline{cd} (as shown in Figure 4.2). We call such an intersection point an *i-point*. Note that the number of *i-points* on each of the segments \overline{ab} and \overline{cd} is $O(k)$.

Observation 4 *Any two consecutive i -points $i_1, i_2 \in \overline{ab}$ and any two consecutive i -points $j_1, j_2 \in \overline{cd}$ form a butterfly $\mathcal{B}_{\overline{i_1 i_2}, \overline{j_1 j_2}}$.*

Consider two polygonal curves P and Q inside K . Let $P_i = \overline{ab}$ be a segment of P , and $Q_j = \overline{cd}$ be a segment of Q . By dividing \overline{ab} and \overline{cd} at i -points, the corresponding cell \mathcal{C}_{ij} in the free-space diagram is decomposed into $O(k^2)$ subcells, where each subcell corresponds to a butterfly (see Figure 4.3).

Let $f(p, q) = \|\pi(p, q)\|$ be a function defined over all $(p, q) \in [a, b] \times [c, d]$. The intersection of the plane $z = \varepsilon$ with the function f determines the boundary of \mathcal{F}_ε inside the cell \mathcal{C}_{ij} . The boundary of \mathcal{F}_ε crosses the boundary of each subcell in at most two points, each of which is called a c -point. The following two lemmas describe the structure of the free space inside \mathcal{C}_{ij} .

Lemma 16 *Any two consecutive c -points on the boundary of \mathcal{F}_ε are connected with a hyperbolic arc, and the line segment connecting the two endpoints of the arc lies completely inside \mathcal{F}_ε .*

Proof: This follows from Lemma 15. □

Lemma 17 *The number of c -points inside a cell is $O(k)$.*

Proof: This follows from the fact that any xy -monotone curve intersecting an $n \times m$ (non-uniform) grid can cross at most $2(n + m)$ cells of the grid. □

Computing c -points. Let \overleftrightarrow{cd} denote the line as a result of extending line segment \overline{cd} . Our algorithm for computing c -points is based on the following observation.

Observation 5 *Consider an hourglass $\mathcal{H}_{\overline{ab}, \overline{cd}}$ and a fixed $\varepsilon > 0$. Let p be a point moving on \overline{ab} , and let q be a point that moves on the line \overleftrightarrow{cd} to maintain geodesic distance ε from p . When p moves monotonically from a to b , q has at most one directional change along \overleftrightarrow{cd} .*

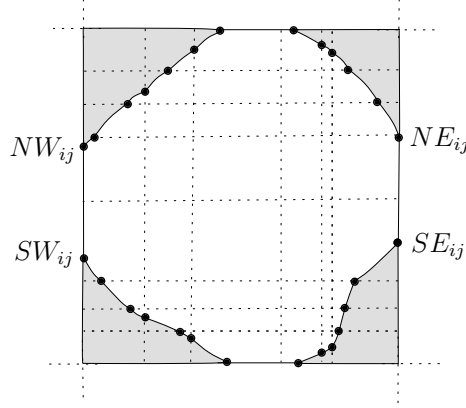


Figure 4.3. The free space inside a cell.

Observation 5 enables us to compute all c -points inside a cell by two linear walks. Details are provided in Algorithm 7. In this algorithm, h_c refers to a point on \overline{ab} which is closest to c , $p_1 \prec_{\overrightarrow{ab}} p_2$ means that p_1 is before p_2 in direction \overrightarrow{ab} , and $F(p, q)$ refers to the unique point in the free-space diagram corresponding to a point $p \in P$ and $q \in Q$. The output of the algorithm is four connected c -point chains as depicted in Figure 4.3.

Algorithm 7 COMPUTING C-POINTS INSIDE A CELL

Input: An hourglass $\mathcal{H}_{\overline{ab}, \overline{cd}}$ corresponding to a cell \mathcal{C}_{ij} and a fixed $\varepsilon > 0$.

- 1: Compute i -points on \overline{ab} and \overline{cd} .
 - 2: Find $q_1, q_2 \in \overleftarrow{cd}$ s.t. $\|\pi(a, q_1)\| = \|\pi(a, q_2)\| = \varepsilon$.
 - 3: Set $\eta_1 = q_1$ and $\eta_2 = q_2$, assuming that $q_1 \prec_{\overrightarrow{cd}} q_2$.
 - 4: Set $\mu = a$.
 - 5: **while** μ has not reached b **do**
 - 6: Move μ in direction \overrightarrow{ab} , and move η_1 on \overleftarrow{cd} s.t. $\|\pi(\mu, \eta_1)\| = \varepsilon$ until either μ or η_1 reaches an i -point.
 - 7: **if** $F(\mu, \eta_1) \in \mathcal{C}_{ij}$ **then**
 - 8: Insert $F(\mu, \eta_1)$ into SW_{ij} if $\mu \prec_{\overrightarrow{ab}} h_c$, otherwise insert $F(\mu, \eta_1)$ into NW_{ij} .
 - 9: Repeat lines 4–8 with η_2 instead of η_1 to obtain NE_{ij} and SE_{ij} .
 - 10: **return** $NW_{ij}, SW_{ij}, NE_{ij}$, and SE_{ij} .
-

4.4 The Decision Problem

In this section, we show how the decision version of our Fréchet distance problem can be solved efficiently. We use the notation of Chapter 3. A path $\mathcal{P} \subset \mathcal{B}_{n \times m}$ is called *slope-constrained* if for any point $(s, t) \in \mathcal{P} \cap \mathcal{C}_{ij}$, the slope of \mathcal{P} at (s, t) is within $\text{minSlope}_{ij} = \bar{v}_{\min}(Q_j)/\bar{v}_{\max}(P_i)$ and $\text{maxSlope}_{ij} = \bar{v}_{\max}(Q_j)/\bar{v}_{\min}(P_i)$. A point $(s, t) \in \mathcal{F}_\varepsilon$ is called *reachable* if there is a slope-constrained path from $(0, 0)$ to (s, t) in \mathcal{F}_ε . As shown in previous chapter, $\delta_{\bar{F}}(P, Q) \leq \varepsilon$ if and only if the point (n, m) is reachable.

Reachable points on the entry side of each cell form a set of $O(n^2)$ disjoint intervals, each of which is called a *reachable interval* (as in previous chapter). To decide if (n, m) is reachable, the general approach is to propagate the reachability information one by one, in row-major order, from $\mathcal{C}_{0,0}$ to \mathcal{C}_{nm} . The propagation in each cell \mathcal{C}_{ij} involves projecting the set of reachable intervals from the entry side of the cell to its exit side.

Since the free space inside a cell is not necessarily convex in our problem, the projection can be affected by the boundary of \mathcal{F}_ε inside a cell (see Figure 4.4). We use the c -point information computed in the previous section to compute projections. Indeed, only c -points on the convex hull of NW_{ij} and SE_{ij} are needed to compute correct projections. Since c -points inside each chain are stored in a sorted x (and y) order, the convex hull of the chains can be computed using a Graham scan in $O(k)$ time. We call the convex hull of NW_{ij} (resp., SE_{ij}) the *left chain* (resp., the *right chain*) of \mathcal{C}_{ij} .

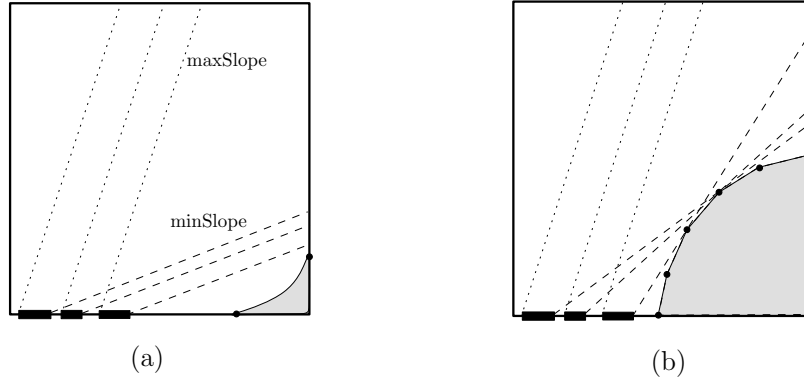
Given a point $p \in \text{entry}(\mathcal{C}_{ij})$, Algorithm 8 computes the projection of p onto $\text{exit}(\mathcal{C}_{ij})$ in $O(\log k)$ time.

Lemma 18 *Given a point $p \in \text{entry}(\mathcal{C}_{ij})$, Algorithm 8 computes the projection of p onto $\text{exit}(\mathcal{C}_{ij})$ in $O(\log k)$ time.*

Proof: Finding each of the two tangents in Line 1 takes $O(\log k)$ time using binary search. The rest of the algorithm takes constant time. \square

Algorithm 8 PROJECTION FUNCTION**Input:** A point $p \in \text{entry}(\mathcal{C}_{ij})$

- 1: Let t_ℓ and t_r be tangents (if they exist) from p to the left and to the right chain of \mathcal{C}_{ij} , respectively.
- 2: Let a_1 and a_2 be the projection of p in directions t_ℓ and maxSlope_{ij} , respectively.
- 3: Let b_1 and b_2 be the projection of p in directions t_r and minSlope_{ij} , respectively.
- 4: **return** $[\max(a_1, a_2), \min(b_1, b_2)]$

**Figure 4.4.** Projecting reachable intervals inside cells with convex and non-convex interior.

Lemma 19 *Given a cell \mathcal{C}_{ij} with r_{ij} reachable intervals on its entry side, Algorithm 8 projects all the reachable intervals onto the exit side of \mathcal{C}_{ij} in $O(k + r_{ij})$ time.*

Proof: Let t_1 be a line in direction minSlope_{ij} tangent to the left chain of \mathcal{C}_{ij} , and let t_2 be a line in direction maxSlope_{ij} tangent to the right chain of \mathcal{C}_{ij} . Let a_1 and a_2 be the intersection points of t_1 and t_2 with $\text{entry}(\mathcal{C}_{ij})$, respectively. For any point $p \in \text{entry}(\mathcal{C}_{ij})$ that lies outside $[a_1, a_2]$, the projection of p is empty. Therefore, we delete those portions of reachable intervals that lie outside $[a_1, a_2]$. Now, the projection of each of the remaining intervals can be simply computed by projecting its two endpoints.

To avoid spending $O(\log k)$ time for projecting each endpoint, we use a cross-ranking technique. This reduces the total time needed for computing the tangents in Algorithm 8. Let T_1 be the list of all endpoints of the reachable intervals on $\text{entry}(\mathcal{C}_{ij})$

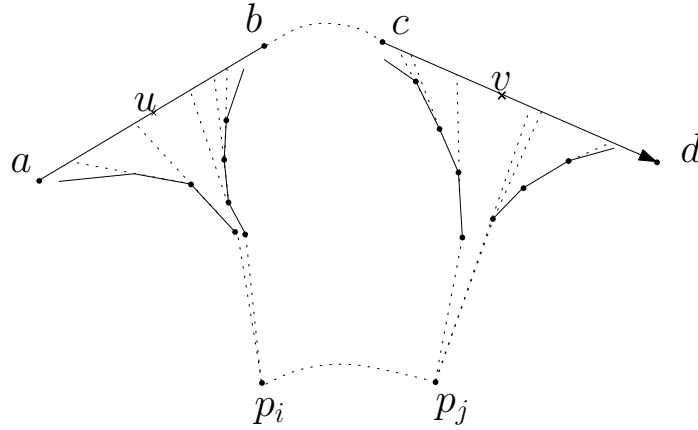


Figure 4.5. Proof of Theorem 20

in \prec order. We construct another list T_2 as follows. Perform an edge traversal of the right chain, starting with the rightmost edge. Each edge encountered is extended to a line until it intersects the entry side at a point which is then added to T_2 . We merge T_1 and T_2 (in \prec order) to create a list T . Each item in T has a pointer to its corresponding c -point or reachable interval endpoint, and vice versa. Moreover, each item in T which comes from T_1 keeps a pointer to its preceding item in T which comes from T_2 . Now, given a reachable interval endpoint p , to compute the tangent from p to the right chain, we simply find the item $t \in T$ corresponding to p , and then find the item in T_2 preceding t in T . This item uniquely determines the c -point at which the tangent from p to the right chain occurs. We process the left chain in the same way. This enables us to compute each tangent in constant time, after the cross-ranking step, leading to $O(k + r_{ij})$ total time for projecting all endpoints. \square

Combined with the fact that $\sum_{0 \leq i, j \leq n} r_{ij} = O(n^3)$ as in Chapter 3, the decision problem can be solved in $O(n^2(k + n))$ time and $O(n^2 + k)$ space.

Theorem 20 *The exact value of $\delta_{\bar{F}}(P, Q)$ between curves P and Q inside polygon K can be computed in $O(kn^3)$ time.*

Proof: We use the same technique as in Section 3.4 to compute $\delta_{\bar{F}}(P, Q)$. There are two critical distances of type (A) and $O(n^2)$ critical distances of type (B). Geodesic

distances inside a simple polygon are computed by the algorithms of Guibas and Hershberger [39, 42]. These algorithms preprocess the polygon in $O(k)$ so that the shortest path queries between two points or between a point and a line segment can be solved in $O(\log k)$ time. Thus, we can compute type (A) and type (B) distances in $O(n^2 \log k)$ time.

As in previous chapter, there are $O(n^3)$ critical distances of type (C). To compute them, we use Algorithm 6 on Page 53, after modifying Line 4 of that algorithm. For the case where P and Q are in the plane and distances are Euclidean, we showed that Line 4 can be done in $O(1)$ time in Lemma 13. Here, because distances are geodesic, the run-time is $O(k)$ as explained in the following.

In the algorithm of Guibas and Hershberger, all shortest paths between a point p_i and a line segment \overline{ab} are represented by a funnel, denoted by $\mathcal{F}_{p_i, \overline{ab}}$ (see Figure 4.5). $\mathcal{F}_{p_i, \overline{ab}}$ is the region bounded by the line segment \overline{ab} and the shortest path chains $\pi(p_i, a)$ and $\pi(p_i, b)$. Extend all line segments in the shortest path chains $\pi(p_i, a)$ and $\pi(p_j, b)$ of funnel $\mathcal{F}_{p_i, \overline{ab}}$ to a line, and find the intersection of those lines with \overline{ab} (see Figure 4.5). Do the same in funnel $\mathcal{F}_{p_j, \overline{cd}}$ with respect to segment \overline{cd} . Now, maintain the list of points which starts at a , the intersection points on \overline{ab} in order, and ends at b , in a list denoted by $L_{\overline{ab}}$. Similarly, compute $L_{\overline{cd}}$. Next, we create two lists $L'_{\overline{ab}}$ and $L'_{\overline{cd}}$ from lists $L_{\overline{ab}}$ and $L_{\overline{cd}}$ to apply the same technique in Algorithm 5 and then, compute critical distances of type (C) in Algorithm 6.

Let $L'_{\overline{ab}} = L_{\overline{ab}}$ and $L'_{\overline{cd}} = L_{\overline{cd}}$. For each point $u \in L_{\overline{ab}}$, compute distance $\|up_i\|$ and find point(s) v on \overline{cd} where $\|up_i\| = \|vp_j\|$, and insert v in $L'_{\overline{cd}}$. Likewise, for each point $v \in L_{\overline{cd}}$, compute distance $\|vp_j\|$ and find point(s) u on \overline{ab} where $\|up_i\| = \|vp_j\|$, and insert u in $L'_{\overline{ab}}$.

The run-time to create these two lists is $O(k)$ because the function which represent distances from a point to a line segment inside a polygon is a bitonic function. Therefore, distances from point p_i (resp., point p_j) to points in $L_{\overline{ab}}$ (resp., to points in $L_{\overline{cd}}$) are increasing or decreasing or bitonic. Thus, $L'_{\overline{ab}}$ and $L'_{\overline{cd}}$ can be computed in $O(k)$ time using the cross-ranking technique.

Having computed these two lists $L'_{\overline{ab}}$ and $L'_{\overline{cd}}$, we can then use two pointers as in

Algorithm 5 and by the same calculation described in Lemma 13, compute critical distances of type (C). Therefore, the run-time of Line 4 of Algorithm 6 is $O(k)$ in this case. Since that line is executed $O(n^3)$ times, type (C) critical distances can be computed in $O(kn^3)$ total time.

After computing all type (A), (B) and (C) critical distances, we sort them and then, we perform binary search equipped with our decision algorithm, to find the exact value of speed-constrained geodesic Fréchet distance. Hence, we obtain an $O(kn^3)$ time algorithm to compute $\delta_{\bar{F}}(P, Q)$ for two curves P and Q inside a simple polygon. \square

4.5 Conclusion

In this chapter, we introduced a variant of the Fréchet distance between two polygonal curves inside a simple polygon, in which the speed of traversal along each segment of the curves is restricted to be within a specified range.

We presented an algorithm that decides in $O(n^2(k+n))$ time whether the speed-constrained geodesic Fréchet distance between two polygonal curves inside a simple polygon is within a given value ε , where n is the number of segments in the curves, and k is the complexity of the polygon.

Several open problems arise from our work. In particular, it is interesting to consider speed limits in other variants of the Fréchet distance studied in the literature, such as the Fréchet distance between two curves lying on a convex polyhedron [52], or on a polyhedral surface [29].

Results of this chapter are presented in 22nd Canadian Conference on Computational Geometry [47].

Chapter 5

Improved Algorithms for Partial Curve Matching

5.1 Introduction

As described in Section 2.1, Alt and Godau [8] showed how the Fréchet distance between two polygonal curves with n and m vertices can be computed in $O(nm \log(nm))$ time. For their solution, they introduced the free-space diagram.

As discussed in Section 2.3, Alt and Godau [8] in their seminal work, studied the partial curve matching problem. Given two polygonal curves P and Q of size n and m , respectively, they presented an algorithm that decides in $O(nm \log(nm))$ time whether there is a subcurve R of P whose Fréchet distance to Q is at most ε , for a given $\varepsilon \geq 0$. Using parametric search, they solved the optimization problem of finding the minimum such ε in $O(nm \log^2(nm))$ time.

Later, Alt *et al.* [7] proposed a generalization of the partial curve matching problem to measure the similarity of a curve to some part of a graph. Given a polygonal curve P and a graph G , they presented an $O(nm \log m)$ -time algorithm to decide whether there is a path π in G whose Fréchet distance to P is at most ε , with n and m being the size of P and G , respectively. A variant of the partial curve matching in the presence of outliers is studied by Buchin *et al.* [20], leading to an algorithm with $O(nm(n+m) \log(nm))$ running time.

Our results. In this chapter, we present a simple data structure, which we call *free-space map*, that enables us to solve several variants of the Fréchet distance problem efficiently. The results we obtain using this data structure are summarized below. In the following, n and m represent the size of the two given polygonal curves P and Q , respectively, and $\varepsilon \geq 0$ is a fixed input parameter.

- *Partial curve matching.* Given two polygonal curves P and Q , we present an algorithm to decide in $O(nm)$ time whether there is a subcurve $R \subseteq P$ whose

Fréchet distance to Q is at most ε . This improves the best previous algorithm for this decision problem due to Alt and Godau [8] (described in Section 2.3), that requires $O(nm \log(nm))$ time. This also leads to an $O(\log(nm))$ faster algorithm for solving the optimization version of the problem, using parametric search.

- *Closed Fréchet metric.* As described in Section 2.2.7, Alt and Godau showed that for two closed curves P and Q , the decision problem of whether the closed Fréchet distance between P and Q (as defined in Section 5.4) is at most ε can be solved in $O(nm \log(nm))$ time. We improve this long-standing result by giving an algorithm that runs in $O(nm)$ time. As a result, we also improve by a $\log(nm)$ -factor the running time of the optimization algorithm for computing the minimum such ε .
- *Minimum/Maximum walk.* We introduce two new variants of the Fréchet distance as generalizations of the partial curve matching problem. Given two curves P and Q and a fixed $\varepsilon \geq 0$, the *maximum walk* problem asks for the maximum-length continuous subcurve of Q whose Fréchet distance to P is at most ε . We show that this optimization problem can be solved efficiently in $O(nm)$ time, without additional $\log(nm)$ factor. The *minimum walk* problem is analogously defined, and can be solved efficiently within the same time bound.
- *Graph matching.* Given a directed acyclic graph G with a straight-line embedding in \mathbb{R}^d , for fixed $d \geq 2$, we present an algorithm to decide in $O(nm)$ time whether a given curve P matches some part of G under a Fréchet distance of ε , with n and m being the size of P and G , respectively. This improves the map matching algorithm of Alt *et al.* [7] (described in Section 2.3.2) by an $O(\log m)$ factor for the particular case in which G is a directed acyclic graph.

The above improved results are obtained using a novel simple approach for propagating the reachability information “sequentially” from bottom side to the top side of

the free-space diagram. Our approach is different from and simpler than the divide-and-conquer approach used by Alt and Godau [8] (explained in Section 2.3), and also, than the approach taken by Alt *et al.* [7] (explained in Section 2.3) which is a mixture of line sweep, dynamic programming, and Dijkstra's algorithm.

The free-space map introduced in this thesis encapsulates all the information available in the standard free-space diagram, yet it is capable of answering a more general type of queries efficiently. Namely, for any query point on the bottom side of the free-space diagram, our data structure can efficiently report all points on the top side of the diagram which are reachable from that query point. Given that our data structure has the same size and construction time as the standard free-space diagram, it can be viewed as a powerful alternative or generalization.

The remainder of this chapter is organized as follows. In Section 5.2, we provide basic definitions and elementary algorithms, such as vertical ray shooting, which will be used in our construction. In Section 5.3, we define the free-space map and show how it can be efficiently constructed. In Section 5.4, we present some applications of the free-space map to problems such as partial curve matching, maximum/minimum walk, and closed Fréchet metric. In Section 5.5, we provide an improved algorithm for matching a curve in a DAG. We conclude in Section 5.6 with some open problems.

5.2 Preliminaries

Here, we borrow some notations from previous chapters. Given a parameter $\varepsilon \geq 0$, the *free space* of the two curves P and Q is defined as

$$\mathcal{F}_\varepsilon(P, Q) = \{(s, t) \in [0, n] \times [0, m] \mid \|P(s), Q(t)\| \leq \varepsilon\}.$$

We call points in $\mathcal{F}_\varepsilon(P, Q)$ *feasible*. The partition of the rectangle $[0, n] \times [0, m]$ into regions formed by feasible and infeasible points is called the *free-space diagram* of P and Q , denoted by $\mathcal{FD}_\varepsilon(P, Q)$ (see Figure 5.1.a).

Let P and Q be two polygonal curves of size n and m , respectively, and $\varepsilon \geq 0$ be a fixed parameter. Following the notation used by Alt *et al.* [7], we denote by \mathcal{FD}_j , for $0 \leq j \leq m$, the one-dimensional free-space diagram $\mathcal{FD}_\varepsilon(P, Q) \cap ([0, n] \times \{j\})$,

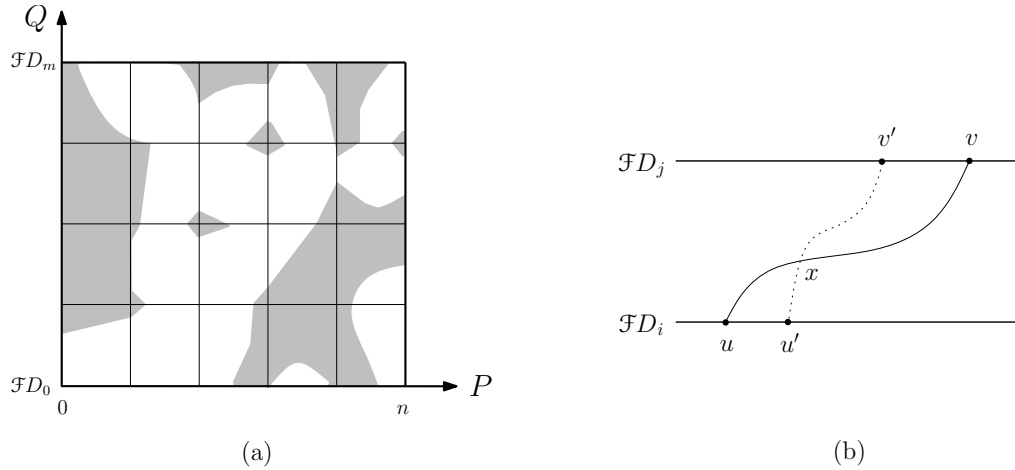


Figure 5.1. (a) An example of a free-space diagram. (b) Proof of the crossing lemma.

corresponding to the curve P and the point $Q(j)$. For each $(i, j) \in \{1 \cdots n\} \times \{1 \cdots m\}$, the intersection of the free-space diagram with the square $[i-1, i] \times [j-1, j]$ is called a *cell* of the diagram. Likewise, we call the intersection of \mathcal{FD}_j with each interval $[i-1, i]$ a cell (or more precisely, the i -th cell) of \mathcal{FD}_j .

A curve is called *feasible* if it lies completely within $\mathcal{F}_\varepsilon(P, Q)$, and is called *monotone* if it is monotone in both x - and y -coordinates. Given two points u and v in the free space, we say that v is *reachable* from u , denoted by $u \rightsquigarrow v$, if there is a monotone feasible curve in $\mathcal{F}_\varepsilon(P, Q)$ from u to v . Alt and Godau [8] showed that $\delta_F(P, Q) \leq \varepsilon$ if and only if $(0, 0) \rightsquigarrow (n, m)$. Clearly, reachability is “transitive”: if $u \rightsquigarrow v$ and $v \rightsquigarrow w$, then $u \rightsquigarrow w$. Given two points a and b in the plane, we write $a < b$ if $a_x < b_x$, and write $a \leq b$ if $a_x \leq b_x$.

Lemma 21 (Crossing Lemma) *Let $u, u' \in \mathcal{F}_i$ and $v, v' \in \mathcal{F}_j$ ($i < j$) such that $u \leq u'$ and $v' \leq v$. If $u \rightsquigarrow v$ and $u' \rightsquigarrow v'$, then $u \rightsquigarrow v'$ and $u' \rightsquigarrow v$.*

Proof: Let π be a monotone feasible curve that connects u to v . Since u' and v' are on different sides of π , any monotone curve that connects u' to v' in $\mathcal{F}_\varepsilon(P, Q)$ intersects π at some point x (see Figure 5.1.b). The concatenation of the subcurve from u to x and the one from x to v' gives a monotone feasible curve from u to v' . Similarly, v is connected to u' by a monotone feasible curve through x . \square

For $0 \leq j \leq m$, we denote by \mathcal{F}_j the set of feasible points in \mathcal{FD}_j . \mathcal{F}_j consists of $O(n)$ feasible intervals, where each feasible interval is a maximal continuous set of feasible points, restricted to be within a cell. For any feasible point set S in $\mathcal{F}_\varepsilon(P, Q)$, we define the *projection* of S on \mathcal{FD}_j as

$$R_j(S) := \{v \in \mathcal{F}_j \mid \exists u \in S \text{ s.t. } u \rightsquigarrow v\}.$$

For an interval I on \mathcal{F}_i , we define the *left pointer* of I on \mathcal{F}_j ($i \leq j$), denoted by $\ell_j(I)$, to be the leftmost point in $R_j(I)$. Similarly, the *right pointer* of I on \mathcal{F}_j , denoted by $r_j(I)$, is defined to be the rightmost point in $R_j(I)$. If $R_j(I)$ is empty, both pointers $\ell_j(I)$ and $r_j(I)$ are set to NIL. These pointers were previously used in [7, 8], and form a main ingredient of our data structure. For a single point u , we simply use $R_j(u)$, $\ell_j(u)$, and $r_j(u)$ instead of $R_j(\{u\})$, $\ell_j(\{u\})$, and $r_j(\{u\})$, respectively. The following observation is an immediate corollary of Lemma 37.

Observation 6 *For any two points $u, v \in \mathcal{F}_i$ with $u \leq v$, and for any $j \geq i$, we have $\ell_j(u) \leq \ell_j(v)$ and $r_j(u) \leq r_j(v)$.*

For an interval I on a horizontal line, we denote by $\text{left}(I)$ and $\text{right}(I)$ the left and the right endpoint of I , respectively. The following simple lemma will be used frequently throughout this chapter.

Lemma 22 *Given two sequences A and B of points on a horizontal line sorted from left to right, we can compute for each point $a \in A$, the leftmost point $b \in B$ with $a \leq b$ in $O(|A| + |B|)$ total time.*

Proof: We scan the two sequences simultaneously from left to right using two pointers. Whenever we reach a point $b \in B$, we advance our pointer on A until we reach the first point $a \in A$ with $a > b$. We then make all points in A scanned during this step up to (not including) a to point to b . We then advance our pointer on B by one, and repeat the above procedure. \square

5.2.1 Vertical Ray Shooting

The following special case of the vertical ray shooting problem appears as a subproblem in our construction. Consider a vertical slab $[0, 1] \times [0, m]$ (see Figure 5.2). For

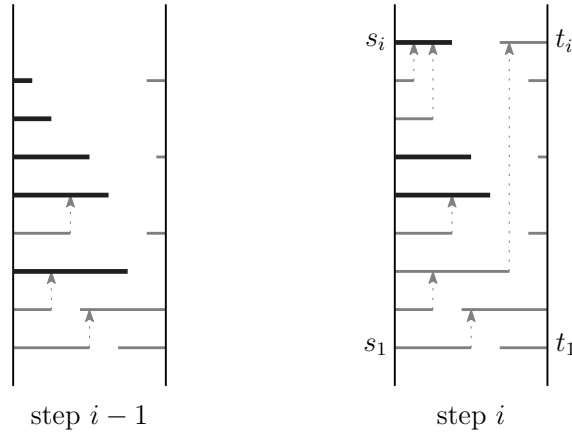


Figure 5.2. An example of the execution of Algorithm 9. Segments in the queue at the end of each step are shown in bold.

each $1 \leq i \leq m$, there are two (possibly empty) segments in the slab at height i , attached to the boundaries of the slab, one from left and the other from right. Given a query point q , the vertical ray shooting problem involves finding the first segment in the slab directly above q . If the query points are restricted to be among the endpoints of the segments, we show below that the vertical ray shooting queries can be answered in $O(1)$ time, after $O(m)$ preprocessing time.

Lemma 23 *Let S be a set of segments $s_i = [0, a_i] \times \{i\}$, and T be a set of segments $t_i = [b_i, 1] \times \{i\}$ with $0 \leq a_i \leq b_i \leq 1$, for $1 \leq i \leq m$. We can find for each segment $s_i \in S$, the first segment in $S \cup T$ directly above $\text{right}(s_i)$ in $O(m)$ total time.*

Proof: Algorithm 9 assigns to each segment s_i of S , an *up* pointer that points to the first segment directly above $\text{right}(s_i)$, if such a segment exists. The algorithm makes use of a double-ended queue Q (a combination of a queue and a stack, commonly known as “deque”), that supports the standard operations $\text{PUSH}()$, $\text{POP}()$, and $\text{TOP}()$, along with two additional operations $\text{BOTTOM}()$ and $\text{BOTTOM-POP}()$, that are analogous to $\text{TOP}()$ and $\text{POP}()$, respectively, but applied to the bottom of the queue.

We say that a segment $s \in S$ is *covered* by a segment $t \in S \cup T$, if a vertical ray from $\text{right}(s)$ intersects t . For $1 \leq i \leq m$, let $S_i = \{s_1, \dots, s_i\}$ and $T_i = \{t_1, \dots, t_i\}$. The following invariant is maintained by the algorithm: At the end of iteration i ,

Algorithm 9 RAY-SHOOTING(S, T)

```

1:  $Q \leftarrow \emptyset$ 
2:  $Q.PUSH(s_1)$ 
3: for  $i$  from 2 to  $m$  do
4:   while  $|Q.TOP()| \leq |s_i|$  do
5:      $Q.POP().up \leftarrow s_i$ 
6:   while  $|Q.BOTTOM()| \geq 1 - |t_i|$  do
7:      $Q.BOTTOM-POP().up \leftarrow t_i$ 
8:    $Q.PUSH(s_i)$ 

```

Q contains a subset of segments from S_i that are not covered by any segment from $S_i \cup T_i$, in a decreasing order of their lengths from bottom to the top of the queue. The invariant clearly holds for $i = 1$. Suppose by induction that the invariant holds for $i - 1$. In the i -th iteration, we first pop off from the top of the queue all segments covered by s_i , in Lines 4–5. Then, we remove from the bottom of the queue all segments covered by t_i , in Lines 6–7. Finally, we add s_i to the top of the queue. (See Figure 5.2 for an illustration.) It is easy to verify that after the insertion of s_i , the segments of Q are still sorted in a decreasing order of their lengths (because we have already removed segments smaller than s_i from Q), and that, no segment of Q is covered by a segment in $S_i \cup T_i$ (because we have removed covered segments from Q). Furthermore, it is clear that any segment s removed from Q is assigned to the first segment that is directly above $\text{right}(s)$, because we are processing segments in order from bottom to the top. The correctness of the algorithm therefore follows. Note that after the termination of the algorithm, Q still contains some uncovered segments from S , whose up pointers are assumed to be NIL, as they are not covered by any segment in $S \cup T$. Since each segment of S is inserted into and removed from the queue at most once, Lines 5 and 7 of the algorithm are executed at most m times, and hence, the whole algorithm runs in $O(m)$ time. \square

Consider the vertical slab $[0, 1] \times [0, m]$, and the two sets of segments S and T as defined above. We call a segment $t_j \in T$ reachable from a segment $s_i \in S$, if there

is a monotone path from a point on s_i to a point on t_j not intersecting any other segment in $S \cup T$. For a segment $s_i \in S$, the *topmost reachable* segment in T is a reachable segment t_j with the maximum index j . In Figure 5.2, for example, the topmost reachable segments for s_1 and s_2 are t_2 and t_i , respectively.

Lemma 24 *Let S and T be the two sets of segments defined in Lemma 23. Then, for each segment $s_i \in S$, $1 \leq i \leq m$, the topmost reachable segment in T can be computed in $O(m)$ total time.*

Algorithm 10 TOPMOST-REACHABLE-SEGMENTS(S, T)

```

1: for  $i$  from  $m$  to 1 do
2:   if  $s_i.\text{up} = \text{null}$  then
3:      $s_i.\text{top} \leftarrow t_m$ 
4:   else if  $s_i.\text{up} \in T$  then
5:      $s_i.\text{top} \leftarrow s_i.\text{up}$ 
6:   else
7:      $s_i.\text{top} \leftarrow s_i.\text{up}.\text{top}$ 

```

Proof: Algorithm 10 scans all segments in S from top to bottom, and assigns to each segment s_i in S a *top* pointer that points to the topmost segment in T reachable from s_i . The algorithm works as follows. Suppose that the top pointers for all segments in S above s_i are computed. At i -th iteration, if s_i is not covered by any other segment above it, (i.e., $s_i.\text{up}$ is null), then the topmost reachable segment of s_i is set to t_m . If s_i is covered by a segment $t_j \in T$, then the topmost reachable segment of s_i is t_j . Otherwise, if s_i is covered by a segment $s_j \in S$, then all segments in T above s_j that are reachable from s_i are also reachable from s_j , and hence, the topmost such segment can be obtained from $s_j.\text{top}$ pointer, which is computed earlier. Therefore, computing all top pointers can be performed in $O(m)$ total time. \square

Analogous to the previous lemma, a result can be stated for a horizontal slab.

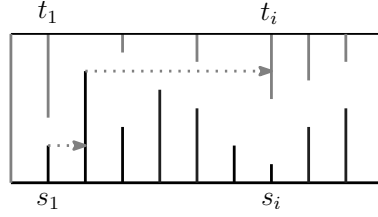


Figure 5.3. A horizontal slab with vertical segments. The rightmost segment reachable from s_1 in this figure is t_i .

Corollary 25 Consider a horizontal slab $[0, n] \times [0, 1]$. Let S be a set of segments $s_i = \{i\} \times [0, a_i]$, and T be a set of segments $t_i = \{i\} \times [b_i, 1]$ with $0 \leq a_i \leq b_i \leq 1$, for $1 \leq i \leq n$ (see Figure 5.3). Then, for all segments $s_i \in S$, the rightmost segment in T reachable from s_i can be computed in $O(n)$ total time.

5.3 The Main Data Structure

In this section, we describe our main data structure that yields improved algorithms for several variants of the Fréchet distance. For $0 \leq j \leq m$, we define the *reachable set* $\mathcal{R}(j) := \mathcal{R}_j(\mathcal{F}_0)$ to be the set of all points in \mathcal{F}_j reachable from \mathcal{F}_0 . We call each interval of $\mathcal{R}(j)$, contained in a feasible interval of \mathcal{F}_j , a *reachable interval*. By our definition, $\mathcal{R}(0) = \mathcal{F}_0$. The following observation is immediate by the transitivity of reachability.

Observation 7 For $0 \leq i < j \leq m$, $\mathcal{R}(j) = \mathcal{R}_j(\mathcal{R}(i))$.

An important property of the reachable sets is described in the following lemma.

Lemma 26 For any two indices i, j ($0 \leq i < j \leq m$) and any point $u \in \mathcal{R}(i)$, $\mathcal{R}_j(u) = \mathcal{R}(j) \cap [\ell_j(u), r_j(u)]$.

Proof: Let $S = [\ell_j(u), r_j(u)]$. By Observation 7, $\mathcal{R}(j) = \mathcal{R}_j(\mathcal{R}(i))$. Thus, it is clear by the definition of pointers that $\mathcal{R}_j(u) \subseteq \mathcal{R}(j) \cap S$. Therefore, it remains to be shown that $\mathcal{R}(j) \cap S \subseteq \mathcal{R}_j(u)$. Suppose, by way of contradiction, that there is a point $v \in \mathcal{R}(j) \cap S$ such that $v \notin \mathcal{R}_j(u)$. Since $v \in \mathcal{R}(j)$, there exists some point $u' \in \mathcal{R}(i)$ such that $u' \rightsquigarrow v$. If u' is to the left (resp., to the right) of u , then the points u, u', v ,

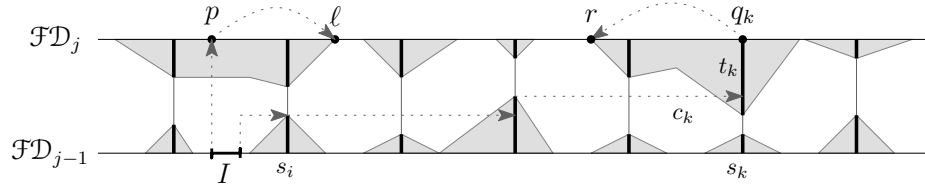


Figure 5.4. Computing $\mathcal{R}(j)$ from $\mathcal{R}(j-1)$.

and $\ell_j(u)$ (resp., $r_j(u)$) satisfy the conditions of Lemma 37. Therefore, by Lemma 37, $u \rightsquigarrow v$, which implies that $v \in \mathcal{R}_j(u)$; a contradiction. \square

Lemma 26 provides an efficient method for storing the sets $\mathcal{R}_j(I)$, for all feasible intervals I on \mathcal{F}_0 . Namely, instead of storing each set $\mathcal{R}_j(I)$ separately, one set per feasible interval I , which takes up to $\Theta(n^2)$ space, we only need to store a single set $\mathcal{R}(j)$, along with the pointers $\ell_j(I)$ and $r_j(I)$, which takes only $O(n)$ space in total. The set $\mathcal{R}_j(I)$, for each interval I on \mathcal{F}_0 , can be then obtained by $\mathcal{R}(j) \cap [\ell_j(I), r_j(I)]$. For each interval I on \mathcal{F}_0 , we call the set $\{\ell_j(I), r_j(I)\}$ a *compact representation* of $\mathcal{R}_j(I)$. The following lemma is a main ingredient of our fast computation of reachable sets.

Lemma 27 *For $0 < j \leq m$, if $\mathcal{R}(j-1)$ is given, then $\mathcal{R}(j)$ can be computed in $O(n)$ time.*

Proof: Let \mathcal{D} be the intersection of the free-space diagram with the rectangle $[0, n] \times [j-1, j]$. \mathcal{D} is composed of n square cells, numbered from left to right by c_1 to c_n . For all reachable intervals I on $\mathcal{R}(j-1)$, we compute pointers $\ell_j(I)$ and $r_j(I)$ in $O(n)$ time as follows. For each cell c_k in \mathcal{D} , the intersection of the right boundary of c_k with the infeasible part of the free-space diagram forms two (possibly empty) vertical segments, denoted by s_k and t_k , respectively, as in Figure 5.4. For each cell c_k , we denote the top-right corner of c_k by q_k . We pre-compute for each point q_i , $1 \leq i \leq n$, a pointer $\text{next}(q_i)$ (resp., $\text{prev}(q_i)$) that points to the first feasible point on or immediately after (resp., before) q_i in $\mathcal{F}\mathcal{D}_j$. Let S be the set of all left and right endpoints of feasible intervals on $\mathcal{F}\mathcal{D}_j$. Since for each point q_i , $\text{next}(q_i)$ and $\text{prev}(q_i)$,

if not null, are included in S , we can compute all next/prev pointers using two linear scans in $O(n)$ time by Lemma 22. After computing $\text{next}(q_i)$ pointers, we can compute $\text{next}(q)$ for any point $q \in \mathcal{FD}_j$ in constant time.

Now, fix an interval I on $\mathcal{R}(j-1)$. We compute $\ell_j(I)$ and $r_j(I)$ as follows. Let c_i be the cell containing I , let p be the vertical projection of $\text{left}(I)$ onto \mathcal{FD}_j , and let t_k be the rightmost segment reachable from s_i , computed by Corollary 25 (see Figure 5.4). We set $\ell = \text{next}(p)$ and $r = \text{prev}(q_k)$. (If $\text{next}(p) > \text{prev}(q_k)$, we set $\ell = r = \text{null}$.) It is easy to verify that no point before ℓ and no point after r on \mathcal{FD}_j can be reachable from I , and that, every feasible point on \mathcal{FD}_j between ℓ and r is reachable from I . Therefore, $\ell_j(I) = \ell$ and $r_j(I) = r$. As a result, computing $\ell_j(I)$ and $r_j(I)$ for each reachable interval I on $\mathcal{R}(j-1)$ takes $O(1)$ time, after $O(n)$ preprocessing time for computing the next/prev pointers. Thus, we can compute $\ell_j(I)$ and $r_j(I)$ for all reachable intervals I on $\mathcal{R}(j-1)$ in $O(n)$ total time.

After computing the left and right pointers, we can produce $\mathcal{R}(j) = \mathbf{R}_j(\mathcal{R}(j-1))$ by identifying those (portions of) intervals on \mathcal{F}_j that lie in at least one interval $[\ell_j(I), r_j(I)]$. Since for all intervals I on $\mathcal{R}(j-1)$ sorted from left to right, $\ell_j(I)$'s and $r_j(I)$'s are in sorted order by Observation 6, we can accomplish this step by a linear scan over the left and right pointers in $O(n)$ time. \square

5.3.1 Data Structure

We now describe our main data structure, which we call free-space map. The data structure maintains reachability information on each row of the free-space diagram, using some additional pointers that help answering reachability queries efficiently. The *free-space map* of two curves P and Q consists of the following:

- (i) the reachable sets $\mathcal{R}(j)$, for $0 \leq j \leq m$,
- (ii) the right pointer $r_j(I)$ for each reachable interval I on $\mathcal{R}(j-1)$, $0 < j \leq m$,
- (iii) the leftmost reachable point after each cell in \mathcal{FD}_j , for $0 < j \leq m$, and
- (iv) the rightmost take-off point before each cell in \mathcal{FD}_j , for $0 \leq j < m$,

where a *take-off* point on \mathcal{FD}_j is a reachable point in $\mathcal{R}(j)$ from which a point on \mathcal{FD}_{j+1} is reachable. For example, in Figure 5.5, ℓ_j is the leftmost reachable point after ℓ' , and r' is the rightmost take-off point before r_{j-1} . For a cell c in \mathcal{FD}_j , by *after c* we mean after $\text{right}(c)$, and by *before c* we mean before $\text{left}(c)$.

Lemma 28 *Given two polygonal curves P and Q of size n and m , respectively, we can build the free-space map of P and Q in $O(nm)$ time.*

Proof: We start from $\mathcal{R}(0) = \mathcal{F}_0$, and construct each $\mathcal{R}(j)$ iteratively from $\mathcal{R}(j-1)$, for j from 1 to m , using Lemma 27. The total time needed for this step is $O(nm)$. The construction of $\mathcal{R}(j)$, as seen in the proof of Lemma 27, involves computing all right (and left) pointers, for all reachable intervals on $\mathcal{R}(j-1)$. Therefore, item (ii) of the data structure can be obtained at no additional cost. Item (iii) is computed as follows. Let S be the set of all left pointers obtained upon constructing $\mathcal{R}(j)$. For each cell c in \mathcal{FD}_j , the leftmost reachable point after c , if any, is a member of S . We can therefore compute item (iii) for each row \mathcal{FD}_j by a linear scan over the cells and the set S using Lemma 22 in $O(n)$ time. For each row, item (iv) can be computed analogous to item (iii), but in a reverse order. Namely, given the set $\mathcal{R}(j)$, we compute the set of points on \mathcal{FD}_{j-1} reachable from $\mathcal{R}(j)$ in the free-space diagram

Algorithm 11 QUERY(u), where $u \in \mathcal{F}_0$

```

1: let  $\ell_0 = r_0 = u$ 
2: for  $j = 1$  to  $m$  do
3:   let  $\ell'$  be the orthogonal projection of  $\ell_{j-1}$  onto  $\mathcal{FD}_j$ 
4:    $\ell_j \leftarrow$  LEFTMOST-REACHABLE( $\ell'$ )
5:   let  $r' =$  RIGHTMOST-TAKE-OFF( $r_{j-1}$ )
6:   if  $r' < \ell_{j-1}$  or  $r' = \text{null}$  then
7:      $r_j \leftarrow \text{null}$ 
8:   else
9:      $r_j \leftarrow r_j(I)$ , for  $I$  being the reachable interval containing  $r'$ 
10:  if  $\ell_j$  or  $r_j$  is null then
11:    return null
12: return  $\ell_m, r_m$ 

```

rotated by 180 degrees. Let S be the set of all left pointers obtained in this reverse computation. For each cell c in \mathcal{FD}_{j-1} , the rightmost take-off point before c , if there is any, is a member of S . We can therefore compute item (iv) for each row by a linear scan over the cells and the set S using Lemma 22 in $O(n)$ time. The total time for constructing the free-space map is therefore $O(nm)$. \square

In the following, we show how the reachability queries can be efficiently answered, using the free-space map. For the sake of describing the query algorithm, we introduce two functions as follows. Given a point $u \in \mathcal{FD}_j$, we denote by LEFTMOST-REACHABLE(u) the leftmost reachable point on or after u on \mathcal{FD}_j . Analogously, we denote by RIGHTMOST-TAKE-OFF(u) the rightmost take-off point on or before u on \mathcal{FD}_j . Note that both these functions can be computed in $O(1)$ time using the pointers stored in the free-space map.

Lemma 29 *Let the free-space map of P and Q be given. Then, for any query point $u \in \mathcal{F}_0$, $\ell_m(u)$ and $r_m(u)$ can be computed in $O(m)$ time.*

Proof: The procedure for computing $\ell_m(u)$ and $r_m(u)$ for a query point $u \in \mathcal{F}_0$ is described in Algorithm 11. The following invariant holds during the execution of the algorithm: After the j -th iteration, $\ell_j = \ell_j(u)$ and $r_j = r_j(u)$. We prove this by induction on j . The base case, $\ell_0 = r_0 = u$, trivially holds. Now, suppose inductively that $\ell_{j-1} = \ell_{j-1}(u)$ and $r_{j-1} = r_{j-1}(u)$. We show that after the j -th iteration, the invariant holds for j . We assume, w.l.o.g., that $\mathcal{R}_j(u)$ is non-empty, i.e., $\ell_j(u) \leq r_j(u)$. Otherwise, the last take-off point from $\mathcal{R}(j-1)$ will be either null, or smaller than ℓ_{j-1} , which is then detected and handled by Lines 6–7.

We first show that $\ell_j = \ell_j(u)$. Suppose by contradiction that $\ell_j \neq \ell_j(u)$. If $\ell_j < \ell_j(u)$, then we draw a vertical line from ℓ_j to \mathcal{FD}_{j-1} (see Figure 5.5). This line crosses any monotone path from $\ell_{j-1} = \ell_{j-1}(u)$ to $\ell_j(u)$ at a point x . The line segment $x\ell_j$ is completely in the free space, because otherwise, it must be cut by an obstacle, which contradicts the fact that the free space inside a cell is convex [8]. But then, ℓ_j becomes reachable from ℓ_{j-1} through x , contradicting the fact that $\ell_j(u)$ is the leftmost reachable point in $\mathcal{R}(j)$. The case, $\ell_j > \ell_j(u)$, cannot arise, because then, $\ell_j(u)$ is a reachable point after ℓ' and before ℓ_j , which contradicts our selection of ℓ_j as the leftmost reachable point of ℓ' in line 4.

We can similarly show that $r_j = r_j(u)$. Suppose by contradiction that $r_j \neq r_j(u)$. The case $r_j > r_j(u)$ is impossible, because otherwise, r_j is a point on $\mathcal{R}(j)$ reachable from $\mathcal{R}(j-1)$ which appears after $r_j(u)$. This contradicts the fact that $r_j(u)$ is the rightmost point on $\mathcal{R}(j)$. If $r_j < r_j(u)$ (see Figure 5.5), then $r_j(u)$ is reachable from a point $x \in \mathcal{R}(j-1)$ with $x < r'$, because r' is the rightmost take-off point on or before r_{j-1} . But then, by Lemma 37, $r_j(u)$ is reachable from r' , which contradicts the fact

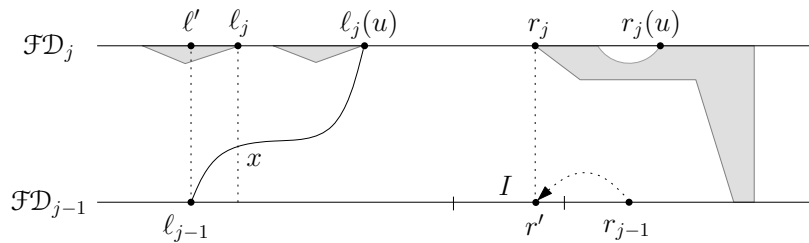


Figure 5.5. Proof of Lemma 29.

that r_j is the left pointer of the reachable interval I containing r' . \square

5.3.2 Improved Query Time

In this section, we show how the query time in the free-space map can be improved by keeping some additional information in our data structure, without increasing either the preprocessing time or space complexity. This improved query time is crucial for applications such as the minimum walk problem.

We use our vertical ray shooting data structure from Section 5.2.1. For each feasible interval I on \mathcal{F}_0 , we partition I into $O(m)$ subintervals, such that for all points u in a subinterval, the first segment directly above u in the ray shooting data structure is the same. Such a partitioning can be obtained by a simple scan on each column of the free-space map from bottom to the top. The total number of subintervals obtained this way is $O(nm)$.

Theorem 30 *Given two polygonal curves P and Q of size n and m , respectively, we can build in $O(nm)$ time a data structure of size $O(nm)$, such that for any query point $u \in \mathcal{F}_0$, a compact representation of $\mathbf{R}_m(u)$ can be reported in $O(\log m)$ time. Furthermore, if the subinterval containing u is given as part of the query, then a compact representation of $\mathbf{R}_m(u)$ can be reported in $O(1)$ time.*

Proof: We first build the free-space map in $O(nm)$ time as per Lemma 28. Let I be a feasible interval on \mathcal{F}_0 . For each $u \in I$, we have $r_m(u) = r_m(I) = r_m(\text{right}(I))$. Therefore, by storing $r_m(I)$ for all feasible intervals I on \mathcal{F}_0 , we can report $r_m(u)$ for each query point $u \in \mathcal{F}_0$ in $O(1)$ time. Since there are $O(n)$ feasible intervals on \mathcal{F}_0 , and computing each right pointer takes $O(m)$ time by Lemma 29, this step takes $O(nm)$ time in total. To report $\ell_m(u)$ quickly, we store for each reachable interval $I \in \mathcal{R}(j)$, $0 < j < m$, the pointer $\ell_m(I)$ in the data structure. We can compute all these left pointers in $O(nm)$ time as follows. We first preprocess each column of the free-space map for vertical ray shooting as in Lemma 23, by assuming horizontal segments to be non-reachable intervals on each row \mathcal{FD}_j . To compute left pointers, we inductively process the free-space map from top to bottom. Suppose that the left

pointers are computed and stored for all reachable intervals above \mathcal{FD}_j , and let I be a reachable interval on \mathcal{FD}_j , with $q = \text{left}(I)$. We can find the first non-reachable segment s above q using our ray shooting data structure in $O(1)$ time. If no such s exists, $\ell_m(q)$ is directly above q on $\mathcal{R}(m)$. Otherwise, as in Algorithm 11, we project q directly to a point $q' \in s$, and then, find the first reachable point p after q' . If such a point p exists, it should be the left endpoint of a reachable interval I' , for which we have already stored the pointer $\ell_m(\text{left}(I'))$. Therefore, $\ell_m(q) = \ell_m(\text{left}(I'))$ can be computed in $O(1)$ time. As a result, finding all left pointers takes $O(n)$ time for each \mathcal{FD}_j , and $O(nm)$ time for the whole free-space map.

Now, for each subinterval J on \mathcal{F}_0 , we compute $\ell_m(J)$ in the same way described above in $O(1)$ time. Namely, we find the unique segment s above J , find the first reachable point p after s , and take the pointer $\ell_m(p)$, which is stored in the data structure. The total time and space needed for this step is therefore $O(nm)$. For any query point $u \in \mathcal{F}_0$, we first locate the subinterval J containing u in $O(\log m)$ time. Now, $\ell_m(u) = \ell_m(J)$ and $r_m(u) = r_m(I)$ for the feasible interval I containing subinterval J , both accessible in $O(1)$ time. Note that the only expensive operation in our query algorithm is to locate the subinterval containing the query point. If the subinterval is given, then the query can be answered in $O(1)$ time. \square

5.4 Applications

In this section, we provide some of the applications of our free-space map data structure.

5.4.1 Partial Curve Matching

Given two polygonal curves P and Q , and an $\varepsilon \geq 0$, the partial curve matching problem involves deciding whether there exists a subcurve $R \subseteq P$ such that $\delta_F(R, Q) \leq \varepsilon$. As noted in [8], this is equivalent to deciding whether there exists a monotone path in the free space from \mathcal{FD}_0 to \mathcal{FD}_m . This decision problem can be efficiently solved

using the free-space map. For each feasible interval I on \mathcal{FD}_0 , we obtain a compact representation of $\mathcal{R}_m(\text{left}(I))$ using Theorem 30 in $O(1)$ time. Observe that $\mathcal{R}_m(I) = \emptyset$ if and only if $\mathcal{R}_m(\text{left}(I)) = \emptyset$. Therefore, we can decide in $O(nm)$ time whether there exists a point on \mathcal{FD}_m reachable from \mathcal{FD}_0 . Furthermore, we can use parametric search as in [8] to find the smallest ε for which the answer to the above decision problem is “YES” in $O(nm \log(nm))$ time. Therefore, we obtain:

Theorem 31 *Given two polygonal curves P and Q of size n and m , respectively, we can decide in $O(nm)$ time whether there exists a subcurve $R \subseteq P$ such that $\delta_F(R, Q) \leq \varepsilon$, for a given $\varepsilon \geq 0$. A subcurve $R \subseteq P$ minimizing $\delta_F(R, Q)$ can be computed in $O(nm \log(nm))$ time.*

5.4.2 Closed Curves

Given two closed curves P and Q , define

$$\delta_C(P, Q) = \inf_{s_1, s_2 \in \mathbb{R}} \delta_F(P \text{ shifted by } s_1, Q \text{ shifted by } s_2)$$

to be the closed Fréchet metric between P and Q .

Consider a diagram \mathcal{D} of size $2n \times m$ obtained from concatenating two copies of the standard free-space diagram of P and Q . Alt and Godau showed that $\delta_C(P, Q) \leq \varepsilon$ if and only if there exists a monotone feasible path in \mathcal{D} from $(t, 0)$ to $(n + t, m)$, for a value $t \in [0, n]$. We show how such a value t , if any exists, can be found efficiently using a free-space map built on top of \mathcal{D} .

Observation 8 *Let i be a fixed integer ($0 < i \leq n$), $I_i = [a, b]$ be the feasible interval on the i -th cell of \mathcal{FD}_0 , and $J_i = [c, d]$ be the feasible interval on the $(i + n)$ -th cell of \mathcal{FD}_m . Then there exists a value $t \in [i - 1, i]$ with $(t, 0) \rightsquigarrow (n + t, m)$ if and only if $\max((\ell_m(I_i))_x, c) \leq b + n$ and $\min((r_m(I_i))_x, d) \geq a + n$.*

We iterate on i from 1 to n , and check for each i if a desired value $t \in [i - 1, i]$ exists using Observation 8. Each iteration involves examining $\ell_m(I_i)$ and $r_m(I_i)$, which are accessible in $O(1)$ time using Theorem 30. The total time is therefore $O(nm)$, required for building the free-space map.

Theorem 32 *Given two closed polygonal curves P and Q of size n and m , respectively, we can decide in $O(nm)$ time whether $\delta_C(P, Q) \leq \varepsilon$, for a given $\varepsilon \geq 0$. Furthermore, $\delta_C(P, Q)$ can be computed in $O(nm \log(nm))$ time.*

5.4.3 Maximum Walk

Another variant of the Fréchet distance problem is the following: Given two curves P and Q and a fixed $\varepsilon \geq 0$, find a maximum-length continuous subcurve of Q whose Fréchet distance to P does not exceed ε . In the dog-person illustration, this problem corresponds to finding the best starting point on P , such that when the person walks the whole curve Q , his or her dog can walk the maximum length on P , without exceeding a leash of length ε . We show that this optimization problem, which is a generalized version of the partial curve matching problem, can be solved efficiently in $O(nm)$ time using the free-space map. The following observation is the main ingredient.

Observation 9 *Let R be a maximum-length subcurve of P such that $\delta_F(R, Q) \leq \varepsilon$. The starting point of R corresponds to the left endpoint of a feasible interval I on \mathcal{FD}_0 , and its ending point corresponds to $r_m(I)$.*

By Observation 9, we only need to test n feasible intervals on \mathcal{FD}_0 , and their right pointer on \mathcal{FD}_m to find the best subcurve R . If we keep the length of P from its beginning to each of its n segments in a table, we can compute the length of each subcurve R of P in $O(1)$ time using two table lookups as it is explained in Chapter 3. Computing the maximum-length subcurve R will therefore take $O(n)$ time for computing the lengths, plus $O(mn)$ time for constructing the free-space map.

Theorem 33 *Given two polygonal curves P and Q of size n and m , respectively, and a parameter $\varepsilon \geq 0$, we can find in $O(nm)$ time a maximum-length subcurve $R \subseteq P$ such that $\delta_F(R, Q) \leq \varepsilon$.*

5.4.4 Minimum Walk

Given two curves P and Q and a fixed $\varepsilon \geq 0$, the *minimum walk* problem asks for the minimum-length continuous subcurve of P that a person can walk while his/her dog walks the whole curve Q without exceeding a leash of length ε . This optimization problem can be again solved efficiently using our free-space map.

Theorem 34 *Given two polygonal curves P and Q of size n and m , respectively, and a parameter $\varepsilon \geq 0$, we can find in $O(nm)$ time a minimum-length subcurve $R \subseteq P$ such that $\delta_F(R, Q) \leq \varepsilon$.*

Proof: Let R be a minimum-length subcurve of P such that $\delta_F(R, Q) \leq \varepsilon$. Observe that the starting point of R corresponds to the right endpoint of a subinterval J on \mathcal{F}_0 , and its ending point corresponds to $\ell_m(J)$. Therefore, to find the best subcurve R , we only need to check the right endpoints of $O(nm)$ subintervals on \mathcal{FD}_0 and their corresponding left pointers. By Theorem 30, this takes $O(1)$ time per subinterval. The total time needed is therefore $O(nm)$. \square

5.5 Matching a Curve in a DAG

Let P be a polygonal curve of size n , and G be a connected geometric graph with m straight-line edges. Alt *et al.* [7] presented an $O(nm \log m)$ -time algorithm to decide whether there is a path π in G with Fréchet distance at most ε to P , for a given $\varepsilon \geq 0$. In this section, we improve this result for the particular case when G is a directed acyclic graph (DAG), by giving an algorithm that runs in only $O(nm)$ time. The idea is to use a sequential reachability propagation approach similar to the one used in Section 5.3. Our approach is structurally different from the one used by Alt *et al.* [7].

We first borrow some notation from [7]. Let $G = (V, E)$ be a connected DAG with m edges, such that $V = \{1, \dots, \nu\}$ corresponds to points $\{v_1, \dots, v_\nu\} \subseteq \mathbb{R}^d$, for $\nu \leq m + 1$. We assume, w.l.o.g., that the elements of V are numbered according to a topological ordering of the vertices of G . Such a topological ordering can be

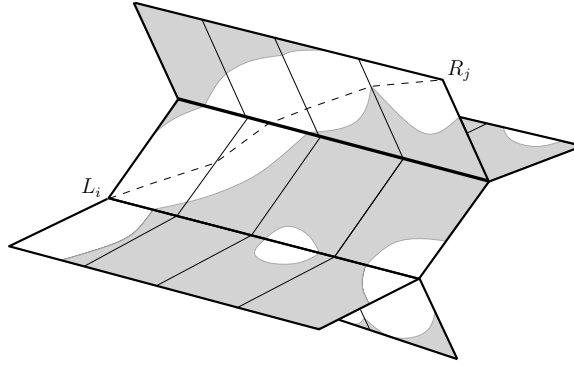


Figure 5.6. An example of a free-space surface.

computed in $O(m)$ time. We embed each edge $(i, j) \in E$ as an oriented line segment s_{ij} from v_i to v_j . Each s_{ij} is continuously parametrized by values in $[0, 1]$ according to its natural parametrization, namely, $s_{ij} : [0, 1] \rightarrow \mathbb{R}^d$.

For each vertex $j \in V$, let $\mathcal{FD}_j := \mathcal{FD}_\varepsilon(P, v_j)$ be the one-dimensional free-space diagram corresponding to the path P and the vertex j . We denote by L_j and R_j the left endpoint and the right endpoint of \mathcal{FD}_j , respectively. Moreover, we denote by \mathcal{F}_j the set of feasible points on \mathcal{FD}_j . For each $(i, j) \in E$, let $\mathcal{FD}_{ij} := \mathcal{FD}_\varepsilon(P, s_{ij})$ be a two-dimensional free-space diagram, which consists of a row of n cells. We glue together the two-dimensional free-space diagrams according to the adjacency information of G , as shown in Figure 5.6. The resulting structure is called the *free-space surface* of P and G , denoted by $\mathcal{FS}_\varepsilon(P, G)$. We denote the set of feasible points in $\mathcal{FS}_\varepsilon(P, G)$ by $\mathcal{F}_\varepsilon(P, G)$.

Given two points $u, v \in \mathcal{F}_\varepsilon(P, G)$, we say that v is *reachable* from u , denoted by $u \rightsquigarrow v$, if there is a monotone feasible curve from u to v in $\mathcal{F}_\varepsilon(P, G)$, where monotonicity in each cell of the surface is with respect to the orientation of the edges of P and G defining that cell. Given a set of points $S \subseteq \mathcal{F}_\varepsilon(P, G)$, we define $\mathcal{R}_j(S) := \{v \in \mathcal{F}_j \mid \exists u \in S \text{ s.t. } u \rightsquigarrow v\}$. Let $\mathbb{L} = \cup_{j \in V} (L_j \cap \mathcal{F}_j)$. For each $j \in V$, we define the *reachable set* $\mathcal{R}(j) := \mathcal{R}_j(\mathbb{L})$. Observe that there is a path π in G with $\delta_F(P, \pi) \leq \varepsilon$ if and only if there is a vertex $j \in V$ with $R_j \in \mathcal{R}(j)$.

Theorem 35 *Given a polygonal curve P of size n and a directed acyclic graph G of size m , we can decide in $O(nm)$ time whether there is a path π in G with $\delta_F(P, \pi) \leq \varepsilon$.*

Algorithm 12 DAG-MATCHING-DECISION(P, G, ε)

- 1: **for all** $j \in V$ in a topological order **do**
 - 2: $\mathcal{R}(j) \leftarrow \mathbf{R}_j(L_j \cap \mathcal{F}_j) \cup (\cup_{(i,j) \in E} \mathbf{R}_j(\mathcal{R}(i)))$
 - 3: let $S = \cup_{j \in V} (\mathbf{R}_j \cap \mathcal{R}(j))$
 - 4: return TRUE if $S \neq \emptyset$, otherwise return FALSE
-

ε , for a given $\varepsilon \geq 0$. A path π in G minimizing $\delta_F(P, \pi)$ can be computed in $O(nm \log(nm))$ time.

Proof: Algorithm 12 computes, for each vertex $j \in V$, the reachable set $\mathcal{R}(j)$ in a topological order. It then returns true only if there is a vertex $j \in V$ such that \mathbf{R}_j is reachable which indicates the existence of a path π in G with $\delta_F(P, \pi) \leq \varepsilon$. To prove the correctness, we only need to show that for every vertex $j \in V$, the algorithm computes $\mathcal{R}(j)$ correctly. We prove this by induction on j . Suppose by induction that the set $\mathcal{R}(i)$ for all $i < j$ is computed correctly. Now consider a point $u \in \mathcal{F}_j$. If $u \in \mathcal{R}(j)$, then there exists a vertex $k < j$ such that L_k is connected to u by a monotone feasible curve \mathcal{C} in $\mathcal{FS}_\varepsilon(P, G)$. If $k = j$, then $u \in \mathcal{R}(j)$ because $\mathbf{R}_j(L_j \cap \mathcal{F}_j)$ is added to $\mathcal{R}(j)$ in line 2. If $k < j$, then the curve \mathcal{C} must pass through a vertex i with $(i, j) \in E$. Since the vertices of V are sorted in a topological order, we have $i < j$, and hence, $\mathcal{R}(i)$ is computed correctly by the induction hypothesis. Hence, letting $x = \mathcal{C} \cap \mathcal{F}_i$, we have $x \in \mathcal{R}(i)$. Furthermore, we know that x is connected to u using the curve \mathcal{C} . Therefore, the point u is in $\mathbf{R}_j(\mathcal{R}(i))$, and hence, is added to $\mathcal{R}(j)$ in Line 2. Similarly, we can show that if $u \notin \mathcal{R}(j)$, then u is not added to $\mathcal{R}(j)$ by the algorithm. Suppose by contradiction that u is added to $\mathcal{R}(j)$ in line 2. Then either $u \in \mathbf{R}_j(L_j \cap \mathcal{F}_j)$ or $u \in \mathbf{R}_j(\mathcal{R}(i))$, for some $i < j$. But by the definition of reachability, both cases imply that u is reachable from a point in \mathbb{L} , which is a contradiction.

For the time complexity, note that each $\mathbf{R}_j(\mathcal{R}(i))$ in Line 2 can be computed in $O(n)$ time using Lemma 27. Moreover, $\mathbf{R}_j(L_j \cap \mathcal{F}_j)$, for each $j \in V$, can be computed by finding the largest feasible interval on \mathcal{F}_j containing L_j in $O(n)$ time. Therefore, processing each edge (i, j) takes $O(n)$ time, and hence, the whole computation takes $O(nm)$ time. Once the algorithm finds a reachable left endpoint v , we can construct

a feasible monotone path connecting a right endpoint $u \in \mathbb{L}$ to v by keeping, for each reachable interval I on $R(j)$, a back pointer to a reachable interval J on $R(i)$, $(i, j) \in E$, from which I is reachable. The path $u \rightsquigarrow v$ can be constructed by following the back pointers from v to u , in $O(m)$ time. For the optimization problem, we use parametric search as in [7, 8] to find the value of $\delta_F(P, \pi)$ by an extra $\log(nm)$ -factor, namely, in $O(nm \log(nm))$ time. \square

Note that Algorithm 12 only works if the input graph is a DAG, because it needs a topological ordering on the vertices in order to sequentially propagate reachability information. By the way, it is straight-forward to modify the algorithm to allow paths in G to start and end anywhere inside edges of the graph, not necessarily at the vertices. This can be easily done by allowing the feasible path found by our algorithm to start and end at any feasible point on the left and right boundary of \mathcal{FD}_{ij} , for each edge $(i, j) \in E$.

5.6 Conclusions

In this chapter, we presented improved algorithms for several variants of the Fréchet distance problem. Our improved results are based on a new data structure, called free-space map, that might be applicable to other problems involving the Fréchet metric. It remains open whether the same improvements obtained here can be achieved for matching curves inside general graphs (see the next section where for complete graphs, we present some improvement). Proving a lower bound better than $\Omega(n \log n)$ is another major problem left open.

Preliminary results of this chapter are presented in the 19th Annual European Symposium on Algorithms (ESA 2011) [49]. The full version of the paper is accepted for publication in *Algorithmica* [51].

Chapter 6

Curve-Pointset Matching Problem (CPM)

Given a point set S and a polygonal curve P in \mathbb{R}^d , we study the problem of finding a polygonal curve Q whose vertices are from S and has minimum Fréchet distance to P . Not all points in S are required to be on Q . Furthermore, a point in S may be present multiple times on Q . We refer to this problem as Curve-Pointset Matching (CPM) Problem. We present an efficient algorithm to solve the decision version of this problem in $O(nk^2)$ time, where n and k represent the sizes of P and S , respectively. Furthermore, if the answer to the decision problem is affirmative, our algorithm can compute the curve with minimum number of segments in ε -Fréchet distance to P . In addition, we show that a curve minimizing the Fréchet distance can be computed in $O(nk^2 \log(nk))$ time. As a by-product, we improve the map matching algorithm of Alt *et al.* by an $O(\log k)$ factor for the case when the map is a complete graph.

6.1 Introduction

In this chapter, we address the following variant of the Fréchet distance problem. Given a point set S and a polygonal curve P in \mathbb{R}^d ($d \geq 2$), find a polygonal curve Q , with its vertices chosen from S , such that the Fréchet distance between P and Q is minimum. Note that in our problem definition, not all points in S need to be chosen as well as a point in S can appear more than once as a vertex in Q . In the decision version of the problem, we want to decide if there is polygonal curve Q through S whose Fréchet distance to P is at most ε , for a given $\varepsilon \geq 0$. An instance of the decision problem is illustrated in Figure 6.1.

One can use the map matching algorithm of Alt *et al.* [7] (described in Section 2.3.2) to solve the decision version of this problem by constructing a complete graph G on top of S , and then running Alt *et al.*'s algorithm on G and P . If n and k represent the sizes of P and S , respectively, this leads to a running time of $O(nk^2 \log k)$ for

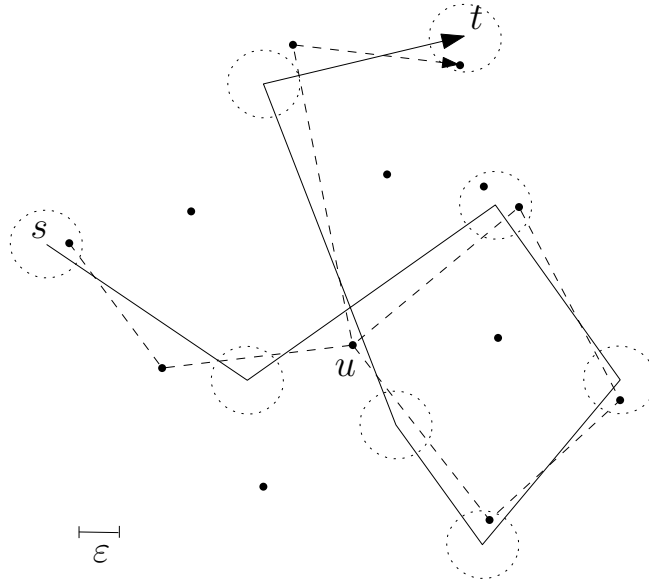


Figure 6.1. A problem instance. The dashed curve is in ε -Fréchet distance to the solid curve. Point u is used multiple times in the dashed curve.

solving the decision problem.

In this chapter, we present a simple algorithm to solve the decision version of the above problem in $O(nk^2)$ time. This improves upon the algorithm of Alt *et al.* [7] by a $O(\log k)$ factor for the case when a curve is matched in a complete graph. Our approach is different from and simpler than the approach taken by Alt *et al.* which is a mixture of line sweep, dynamic programming, and Dijkstra's algorithm.

6.2 Preliminaries

Let $\varepsilon \geq 0$ be a real number, and $d \geq 2$ be a fixed integer. For any point $p \in \mathbb{R}^d$, we define $\mathcal{B}(p, \varepsilon) \equiv \{q \in \mathbb{R}^d : \|pq\| \leq \varepsilon\}$ to be a *ball* of radius ε centered at p , where $\|\cdot\|$ denotes the Euclidean distance. Given a line segment $L \subset \mathbb{R}^d$, we define $\mathcal{C}(L, \varepsilon) \equiv \cup_{p \in L} \mathcal{B}(p, \varepsilon)$ to be a *cylinder* of radius ε around L (see Figure 6.2).

A curve in \mathbb{R}^d can be represented as a continuous function $P : [0, 1] \rightarrow \mathbb{R}^d$. Given two points $u, v \in P$, we write $u \prec v$, if u is located before v on P . The relation \preceq is defined analogously. For a subcurve $R \subseteq P$, we denote by $\text{left}(R)$ and $\text{right}(R)$ the first and the last point of R along P , respectively.

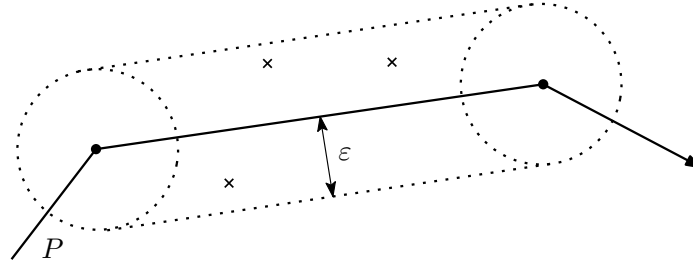


Figure 6.2. A cylinder of radius ε around segment L .

Given two curves $\alpha, \beta : [0, 1] \rightarrow \mathbb{R}^d$, the *Fréchet distance* between α and β is defined as $\delta_F(\alpha, \beta) = \inf_{\sigma, \tau} \max_{t \in [0, 1]} \|\alpha(\sigma(t)), \beta(\tau(t))\|$, where $\sigma, \tau : [0, 1] \rightarrow [0, 1]$ range over all continuous non-decreasing surjective functions. The following two observations are immediate.

Observation 10 *Given four points $a, b, c, d \in \mathbb{R}^d$, if $\|ab\| \leq \varepsilon$ and $\|cd\| \leq \varepsilon$, then $\delta_F(\vec{ac}, \vec{bd}) \leq \varepsilon$.*

Observation 11 *Let $\alpha_1, \alpha_2, \beta_1$, and β_2 be four curves such that $\delta_F(\alpha_1, \beta_1) \leq \varepsilon$ and $\delta_F(\alpha_2, \beta_2) \leq \varepsilon$. If the ending point of α_1 (resp., β_1), is the same as the starting point of α_2 (resp., β_2), then $\delta_F(\alpha_1 + \alpha_2, \beta_1 + \beta_2) \leq \varepsilon$, where $+$ denotes the concatenation of two curves.*

6.3 The Decision Algorithm

Let P be a polygonal curve composed of n line segments P_1, \dots, P_n , and let S be a set of k points in \mathbb{R}^d . In this section, we provide an algorithm to decide whether there exists a polygonal curve Q whose vertices are chosen from S , such that $\delta_F(P, Q) \leq \varepsilon$, for a given $\varepsilon \geq 0$.

We denote by s and t the starting and the ending point of P , respectively. For each segment P_i of P , we denote by C_i the cylinder $\mathcal{C}(P_i, \varepsilon)$, and by S_i the set $S \cap C_i$. Furthermore, for each point $u \in C_i$, we denote by $P_i[u]$ the line segment $P_i \cap \mathcal{B}(u, \varepsilon)$.

We call a polygonal curve Q *feasible* if all its vertices are from S , and $\delta_F(Q, P') \leq \varepsilon$ for a subcurve $P' \subseteq P$ starting at s . If Q ends at a point $v \in S$ and P' ends at a

point $p \in P$, we call the pair (v, p) a *feasible pair*. A point $v \in S_i$ is called *reachable* (at cylinder C_i) if there is a feasible curve ending at v in C_i .

Consider a feasible curve Q starting at a point $u \in S_1$ and ending at a point $v \in S_i$. Since no backtracking is allowed in the definition of Fréchet distance, Q traverses all cylinders C_1 to C_i in order, until it reaches v . Moreover, by our definition of reachability, each vertex of Q is reachable at some cylinder C_j , $1 \leq j \leq i$.

Our approach for solving the decision problem is to process the cylinders one by one from C_1 to C_n , and identify at each cylinder C_i all points of S which are reachable at C_i . The decision problem will be then reduced (by Observation 11) to checking whether there is a reachable point in the ball $\mathcal{B}(t, \varepsilon)$.

To propagate the reachability information through the cylinders, we need a primitive operation described below. Let $u \in S_i$ be a point reachable at cylinder C_i , and let Q be a feasible curve ending at u . For each point $v \in S$, we denote by $r_i(u, v)$ the index of the furthest cylinder we can reach by the curve $Q + \vec{uv}$. In other words, $r_i(u, v)$ is the largest index $\ell \geq i$ such that $v \in S_\ell$ is reachable via $u \in S_i$. If $Q + \vec{uv}$ is not feasible, we set $r_i(u, v) = 0$. The following lemma is a direct corollary of a similar one proved in [7] (Lemma 3) for computing the so-called right pointers.

Lemma 36 ([7]) *Given two points $u, v \in S$, we can compute $r_i(u, v)$ for all $1 \leq i \leq n$ in $O(n)$ total time.*

We use the following lemma for our algorithm.

Lemma 37 *Let $r_i(u, v) = \ell$. For all $i \leq j \leq \ell$, if $v \in S_j$, then v is reachable at C_j .*

Proof: Let Q be a feasible curve starting at a point $w \in S \cap \mathcal{B}(s, \varepsilon)$ and ending at u , and let $Q' = Q + \vec{uv}$. Since v is reachable at C_ℓ via Q' , there is a subcurve P' of P starting at s and ending at a point $p \in P_\ell[v]$ (see Figure 6.3). Consider two point objects \mathcal{O}_P and \mathcal{O}_Q traversing P' and Q' , respectively, from beginning to end, while keeping ε distance to each other. Since v is reachable via $u \in S_i$, \mathcal{O}_P is at a point $a \in P_i$ when \mathcal{O}_Q is at u . Fix a cylinder C_j , $i < j \leq \ell$, such that $v \in C_j$. When \mathcal{O}_P reaches the point $b = \text{left}(P_j[v])$, \mathcal{O}_Q is at a point $x \in \vec{uv}$ such that $\|bx\| \leq \varepsilon$.

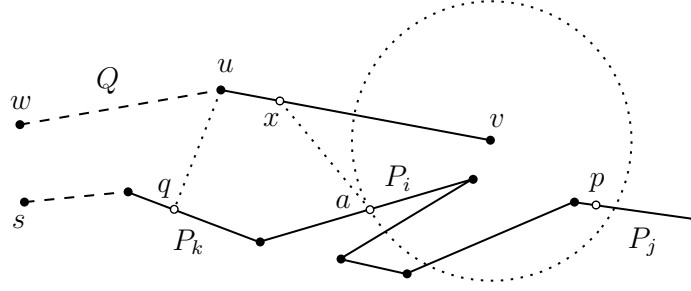


Figure 6.3. Proof of Lemma 37

The subcurve of Q' from w to x has Fréchet distance at most ε to the subcurve of P from s to b , and the segment \overline{xv} has Fréchet distance at most ε to the point b by Observation 10. Therefore, by Observation 11, the whole curve Q' has Fréchet distance at most ε to the subcurve P' from s to b , meaning that v is reachable at C_j . \square

The above proof, not only shows that v is reachable at C_j , but also that the pair $(v, \text{left}(P_j[v]))$ is feasible. The following lemma is therefore immediate.

Lemma 38 *If $r_i(u, v) = \ell$ and $v \in S_j$, $i < j \leq \ell$, then $(v, \text{left}(P_j[v]))$ is a feasible pair.*

The Algorithm Our algorithm for solving the decision problem is provided in Algorithm 13. It maintains, for each cylinder C_i , a set \mathcal{R}_i of all points in S_i which are reachable at C_i . To handle the base case more easily, we assume, w.l.o.g., that the curve P starts with a segment P_0 consisting of a single point $\{s\}$. Every point of S inside the cylinder $C_0 = \mathcal{B}(s, \varepsilon)$ is reachable by definition. Therefore, we initially set $\mathcal{R}_0 = S \cap \mathcal{B}(s, \varepsilon)$ (in line 4).

For each point $v \in S$, the algorithm maintains an index ℓ_v , whose value at the beginning of each iteration i is the following: $\ell_v = \max_{0 \leq j < i, u \in \mathcal{R}_j} r_j(u, v)$. In other words, ℓ_v points to the largest index ℓ for which v is reachable at C_ℓ via a reachable point u in some earlier cylinder C_j , $j < i$. Initially, we set $\ell_v = 1$ for all points in \mathcal{R}_0 , because all points in \mathcal{R}_0 are also reachable in C_1 , as $C_0 \subseteq C_1$. For all other

Algorithm 13 DECISION(S, P, ε)

```

1: Initialize:
2:   compute  $r_i(u, v)$  for all  $u, v \in S$  and  $1 \leq i \leq n$ 
3:   set  $\ell_v = 0$  for all  $v \in S$ 
4:   let  $\mathcal{R}_0 = S \cap \mathcal{B}(s, \varepsilon)$ 
5:   set  $\ell_v = 1$  for all  $v \in \mathcal{R}_0$ 
6: for  $i = 1$  to  $n$  do
7:   let  $\mathcal{R}_i = \{v \in S_i : \ell_v \geq i\}$ 
8:   let  $q = \min_{v \in \mathcal{R}_i} \text{left}(P_i[v])$ 
9:   for all  $v \in S_i \setminus \mathcal{R}_i$  do
10:    if  $q \preceq \text{right}(P_i[v])$  then
11:      add  $v$  to  $\mathcal{R}_i$ 
12:   for all  $(u, v) \in \mathcal{R}_i \times S$  do
13:      $\ell_v \leftarrow \max\{\ell_v, r_i(u, v)\}$ 
14: return YES if  $\mathcal{R}_n \cap \mathcal{B}(t, \varepsilon) \neq \emptyset$ 

```

points, ℓ_v is set to 0 in the initialization step. The following invariant holds during the execution of the algorithm.

Lemma 39 *After the i -th iteration of Algorithm 13, the set \mathcal{R}_i consists of all points in S_i which are reachable at cylinder C_i .*

Proof: We prove the lemma by induction on i . The base case $i = 0$ trivially holds. Suppose by induction that, for each $0 \leq j < i$, the set \mathcal{R}_j is computed correctly. In the i -th iteration, we first add to \mathcal{R}_i (in Line 7) all points in S_i which are reachable through a point in a set \mathcal{R}_j , for $1 \leq j < i$. We call these points *entry points* of cylinder C_i . We then add to \mathcal{R}_i in lines 8–11 all points in S_i which are reachable through the entry points of C_i (see Figure 6.4 for an example).

We first show that all points added to \mathcal{R}_i are reachable at C_i . For each point $v \in S_i$ added to \mathcal{R}_i in Line 7, we have $\ell_v \geq i$. It means that there is a point $u \in \mathcal{R}_j$, for some $j < i$, such that $r_j(u, v) \geq i$. Therefore, Lemma 37 implies that v is reachable

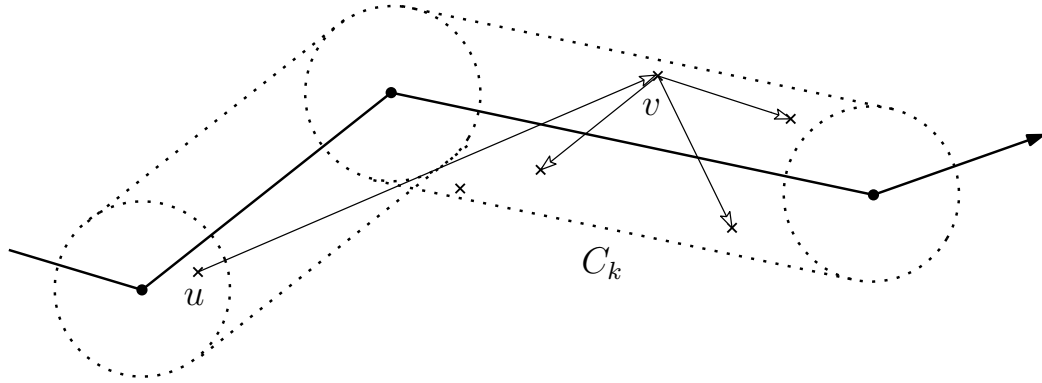


Figure 6.4. Point v is an entry point of C_i .

at C_i . Now, consider a point v added to \mathcal{R}_i in line 11. According to the condition in line 10, there is an entry point w in C_i such that $\text{left}(P_i[w]) \preceq \text{right}(P_i[v])$. By Observation 10, the segment \overrightarrow{wv} is within ε Fréchet distance to the line segment from $\text{left}(P_i[w])$ to $\text{right}(P_i[v])$. Moreover, by Lemma 38, $(w, \text{left}(P_i[w]))$ is a feasible pair. Therefore, by Observation 11, v is reachable.

Next, we show that any reachable point at C_i is added to \mathcal{R}_i by the algorithm. Suppose that there is a point $v \in S_i$ which is reachable at C_i , but is not added to \mathcal{R}_i . Let Q be a feasible curve ending at v , and w be the first point on Q which is reachable at C_i . By our definition, w is an entry point of C_i . If $w = v$, then v must be added to R_i in Line 7, which is a contradiction. If w is before v on Q , then we have $\text{left}(P_i[w]) \preceq \text{right}(P_i[v])$. Now, by our selection of q in Line 8, we have $q \preceq \text{left}(P_i[w]) \preceq \text{right}(P_i[v])$, and hence, v is added to R_i in line 11, which is again a contradiction. \square

Theorem 40 *Given a polygonal curve P of n segments and a set S of k points in \mathbb{R}^d , we can decide in $O(nk^2)$ time whether there is a polygonal curve Q through S such that $\delta_F(P, Q) \leq \varepsilon$, for a given $\varepsilon \geq 0$. A polygonal curve Q through S of size $O(\min\{n, k\})$ minimizing $\delta_F(P, Q)$ can be computed in $O(nk^2 \log(nk))$ time.*

Proof: The correctness of the decision algorithm (Algorithm 13) directly follows from Lemma 39. Line 2 of the algorithm takes $O(nk^2)$ time by Lemma 36. The other three

lines in the initialization step (lines 3–5) take only $O(k)$ time. In the main loop, lines 7–11 take $O(k)$ time, and lines 12–13 require $O(k^2)$ time. Therefore, the whole loop takes $O(nk^2)$ time in total.

Once the algorithm finds a reachable point $v \in S_n \cap \mathcal{B}(t, \varepsilon)$, we can construct a feasible curve Q ending at v by keeping, for each reachable point u at a cylinder C_i , a back-pointer to a reachable point w at C_j , $j \leq i$, from which u is reachable. The feasible curve Q can be then constructed by following the back pointers from v to a point in $S_1 \cap \mathcal{B}(s, \varepsilon)$. Since at most two points from each cylinder are selected in this process, the curve Q has $O(\min\{n, k\})$ segments. For the optimization problem, we use parametric search as in [7, 8], to find a curve minimizing $\delta_F(P, Q)$ by an extra $\log(nk)$ -factor in $O(nk^2 \log(nk))$ time. \square

6.4 Conclusions

In this chapter, we presented a simple efficient algorithm for finding a polygonal curve through a given point set S in \mathbb{R}^d such that its Fréchet distance to a given polygonal curve P is minimized. Several interesting problems remain open. For a fixed ε , one can easily modify the algorithm provided here to find a curve with a minimum number of segments, having Fréchet distance at most ε to P . It can be done by keeping reachable points in a priority queue, and propagating the reachability information in a Dijkstra-like manner. However, we cannot see any easy adaptation of our algorithm to find a curve passing through a maximum number of points for a fixed ε .

The algorithm presented in this chapter improves the map matching algorithm of Alt *et al.* [7] for the case of matching a curve in a complete graph. The current lower bound available for the problem is $\Omega((n+k) \log(n+k))$ due to Buchin *et al.* [16]. It is therefore open whether a better algorithm is available, or whether the algorithm obtained in this chapter is optimal.

Results of this chapter are presented in 23rd Canadian Conference on Computational Geometry [50].

Chapter 7

All-Points CPM Problem is NP-complete

7.1 Introduction

In this chapter, we study a variant of the problem discussed in the previous chapter. We refer to this variant as the All-Points CPM problem. We address the following: Consider a pointset $S \subseteq \mathbb{R}^d$ and a polygonal curve P in \mathbb{R}^d , for $d \geq 2$ being a fixed dimension. The objective is to decide whether there exists a polygonal curve Q in ε -Fréchet distance to P such that the vertices of Q are all chosen from the pointset S . Moreover, curve Q has to visit every point of S and it can visit a point multiple times. We prove that this problem is NP-complete by reducing from 3CNF-SAT problem. In an independent work [1] (which is done after our NP-completeness result), the authors have shown that the version of this problem where points in S has to be visited only once, is NP-complete too. Their proof is obtained via reduction from a restricted version of the 3SAT problem, called (3,B2)-SAT problem, where the input to formulas is restricted in which each literal occurs exactly twice. In [60], Wylie and Zhu studied All-points CPM problem from the perspective of discrete Fréchet distance and they showed that it is solvable in $O(nk)$ time (n is the size of curve P and k is the size of pointset S). Furthermore, they showed that the version of the problem in which each point of S can only used once in Q is NP-complete.

7.2 General Case is NP-complete

7.2.1 Preliminaries

Notation. We denote by $P = \langle p_1 p_2 p_3 \dots p_n \rangle$, a polygonal curve P with vertices $p_1 p_2 \dots p_n$ in order and by $start(P)$ and $end(P)$, we denote the starting and ending point of P , respectively. For a curve P and a point x , by $P \oplus x$, we mean connecting $end(P)$ to point x . We use the same notation $P \oplus Q$ to show the concatenation of two

curves P and Q (which means connecting $end(P)$ to $start(Q)$). Let $M(\overline{ab})$ denote the midpoint of line segment \overline{ab} . For a point q in the plane, let $x(q)$ and $y(q)$ denote the x and y coordinate of q , respectively.

For two intersecting line segments \overline{ab} and \overline{cd} , let $\overline{ab} \dashv \overline{cd}$ denote the intersection point of them. Let \overleftrightarrow{bc} denote the line as a result of extending line segment \overline{bc} . For a point p and a line segment \overline{bc} , let $p \perp \overline{bc}$ denote the point on line \overleftrightarrow{bc} , located on the perpendicular from p to \overleftrightarrow{bc} .

Definition 2 Given a pointset S in the plane, let $Curves(S)$ be a set of polygonal curves $Q = \langle q_1 q_2 \dots q_n \rangle$ where:

$$\forall q_i : q_i \in S \text{ and } \forall a \in S : \exists q_i \text{ s.t. } q_i = a.$$

Definition 3 Given a pointset S , a polygonal curve P and a distance ε , a polygonal curve Q is called feasible if: $Q \in Curves(S)$ and $\delta_F(P, Q) \leq \varepsilon$.

We show that the problem of deciding whether a feasible curve exists or not is NP-complete. It is easy to see that this problem is in NP, since one can polynomially check whether $Q \in Curves(S)$ and also $\delta_F(P, Q) \leq \varepsilon$, using the algorithm in [8] (explained in Section 2.1).

7.2.2 Reduction Algorithm

We reduce in Algorithm 14, an instance of 3CNF-SAT formula ϕ to an instance of our problem. The input is a boolean formula ϕ with k clauses C_1, C_2, \dots, C_k and n variables x_1, x_2, \dots, x_n and the output is a pointset S , a polygonal curve P in the plane and a distance $\varepsilon = 1$.

We construct the pointset S as follows. For each clause C_j , $1 \leq j \leq k$, in the formula ϕ , we place three points $\{s_j, g_j, c_j\}$ in the plane, which are computed in the j -th iteration of Algorithm 14 (from Line 3 to Line 13). We define o_j to be $M(\overline{s_j g_j})$. By \mathcal{SQ}_j , $1 \leq j \leq k$, we denote a square in the plane, centered at o_j , with diagonal $\overline{s_j g_j}$. We refer to \mathcal{SQ}_j , $1 \leq j \leq k$, as c -squares. For an example of a pointset S corresponding to a formula, see Figure 7.1a.

Our reduction algorithm constructs the polygonal curve P through n iterations. In the i -th iteration, $1 \leq i \leq n$, it builds a subcurve l_i corresponding to a variable x_i in the formula ϕ and appends that curve to P . In addition to those n subcurves, two curves l_{n+1} and l_{n+2} are appended to P . We will later discuss the reason we add those two curves. Every subcurve l_i of P starts at point u and ends at point v . Furthermore, each l_i goes through \mathcal{SQ}_1 to \mathcal{SQ}_k in order, enters each c-square \mathcal{SQ}_j from the side $\overline{c_j s_j}$ and exists that square from the side $\overline{c_j g_j}$ (for an illustration, see Figure 7.1a). Curve l_i itself is built incrementally through iterations of the loop at line 29 of Algorithm 14. In the j -th iteration, when l_i goes through \mathcal{SQ}_j , three points, which are within \mathcal{SQ}_j , are added to l_i (these three points are computed through Lines 30 to 35). Next, before l_i reaches \mathcal{SQ}_{j+1} , two points, denoted by α_j and β_j , are added to that curve (these two points are computed in Lines 37 and 38).

Each l_i corresponds to variable x_i in our approach. We simulate 1 or 0 values of x_i as follows. Consider a point object \mathcal{O}_L traversing l_i , from starting point u to ending point v . Consider another point object \mathcal{O}_2 which wants to walk from u to v on a path whose vertices are from points in S and it wants to stay in distance one to \mathcal{O}_L . We will show that by our construction, object \mathcal{O}_2 has two options, either taking the path $A = \langle u s_1 g_2 s_3 \dots v \rangle$ or the path $B = \langle u g_1 s_2 g_3 \dots v \rangle$ (See Figure 7.1a and 7.1b for an illustration). Choosing path A by \mathcal{O}_2 means $x_i = 1$ and choosing path B means $x_i = 0$. We first prove in Lemma 41 that $\delta_F(l_i, A) \leq 1$ and in Lemma 42 that $\delta_F(l_i, B) \leq 1$. Furthermore, in Lemma 43, we prove that as soon as \mathcal{O}_2 chooses path A at point u to walk towards v , it can not switch to any vertex on path B . Analogously, we show that as soon as \mathcal{O}_2 chooses path B at point u to walk towards v , it can not switch to any vertex on path A . In addition, in Lemmas 44 and 45, we prove that if x_i appears in clause C_j , \mathcal{O}_2 could visit point c_j via the path A and not B . In contrast, when $\neg x_i$ appears in the clause C_j , \mathcal{O}_2 could visit point c_j via the path B and not A . However, when none of x_i or $\neg x_i$ appear in C_j , \mathcal{O}_2 can take neither A nor B to visit c_j . Thus, c_j can be visited, if and only if there is an i such that either x_i or $\neg x_i$ are in clause C_j .

Algorithm 14 REDUCTION ALGORITHM**Input:** 3SAT formula ϕ with k clauses $C_1 \dots C_k$ and n variables $x_1 \dots x_n$ **Construct pointset S :**

```

1:  $S \leftarrow \emptyset$ 
2:  $g_1 = (1, 1)$ 
3: for  $j = 1$  to  $k$  do
4:    $s_j \leftarrow (x(g_j) - 2, y(g_j) - 2)$ 
5:    $o_j \leftarrow M(\overline{s_j g_j})$ 
6:   if ( $j$  is odd) then
7:      $c_j \leftarrow (x(s_j), y(g_j)), w_j \leftarrow (x(o_j) + \frac{1}{4}, y(o_j) - \frac{1}{4})$ 
8:      $g_{j+1} \leftarrow (x(s_j) + \frac{1}{4} + 8, y(s_j) + \frac{7}{4} + 15)$ 
9:   else
10:     $c_j \leftarrow (x(g_j), y(s_j)), w_j \leftarrow (x(o_j) - \frac{1}{4}, y(o_j) + \frac{1}{4})$ 
11:     $g_{j+1} \leftarrow (x(s_j) + \frac{7}{4} + 15, y(s_j) + \frac{1}{4} + 8)$ 
12:     $z_j = M(\overline{c_j w_j})$ 
13:     $S = S \cup \{s_j, g_j, c_j\}$ 
14:   if ( $k$  is odd) then
15:      $\eta \leftarrow (x(o_k) + 1, y(o_k) + 4)$ 
16:      $v \leftarrow (x(o_k) + 1, y(o_k) + 9)$ 
17:   else
18:      $\eta \leftarrow (x(o_k) + 4, y(o_k) + 1)$ 
19:      $v \leftarrow (x(o_k) + 9, y(o_k) + 1)$ 
20:    $u = (-9, -1)$ 
21:    $t \leftarrow (x(v), y(u) - 20)$ 
22:    $S = S \cup \{u, v, t\}$ 

```

Construct polygonal curve P :

```

23:  $P \leftarrow \emptyset$ 
24:  $P \leftarrow P \oplus t$ 
25: for  $i = 1$  to  $n + 2$  do
26:    $l_i \leftarrow \emptyset$ 
27:    $l_i \leftarrow l_i \oplus u$ 
28:    $l_i \leftarrow l_i \oplus (-4, -1)$ 
29:   for  $j = 1$  to  $k$  do
30:     if ( $x_i \in C_j$  and  $j$  is odd ) or ( $\neg x_i \in C_j$  and  $j$  is even ) then
31:        $l_i \leftarrow l_i \oplus M(\overline{s_j c_j}) \oplus c_j \oplus w_j$ 
32:     else if ( $\neg x_i \in C_j$  and  $j$  is odd ) or ( $x_i \in C_j$  and  $j$  is even ) then
33:        $l_i \leftarrow l_i \oplus w_j \oplus c_j \oplus M(\overline{g_j c_j})$ 
34:     else
35:        $l_i \leftarrow l_i \oplus w_j \oplus c_j \oplus w_j$ 
36:     if  $j \neq k$  then
37:        $\alpha_j = \frac{4}{5}g_j + \frac{1}{5}g_{j+1}$ 
38:        $\beta_j = \frac{1}{5}s_j + \frac{4}{5}s_{j+1}$ 
39:        $l_i \leftarrow l_i \oplus \alpha_j \oplus \beta_j$ 
40:    $l_i \leftarrow l_i \oplus \eta \oplus v$ 
41:    $P \leftarrow P \oplus l_i$ 
42:    $P \leftarrow P \oplus t$ 
43: return pointset  $S$ , polygonal curve  $P$  and distance  $\varepsilon = 1$ 

```

if $x_i \in C_1$	location of \mathcal{O}_A	location of \mathcal{O}_L
	u h_1 s.t. $\ h_1\mu_1\ \leq \varepsilon$ s_1	u $\mu_1 = (-4, -1)$ $M(\overline{s_1c_1})$
if $\neg x_i \in C_1$	u h_1 s.t. $\ h_1\mu_1\ \leq \varepsilon$ s_1	u $\mu_1 = (-4, -1)$ $\overrightarrow{\mu_1 w_1} \dashv \overline{s_1 c_1}$
if $x_i \notin C_1 \& \neg x_i \notin C_1$	u h_1 s.t. $\ h_1\mu_1\ \leq \varepsilon$ s_1	u $\mu_1 = (-4, -1)$ $\overrightarrow{\mu_1 w_1} \dashv \overline{s_1 c_1}$

Table 7.1. Proof of Lemma 41, the base case of induction

Lemma 41 Consider any subcurve l_i , $1 \leq i \leq n+2$, which is built through Lines 25 to 40 of Algorithm 14. Let A be the polygonal curve $\langle us_1g_2s_3g_4..v \rangle$. Then, $\delta_F(l_i, A) \leq 1$.

Proof: We prove the lemma by induction on the number of segments along A . Consider two point objects \mathcal{O}_L and \mathcal{O}_A traversing l_i and A , respectively (Figure 7.1a depicts an instance of l_i and A). We show that \mathcal{O}_L and \mathcal{O}_A can walk their respective curve, from the beginning to end, while keeping distance 1 to each other.

The base case of induction trivially holds as follows (see Figure 7.2 for an illustration). Table 7.1 lists pairwise locations of \mathcal{O}_L and \mathcal{O}_A , where the distance of each pair is at most 1. Hence, \mathcal{O}_A can walk from u to s_1 on the first segment of A (segment $\overrightarrow{us_1}$), while keeping distance ≤ 1 to \mathcal{O}_L .

Assume inductively that \mathcal{O}_L and \mathcal{O}_A have feasibly walked along their respective curves, until \mathcal{O}_A reached s_j . Then, as the induction step, we show that \mathcal{O}_A can walk to g_{j+1} and then to s_{j+2} , while keeping distance 1 to \mathcal{O}_L . Table 7.2 lists pairwise locations of \mathcal{O}_A and \mathcal{O}_L such that \mathcal{O}_A could reach s_{j+2} . One can easily check that the distance between the pair of points in that table is at most one. (For an illustration, see Figure 7.3).

Finally, if k is an odd number, then $\overrightarrow{s_k v}$ is the last segment along B , otherwise, $\overrightarrow{g_k v}$ is the last one. In either case, that edge crosses the circle $\mathcal{B}(\eta, 1)$, where η is the last vertex of l_i before v (point η is computed in line 14 of Algorithm 14). Therefore, \mathcal{O}_A can walk to v , while keeping distance 1 to \mathcal{O}_L .

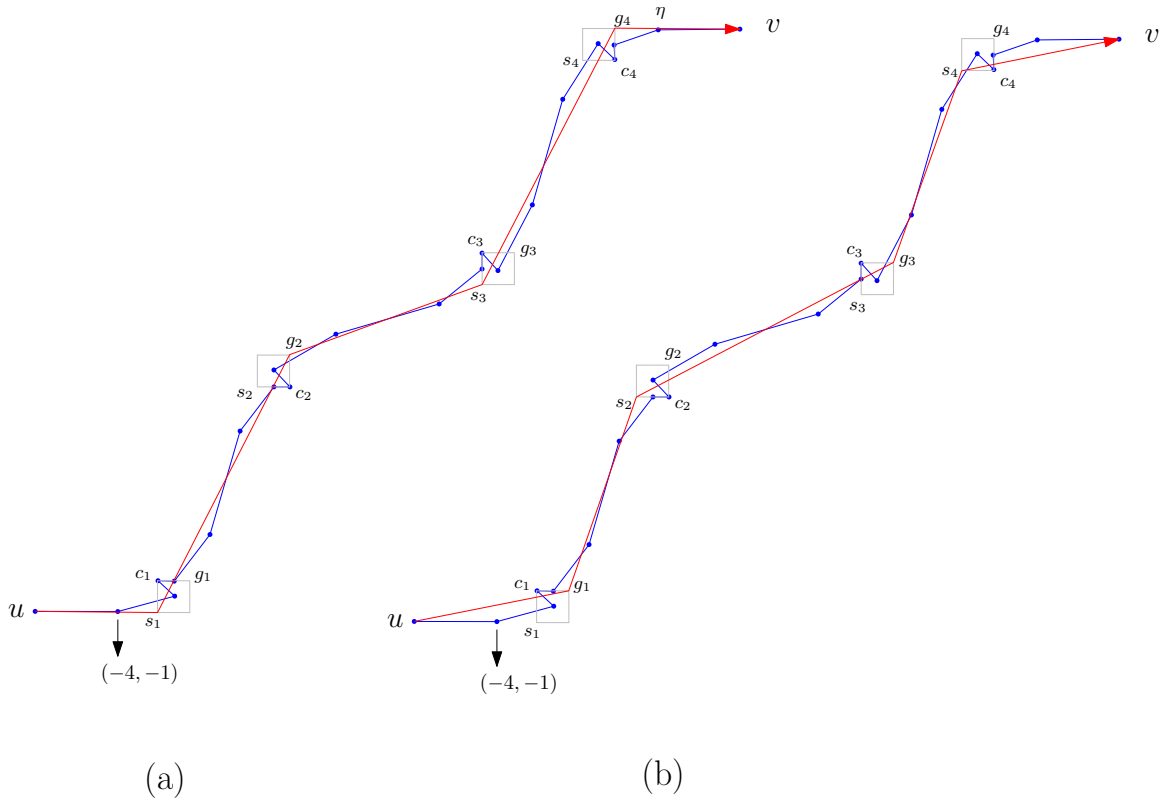


Figure 7.1. Blue curve is an example of curve l_i which corresponds to variable x_i in formula ϕ . The formula has four clauses C_1, C_2, C_3 and C_4 , where the occurrence of variable x_i in those clauses is: $\neg x_i \in C_1, \neg x_i \in C_2, x_i \in C_3$ and $x_i \in C_4$. For each clause C_i , the reduction algorithm places three point s_i, g_i and c_i in the plane. (a) Red curve is curve A . (b) Red curve is curve B .

□

Lemma 42 Consider any subcurve $l_i, 1 \leq i \leq n + 2$, constructed through Lines 25 to 40 of Algorithm 14. Let B be the polygonal curve $\langle u g_1 s_2 g_3 s_4 . v \rangle$. Then, $\delta_F(l_i, B) \leq 1$.

Proof: Consider two point objects \mathcal{O}_L and \mathcal{O}_B traversing l_i and B , respectively (Figure 7.1b depicts an instance of l_i and B). To prove the lemma, we show that \mathcal{O}_L and \mathcal{O}_B can walk along their respective curves, from beginning to the end, while keeping distance 1 to each other.

The base case of induction holds as follows (see Figure 7.4 for an illustration). Table 7.3 lists pairwise locations of \mathcal{O}_L and \mathcal{O}_B , where the distance of each pair is less or equal to 1. Therefore, \mathcal{O}_B can walk from u to g_1 while keep distance one to \mathcal{O}_L .

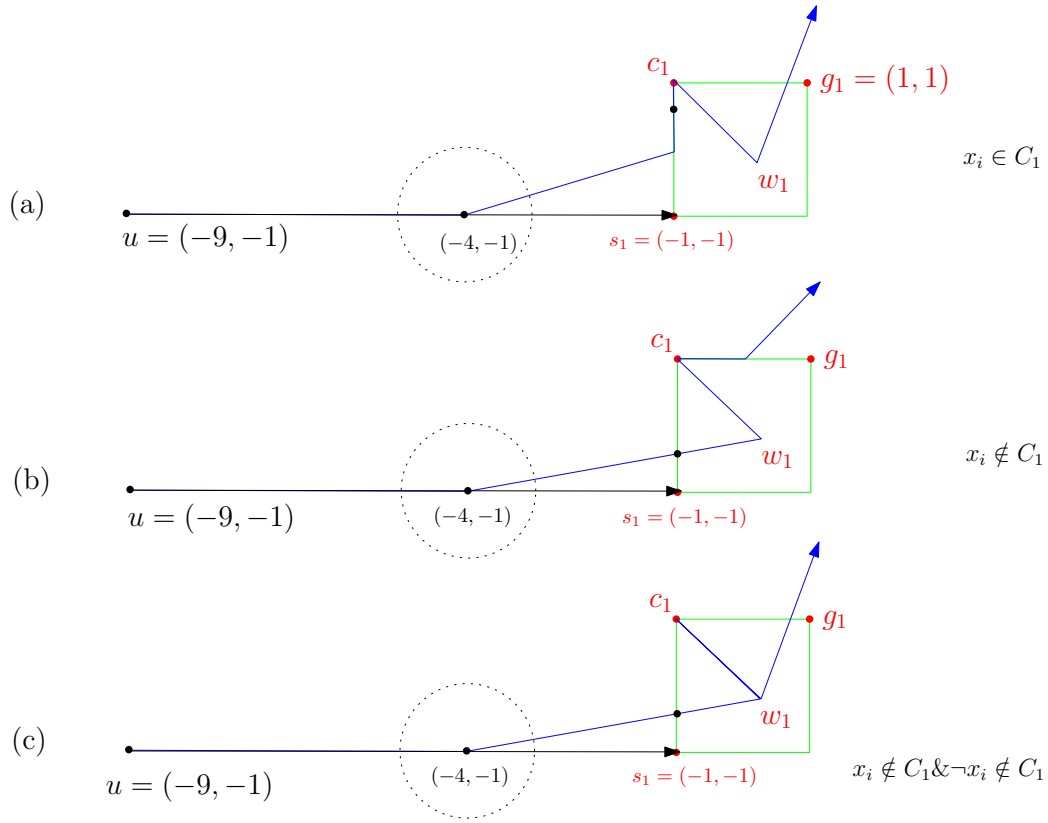


Figure 7.2. Base case of induction in the proof of Lemma 41

Assume inductively that \mathcal{O}_L and \mathcal{O}_B have feasibly walked along their respective curves, until \mathcal{O}_B reached g_j . Then, as the induction step, we show that \mathcal{O}_B can walk to s_{j+1} and then to g_{j+2} , while keeping distance 1 to \mathcal{O}_L . This is shown in Table 7.4 (see Figure 7.5 for an illustration).

Finally, if k is an odd number, then $\overrightarrow{g_k v}$ is the last segment along B , otherwise, $\overrightarrow{s_k v}$ is the last one. In any case, that edge crosses circle $\mathcal{B}(\eta, 1)$, where η is the last vertex of l_i before v (point η is computed after the condition checking in line 14 of Algorithm 14). Therefore, \mathcal{O}_B can walk to v , while keeping distance 1 to \mathcal{O}_L .

□

Lemma 43 Consider any curve $l_i \subset P$, $1 \leq i \leq n + 2$. Imagine that a point object \mathcal{O}_L is walking from u to v on l_i . Furthermore, imagine two point objects \mathcal{O}_A and \mathcal{O}_B

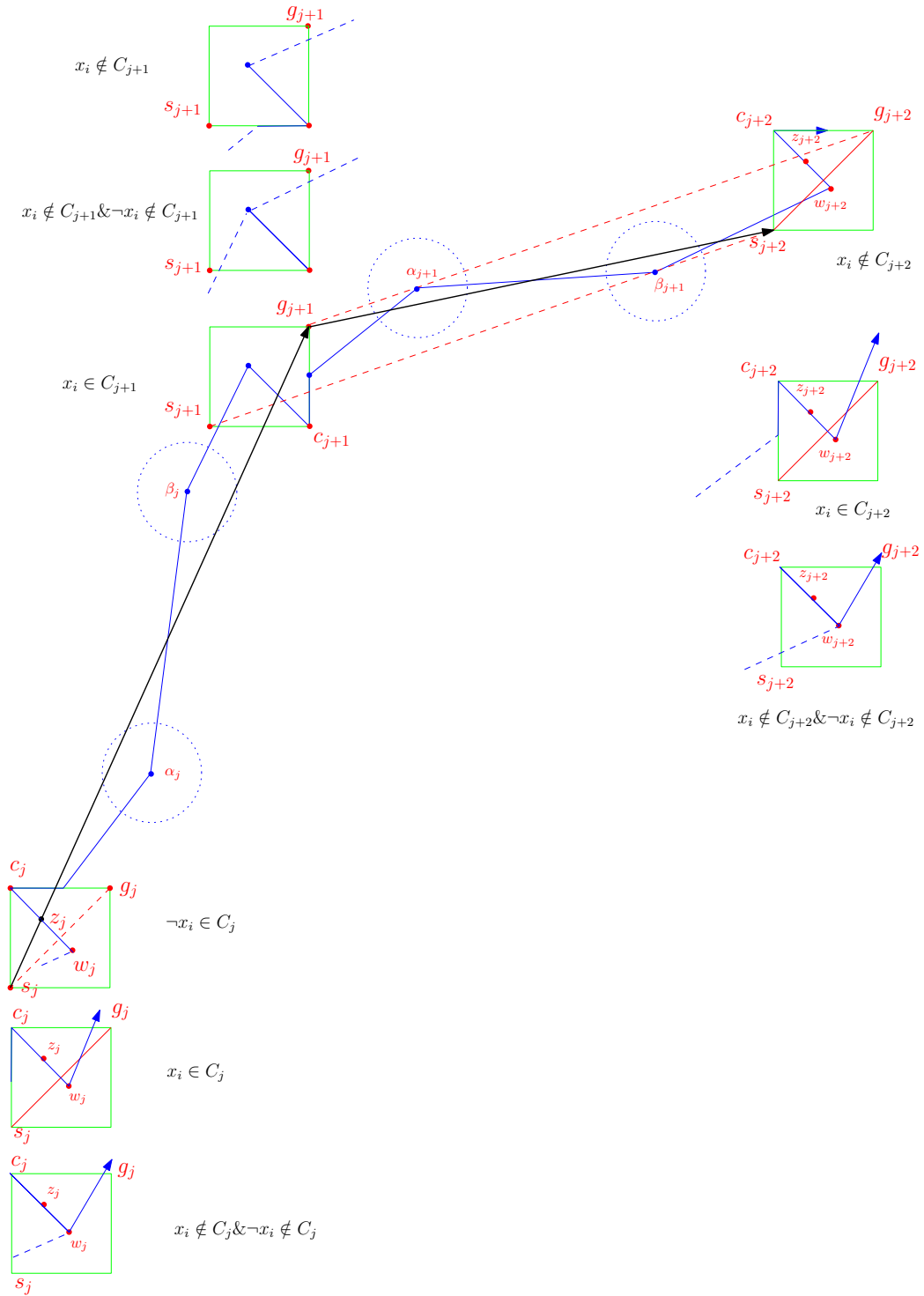


Figure 7.3. Proof of Lemma 41

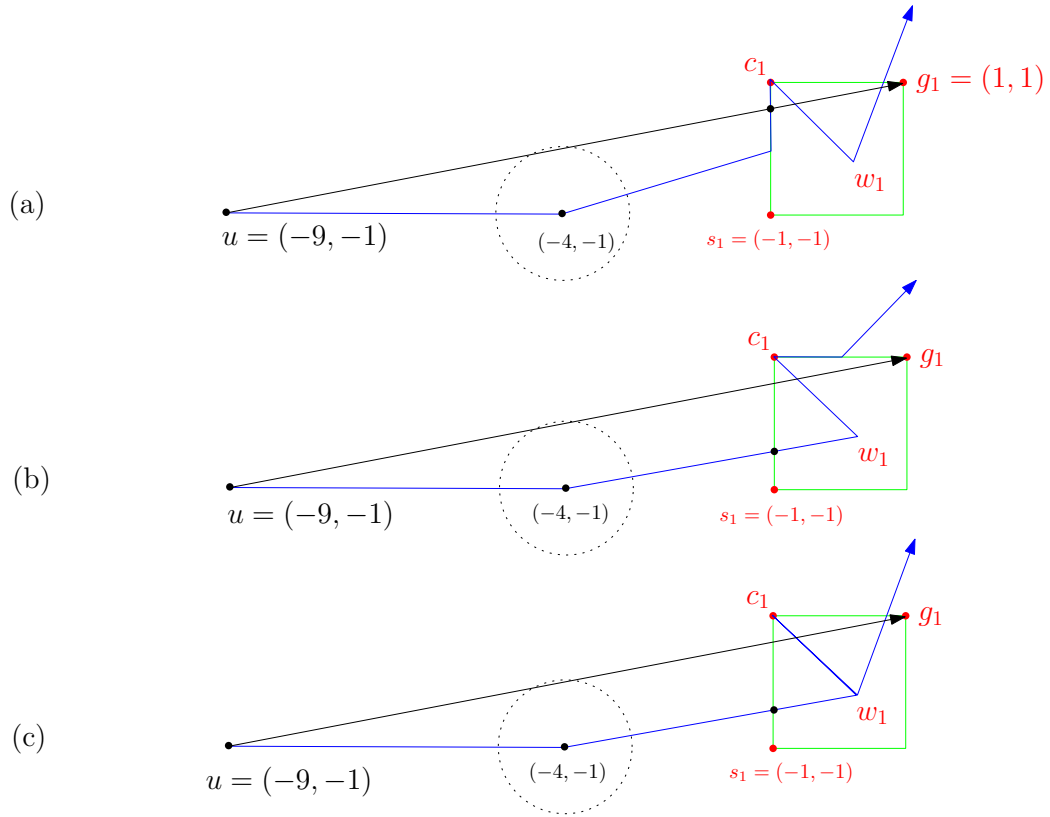


Figure 7.4. Base case of induction in the proof of Lemma 42

which are walking on curves A and B (from Lemmas 41 and 42), respectively, while keeping distance 1 to \mathcal{O}_L . If \mathcal{O}_A goes to any vertex of B or \mathcal{O}_B goes to any vertex of A , then they loose distance ≤ 1 to \mathcal{O}_L .

Proof: Let cl_i refer to points $\{s_i, g_i, c_i\}$. Notice that we have placed the cl_{i+1} points far enough from the cl_i points so that no curve can go to cl_{i+1} and come back to cl_i and stay in Fréchet distance 1 to l_i . Therefore, to prove the lemma, we only focus on two consecutive c-squares. We show that no subcurve $l' \subseteq l_i$ exists such that (for an illustration, see Figure 7.6) :

- $\delta_F(l', \overrightarrow{s_j g_j}) \leq 1$ because:

for all j , $1 \leq j \leq k$, point c_j is always a vertex of l_i . A point on l_i at distance 1 to s_j lies before c_j in direction $\overrightarrow{l_i}$, while a point on l_i at distance 1 to point g_j

lies after c_j in direction \vec{l}_i . Since $\text{dist}(c_j, \overline{s_j g_j}) > 1$, no subcurve $l' \subseteq l_i$ exists such that $\delta_F(l', \overline{s_j g_j}) \leq 1$.

- $\delta_F(l', \langle s_j c_j g_j \rangle) \leq 1$ or $\delta_F(l', \langle g_j c_j s_j \rangle) \leq 1$, because:

For all j , $1 \leq j \leq k$, w_j is a vertex of l_i . A point on l_i at distance 1 to s_j lies before w_j in direction \vec{l}_i , while a point on l_i at distance 1 to point g_j lies after w_j in direction \vec{l}_i . Since $\text{dist}(w_j, \overline{s_j c_j}) > 1$ and $\text{dist}(w_j, \overline{g_j c_j}) > 1$, no subcurve $l' \subseteq l_i$ exists such that $\delta_F(l', \langle s_j c_j g_j \rangle) \leq 1$. Similarly, no subcurve $l' \subseteq l_i$ exists such that $\delta_F(l', \langle g_j c_j s_j \rangle) \leq 1$.

- $\delta_F(l', \langle s_j s_{j+1} \rangle) \leq 1$ or $\delta_F(l', \langle g_j g_{j+1} \rangle) \leq 1$ because:

Vertex α_i of l_i guarantees the first part as $\text{dist}(\alpha_i, \overline{s_j s_{j+1}}) > 1$, and vertex β_i of l_i guarantees the second part, as $\text{dist}(\beta_i, \overline{g_j g_{j+1}}) > 1$.

- $\delta_F(l', \langle c_j c_{j+1} \rangle) \leq 1$, because $\text{dist}(\alpha_i, \overline{c_j c_{j+1}}) > 1$
- $\delta_F(l', \langle u c_1 \rangle) \leq 1$, because $\text{dist}((-4, -1), \overline{u c_1}) > 1$
- $\delta_F(l', \langle c_j g_{j+1} \rangle) \leq 1$, because $\text{dist}(\alpha_i, \overline{c_j g_{j+1}}) > 1$
- $\delta_F(l', \langle c_j s_{j+1} \rangle) \leq 1$, because $\text{dist}(\alpha_i, \overline{c_j s_{j+1}}) > 1$
- $\delta_F(l', \langle c_k v \rangle) \leq 1$, because $\text{dist}(\eta, \overline{c_k v}) > 1$

□

To establish the correctness of our reduction algorithm, from now on, we define: $(a_i = s_i, b_i = g_i)$, when i is an odd number, and $(a_i = g_i, b_i = s_i)$, when i is an even number, for $1 \leq i \leq k$.

Lemma 44 *Consider the curve $A = \langle u a_1 a_2 a_3 \dots a_k v \rangle$ from Lemma 41. Let A_1 be a subcurve of A which starts at u and ends at a_j , $1 \leq j \leq k$. Furthermore, let A_2 be a subcurve of A which starts at a_j and ends at v . For any curve l_i , $1 \leq i \leq n + 2$, if $x_i \in C_j$, $\delta_F(A_1 \oplus c_j \oplus A_2, l_i) \leq \varepsilon$. Similarly, consider the curve $B = \langle u b_1 b_2 b_3 \dots b_k v \rangle$*

from Lemma 42. Let B_1 be a subcurve of B which starts at u and ends at b_j , $1 \leq j \leq k$. Furthermore, let B_2 be a subcurve of B which starts at b_j and ends at v . For any curve l_i , $1 \leq i \leq n + 2$, if $\neg x_i \in C_j$, $\delta_F(B_1 \oplus c_j \oplus B_2, l_i) \leq \varepsilon$.

Proof: When x_i appears in clause C_j , point $z = M(\overline{c_j a_j})$ is a vertex of l_i . Since $\|c_j a_j\| = 2$ and z is the midpoint of $\overline{c_j a_j}$, \mathcal{O}_L can wait at z while \mathcal{O}_A visits c_j . Therefore, as the lemma states, we can cut curve A at vertex a_j , add two edges $\overrightarrow{a_j c_j}$ and then $\overrightarrow{c_j a_j}$ to A , and continue with the same curve A from a_j to A 's endpoint. For the modified A , still $\delta_F(A, l_i) \leq \varepsilon$ holds.

When $\neg x_i$ appears in clause C_j , point $z = M(\overline{c_j b_j})$ is a vertex of l_i . Since $\|c_j b_j\| = 2$ and z is the midpoint of $\overline{c_j b_j}$, \mathcal{O}_L can wait at z while \mathcal{O}_A visits c_j and comes back to b_j . Therefore, as the lemma says, we can cut curve B at vertex b_j , add two edges $\overrightarrow{b_j c_j}$ and then $\overrightarrow{c_j b_j}$ to B , and continue with the same curve B from b_j to B 's endpoint. For the modified B , still $\delta_F(B, l_i) \leq \varepsilon$ holds.

□

Lemma 45 Consider curve A (respectively, B) from previous lemma. For any curve l_i , $1 \leq i \leq n + 2$, when $x_i \notin C_j$ and $\neg x_i \notin C_j$, curve A (resp., B) can not be modified to visit c_j .

Proof: This holds because $dist(w_j, \overline{a_j c_j}) > 1$ and $dist(w_j, \overline{b_j c_j}) > 1$.

□

Theorem 46 Given a formula ϕ with k clauses C_1, C_2, \dots, C_k and n variables x_1, x_2, \dots, x_n , as input, let curve P and pointset S be the output of Algorithm 14. Then, ϕ is satisfiable iff a curve $Q \in Curves(S)$ exists such that $\delta_F(P, Q) \leq 1$.

Proof: For (\Rightarrow): Assume that formula ϕ is satisfiable. In Algorithm 15, we show that knowing the truth value of the literals in ϕ , we can build a curve Q which visits every point in S and $\delta_F(P, Q) \leq 1$.

First, we show $\delta_F(P, Q) \leq 1$, where Q is the output curve of Algorithm 15. Recall that by Algorithm 14, curve P includes n subcurves l_i each corresponds to a variable

x_i . Both curves P and Q start and end at a same point t . For each curve π which is appended to Q in the i -th iteration of Algorithm 15 (Line 10 or Line 17), $\delta_F(\pi, l_i) \leq 1$ by Lemma 44. Notice that P also includes two additional subcurves l_{n+1} and l_{n+2} whereas there is no variable x_{n+1} and x_{n+2} in formula ϕ . These two curves are to resolve two special cases: when all variables x_i are 1, no $\neg x_i$ appears in ϕ , and when all variables x_i are 0, no x_i appears in ϕ . Because of these two curves, we added two additional curves in line 19 and 21 to Q . Finally, by Observation 11, $\delta_F(P, Q) \leq 1$.

Next, we show that curve Q visits every point in S . First of all, by the curves added to Q in Line 19 and 21, all a_j and b_j , $1 \leq j \leq k$, in S will be visited. It is sufficient to show that Q will visit all c_j points in S as well. Since formula ϕ is satisfied, every clause C_i in ϕ must be satisfied too. Fix clause C_j . At least one of the literals in C_j must have a truth value 1. If $x_i \in C_j$ and $x_i = 1$, then by line 9, curve Q visits c_j . On the other hand, if $\neg x_i \in C_j$ and $x_i = 0$, by Line 16, curve Q visits c_j . We conclude that curve Q is feasible.

Now (\Leftarrow) part:

Let Q be a feasible curve with respect to P and pointset S . Notice that curve P consists of n subcurves l_i , $1 \leq i \leq n$, where each corresponds to one variable x_i . From the configuration of each l_i in c-squares, one can easily construct formula ϕ with all of its clauses and literals.

Imagine two point objects \mathcal{O}_Q and \mathcal{O}_P walk on P and Q , respectively. We find the truth value of variable x_i in the formula by looking at the path that \mathcal{O}_Q takes to stay in Fréchet distance 1 to \mathcal{O}_P , when \mathcal{O}_P walks on curve l_i corresponding to x_i . If \mathcal{O}_Q takes path A from Lemma 41 while \mathcal{O}_P is walking on l_i , then $x_i = 1$. But if \mathcal{O}_Q takes path B from Lemma 42 while \mathcal{O}_P is walking on l_i , then $x_i = 0$. Object \mathcal{O}_Q decides between path A or B , when both \mathcal{O}_Q and \mathcal{O}_P are at point u . Lemma 43 ensures that once they start walking, \mathcal{O}_Q can not change its path from A to B or from B to A . Therefore, the truth value of a variable x_i is consistent.

The only thing left to show is the reason that formula ϕ is satisfiable. It is sufficient to show every clause of ϕ is satisfiable. Consider any clause C_j . Since curve Q is feasible, it uses every point in S . Assume w.l.o.g. that \mathcal{O}_Q visits c_j when \mathcal{O}_P

is walking along curve l_i . By Lemmas 43 and 44, this only happens when either $(x_i$ appears in C_i and $x_i = 1$) or $(\neg x_i$ appears in C_i and $x_i = 0$). Therefore, C_j is satisfiable.

The last ingredient of the NP-completeness proof is to show that the reduction takes polynomial time. One can easily see that Algorithm 14 has running time $O(nk)$, where n is the number of variables in the input formula with k clauses.

□

7.2.3 Implementation Results

To show the simplicity of our reduction algorithm, we have implemented it in Java. The figures in this chapter are all generated by our program. Our test case, as an input to the program, is a formula ϕ with four clauses. The output is three sets S , L and C as follows.

Set S is a pointset computed by Algorithm 14. Since ϕ has four clauses, S contains the following points:

$$S = \{s_1, g_1, c_1, s_2, g_2, c_2, s_3, g_3, c_3, s_4, g_4, c_4, u, v, t\}.$$

Set L is a set of curves, where each of it is a configuration of l_i in the reduction algorithm. Choosing a formula with four clauses as an input, enables us to check all possible configurations of curve l_i built by Algorithm 14. Let x_i be a variable in formula ϕ . Since x_i or $\neg x_i$ or none could appear in a clause, and the formula has four clauses, set L contains 81 curves l_i .

Set C contains all possible curves α , each built in this way: α starts from point u , goes through arbitrary points from $\{g_1, c_1, s_1\}$, then to arbitrary points in $\{g_2, c_2, s_2\}$, next to arbitrary points from $\{g_3, c_3, s_3\}$, and lastly from $\{g_4, c_4, s_4\}$ and at the end, α ends at v . Therefore, set C has almost 1,000,000,000 polygonal curves.

Let α be any curve in C and ℓ be any curve in L . We compute in our program, the Fréchet distance between every curve α and ℓ . Notice that C has huge amounts of curve data. We implemented our program in an efficient way so that we could do this computation in a fair amount of time. First, all 81 curves ℓ are computed and then, by computing each α in C , we compute 81 Fréchet distances $\delta_F(\alpha, \ell)$. Therefore,

in total, almost $81 \times 1,000,000,000$ Fréchet distances have been computed by our program. The experiment is performed on four machines in parallel, each has an Intel(R) Core(TM) i7 CPU 2.67GHz and 12GB RAM.

The results show that in all cases, $\delta_F(\alpha, \ell) > 1$ except for the following cases:

Case I: $\alpha = \langle u, s_1, g_2, s_3, g_4, v \rangle$, then $\delta_F(\alpha, \ell) \leq 1$, for any curve ℓ in L .

Case II: $\alpha = \langle u, g_1, s_2, g_3, s_4, v \rangle$, then $\delta_F(\alpha, \ell) \leq 1$, for any curve ℓ in L .

Case III: $\alpha = \langle u, g_1, c_1, g_1, s_2, g_3, s_4, v \rangle$, then $\delta_F(\alpha, \ell) \leq 1$, for ℓ corresponding to the case where $\neg x_i$ appeared in the first clause.

Case IV: $\alpha = \langle u, s_1, c_1, s_1, g_2, s_3, g_4, v \rangle$, then $\delta_F(\alpha, \ell) \leq 1$, for ℓ corresponding to the case where x_i appeared in the first clause and so on for other occurrence of variable x_i in other clauses.

Case I confirms Lemma 41, case II confirms Lemma 42, cases III and IV confirm Lemma 44, and all together confirm Lemma 43.

7.3 Conclusions

In this chapter, we investigated the problem of deciding whether a polygonal curve through a given pointset S exists, which visits every point in S and is in ε -Fréchet distance to a curve P . We showed that this problem is NP-complete.

	location of \mathcal{O}_A	location of \mathcal{O}_L
if $x_i \in C_j$	s_j z_j	$M(\overline{c_j s_j})$ c_j w_j
if $\neg x_i \in C_j$	$\overline{c_j g_j} \dashv \overline{s_j g_{j+1}}$ s_j $w_j \perp \overline{s_j g_{j+1}}$ z_j	$\overline{w_j \alpha_j} \dashv \overline{c_j g_j}$ $\beta_{j-1} w_j \dashv \overline{c_j s_j}$ w_j z_j c_j
if $x_i \notin C_j \& \neg x_i \notin C_j$	$\overline{c_j g_j} \dashv \overline{s_j g_{j+1}}$ s_j $w_j \perp \overline{s_j g_{j+1}}$ z_j	$M(\overline{c_j g_j})$ $\beta_{j-1} w_j \dashv \overline{c_j s_j}$ w_j z_j c_j w_j
	$\overline{c_j g_j} \dashv \overline{s_j g_{j+1}}$	$\overline{w_j \alpha_j} \dashv \overline{c_j g_j}$
	h_1 s.t. $\ h_1 \alpha_j\ \leq \varepsilon$ h_2 s.t. $\ h_2 \beta_j\ \leq \varepsilon$	α_j β_j
if $x_i \in C_{j+1}$	$\overline{s_{j+1} c_{j+1}} \dashv \overline{s_j g_{j+1}}$ z_{j+1}	$\beta_j w_{j+1} \dashv \overline{c_{j+1} s_{j+1}}$ w_{j+1} z_{j+1} c_{j+1}
if $\neg x_i \in C_{j+1}$	g_{j+1} $\overline{s_{j+1} c_{j+1}} \dashv \overline{s_j g_{j+1}}$ z_{j+1}	$M(\overline{c_{j+1} g_{j+1}})$ $M(\overline{s_{j+1} c_{j+1}})$ c_{j+1} w_{j+1}
if $x_i \notin C_{j+1} \& \neg x_i \notin C_{j+1}$	g_{j+1} $\overline{s_{j+1} c_{j+1}} \dashv \overline{s_j g_{j+1}}$ z_{j+1}	$\overline{g_{j+1} c_{j+1}} \dashv \overline{w_{j+1} \alpha_{j+1}}$ $\beta_j w_{j+1} \dashv \overline{c_{j+1} s_{j+1}}$ w_{j+1} c_{j+1} w_{j+1}
	g_{j+1}	$\overline{g_{j+1} c_{j+1}} \dashv \overline{w_{j+1} \alpha_{j+1}}$
	h_3 s.t. $\ h_3 \alpha_{j+1}\ \leq \varepsilon$ h_4 s.t. $\ h_4 \beta_{j+1}\ \leq \varepsilon$	α_{j+1} β_{j+1}
if $\neg x_i \in C_{j+2}$	s_{j+2}	$\overline{\alpha_{j+1} w_{j+2}} \dashv \overline{c_{j+2} s_{j+2}}$
if $x_i \in C_{j+2}$	s_{j+2}	$M(\overline{c_{j+2} s_{j+2}})$
if $x_i \notin C_{j+2} \& \neg x_i \notin C_{j+2}$	s_{j+2}	$\overline{\alpha_{j+1} w_{j+2}} \dashv \overline{c_{j+2} s_{j+2}}$

Table 7.2. Distance between pair of points is less or equal to one

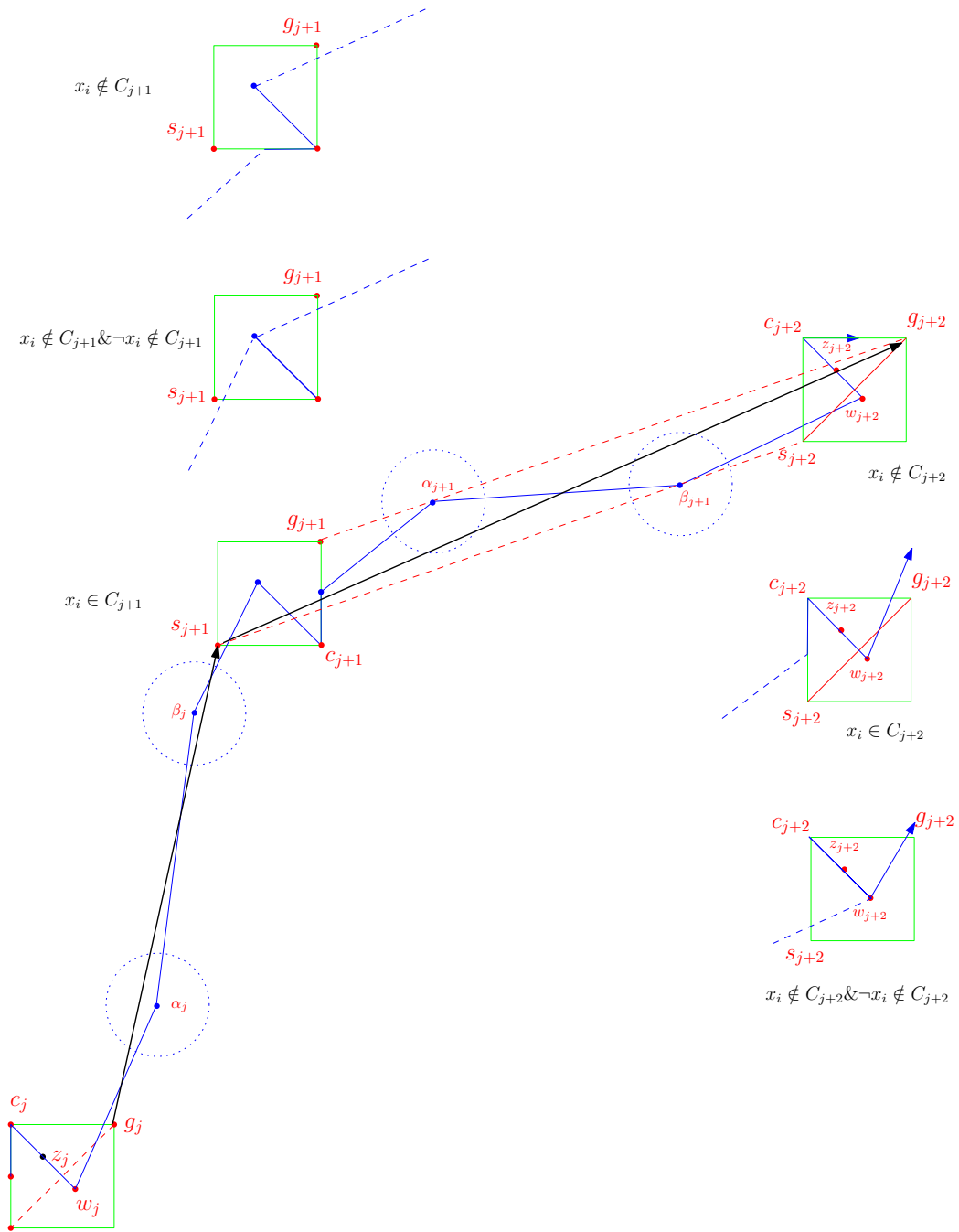


Figure 7.5. Proof of Lemma 42

if $x_i \in C_1$	location of \mathcal{O}_B	location of \mathcal{O}_L
	u h_1 s.t. $\ h_1\mu_1\ \leq \varepsilon$ $h_2 = \overrightarrow{ug_1} \dashv \overline{s_1c_1}$ h_2 $\overline{ug_1} \dashv \overline{c_1w_1}$ $w_1 \perp ug_1$ g_1	u $\mu_1 = (-4, -1)$ $\mu_2 = M(s_1c_1)$ c_1 $\overline{ug_1} \dashv \overline{c_1w_1}$ w_1 $\overline{w_1\alpha_1} \dashv \overline{c_1g_1}$
if $\neg x_i \in C_1$	u h_1 s.t. $\ h_1\mu\ \leq \varepsilon$ $h_2 = \overrightarrow{ug_1} \dashv \overline{s_1c_1}$ $\overline{ug_1} \dashv \overline{c_1w_1}$ g_1	u $\mu_1 = (-4, -1)$ $\mu_2 = \overrightarrow{\mu_1w_1} \dashv \overline{s_1c_1}$ w_1 c_1 $M(c_1g_1)$
if $x_i \notin C_1 \& \neg x_i \notin C_1$	u h_1 s.t. $\ h_1\mu\ \leq \varepsilon$ $h_2 = \overrightarrow{ug_1} \dashv \overline{s_1c_1}$ $\overline{ug_1} \dashv \overline{c_1w_1}$ g_1	u $\mu_1 = (-4, -1)$ $\mu_2 = \overrightarrow{\mu_1w_1} \dashv \overline{s_1c_1}$ w_1 c_1 w_1 $\overline{w_1\alpha_1} \dashv \overline{c_1g_1}$

Table 7.3. Pairwise location of \mathcal{O}_B and \mathcal{O}_L , to prove the base case of induction in Lemma 42

	location of \mathcal{O}_B	location of \mathcal{O}_L
if $x_i \in C_j$	g_j	$\overline{\alpha_{j-1}w_j} \dashv \overline{c_jg_j}$
if $\neg x_i \in C_j$	g_j	$M(\overline{c_jg_j})$
if $x_i \notin C_j \& \neg x_i \notin C_j$	g_j	$\overline{\alpha_{j-1}w_j} \dashv \overline{c_jg_j}$
	h_3 s.t. $\ h_3\alpha_j\ \leq \varepsilon$	α_j
	h_4 s.t. $\ h_4\beta_j\ \leq \varepsilon$	β_j
if $x_i \in C_{j+1}$	s_{j+1} $w_{j+1} \perp \overline{s_{j+1}g_{j+2}}$ z_{j+1} $\overline{g_{j+1}c_{j+1}} \dashv \overline{s_{j+1}g_{j+2}}$	$\overline{\beta_j w_{j+1}} \dashv \overline{c_{j+1}s_{j+1}}$ w_{j+1} z_{j+1} c_{j+1} $M(\overline{c_{j+1}g_{j+1}})$
if $\neg x_i \in C_{j+1}$	s_{j+1} z_{j+1} $\overline{g_{j+1}c_{j+1}} \dashv \overline{s_{j+1}g_{j+2}}$	$M(\overline{s_{j+1}c_{j+1}})$ c_{j+1} w_{j+1} $\overline{g_{j+1}c_{j+1}} \dashv \overline{w_{j+1}\alpha_{j+1}}$
if $x_i \notin C_{j+1} \& \neg x_i \notin C_{j+1}$	s_{j+1} z_{j+1} $\overline{g_{j+1}c_{j+1}} \dashv \overline{s_{j+1}g_{j+2}}$	$\overline{\beta_j w_{j+1}} \dashv \overline{c_{j+1}s_{j+1}}$ w_{j+1} c_{j+1} w_{j+1} $\overline{g_{j+1}c_{j+1}} \dashv \overline{w_{j+1}\alpha_{j+1}}$
	h_5 s.t. $\ h_5\alpha_{j+1}\ \leq \varepsilon$	α_{j+1}
	h_6 s.t. $\ h_6\beta_{j+1}\ \leq \varepsilon$	β_{j+1}
if $x_i \in C_{j+2}$	$\overline{s_{j+2}c_{j+2}} \dashv \overline{s_{j+1}g_{j+2}}$ z_{j+2}	$M(\overline{s_{j+2}c_{j+2}})$ c_{j+2} w_{j+2}
if $\neg x_i \in C_{j+2}$	g_{j+2} $\overline{s_{j+2}c_{j+2}} \dashv \overline{s_{j+1}g_{j+2}}$ z_{j+2}	$\overline{g_{j+2}c_{j+2}} \dashv \overline{w_{j+2}\alpha_{j+2}}$ $\overline{s_{j+2}c_{j+2}} \dashv \overline{\beta_{j+1}w_{j+2}}$ w_{j+2} c_{j+2}
if $x_i \notin C_{j+2} \& \neg x_i \notin C_{j+2}$	g_{j+2} $\overline{s_{j+2}c_{j+2}} \dashv \overline{s_{j+1}g_{j+2}}$ z_{j+2} g_{j+2}	$M(\overline{c_{j+2}g_{j+2}})$ $\overline{s_{j+2}c_{j+2}} \dashv \overline{\beta_{j+1}w_{j+2}}$ w_{j+2} c_{j+2} w_{j+2} $\overline{g_{j+2}c_{j+2}} \dashv \overline{w_{j+2}\alpha_{j+2}}$

Table 7.4. Distance between pair of points is less or equal to one

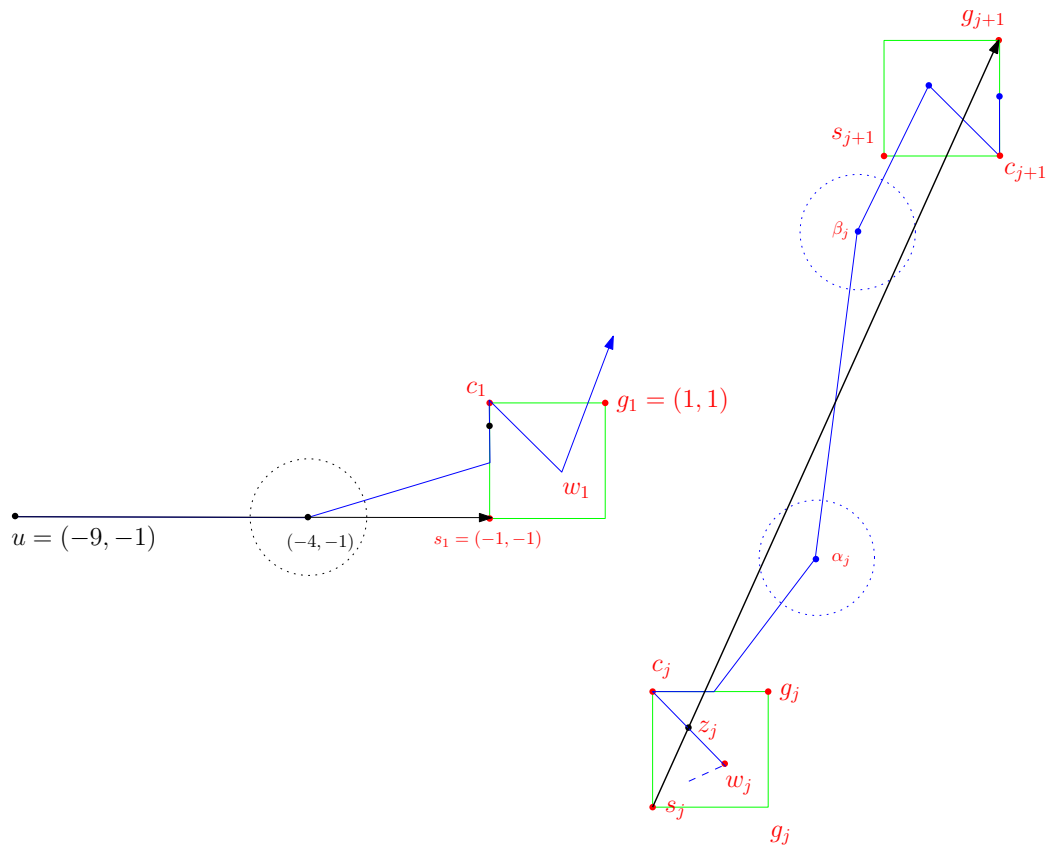


Figure 7.6. Proof of Lemma 43

Algorithm 15 BUILD A FEASIBLE CURVE Q

Input: Truth table of variables x_1, x_2, \dots, x_n in ϕ

```

1:  $Q \leftarrow \emptyset$ 
2:  $Q \leftarrow Q \oplus t$ 
3: for  $i = 1$  to  $n$  do
4:   if  $(x_i = 1)$  then
5:      $\pi \leftarrow \langle ua_1a_2a_3 \dots a_kv \rangle$ 
6:     for all  $C_j$  clauses, if  $x_i \in C_j$  do
7:       let  $\pi_1$  be subcurve of  $\pi$  from  $u$  to  $a_j$ 
8:       let  $\pi_2$  be subcurve of  $\pi$  from  $a_j$  to  $v$ 
9:        $\pi \leftarrow \pi_1 \oplus c_j \oplus \pi_2$ 
10:     $Q \leftarrow Q \oplus \pi$ 
11:   else
12:      $\pi \leftarrow \langle ub_1b_2b_3 \dots b_kv \rangle$ 
13:     for all  $C_j$  clauses, if  $\neg x_i \in C_j$  do
14:       let  $\pi_1$  be subcurve of  $\pi$  from  $u$  to  $b_j$ 
15:       let  $\pi_2$  be subcurve of  $\pi$  from  $b_j$  to  $v$ 
16:        $\pi \leftarrow \pi_1 \oplus c_j \oplus \pi_2$ 
17:      $Q \leftarrow Q \oplus \pi$ 
18:    $Q \leftarrow Q \oplus t$ 
19:  $Q \leftarrow Q \oplus \langle ua_1a_2a_3 \dots a_kv \rangle$ 
20:  $Q \leftarrow Q \oplus t$ 
21:  $Q \leftarrow Q \oplus \langle ub_1b_2b_3 \dots b_kv \rangle$ 
22:  $Q \leftarrow Q \oplus t$ 
23: return  $Q$ 

```

Bibliography

- [1] P. Accisano and A. Üngör. Hardness results on curve/point set matching with Fréchet distance. *CoRR*, abs/1211.2030, 2012.
- [2] P. K. Agarwal, R. B. Avraham, H. Kaplan, and M. Sharir. Computing the discrete Fréchet distance in subquadratic time. In *Proceedings of the 24th Annual ACM-SIAM Symposium on Discrete Algorithms*, SODA '13, pages 156–168. SIAM, 2013.
- [3] P. K. Agarwal, S. Har-Peled, N. H. Mustafa, and Y. Wang. Near-linear time approximation algorithms for curve simplification in two and three dimensions. *Algorithmica*, 42(3-4):203–219, 2005.
- [4] H. Alt. Communicated during the Ph.D. thesis defence of Kaveh Shahbaz, 8th of May 2013, Carleton University.
- [5] H. Alt. The computational geometry of comparing shapes. In *Efficient Algorithms*, volume 5760 of *Lecture Notes Comput. Sci.*, pages 235–248. Springer, 2009.
- [6] H. Alt and M. Buchin. Can we compute the similarity between surfaces? *Discrete Comput. Geom.*, 43(1):78–99, 2010.
- [7] H. Alt, A. Efrat, G. Rote, and C. Wenk. Matching planar maps. *J. Algorithms*, 49(2):262–283, 2003.
- [8] H. Alt and M. Godau. Computing the Fréchet distance between two polygonal curves. *Int. J. Comput. Geometry Appl.*, 5:75–91, 1995.
- [9] H. Alt, C. Knauer, and C. Wenk. Matching polygonal curves with respect to the Fréchet distance. In *Proc. 18th Sympos. Theoret. Aspects Comput. Sci.*, volume 2010 of *Lecture Notes Comput. Sci.*, pages 63–74. Springer, 2001.
- [10] H. Alt, C. Knauer, and C. Wenk. Comparison of distance measures for planar curves. *Algorithmica*, 38(1):45–58, 2003.
- [11] E. M. Arkin, L. P. Chew, D. P. Huttenlocher, K. Kedem, and J. S. B. Mitchell. An efficiently computable metric for comparing polygonal shapes. *IEEE Trans. Pattern Anal. Mach. Intell.*, 13(3):209–216, 1991.
- [12] B. Aronov, S. Har-Peled, C. Knauer, Y. Wang, and C. Wenk. Fréchet distance for curves, revisited. In *Proc. 14th Annu. European Sympos. Algorithms*, volume 4168 of *Lecture Notes Comput. Sci.*, pages 52–63. Springer, 2006.

- [13] S. Bereg. An approximate morphing between polylines. *Int. J. Comput. Geometry Appl.*, 15(2):193–208, 2005.
- [14] S. Brakatsoulas, D. Pfoser, R. Salas, and C. Wenk. On map-matching vehicle tracking data. In *Proceedings of the 31st international conference on Very large data bases, VLDB '05*, pages 853–864. VLDB Endowment, 2005.
- [15] K. Buchin, M. Buchin, and J. Gudmundsson. Constrained free space diagrams: a tool for trajectory analysis. *International Journal of Geographical Information Science*, 24(7):1101–1125, 2010.
- [16] K. Buchin, M. Buchin, C. Knauer, G. Rote, and C. Wenk. How difficult is it to walk the dog. In *Proc. 23rd European Workshop on Computational Geometry*, pages 170–173, 2007.
- [17] K. Buchin, M. Buchin, W. Meulemans, and W. Mulzer. Four Soviets walk the dog - with an application to Alt’s conjecture. *CoRR*, abs/1209.4403, 2012.
- [18] K. Buchin, M. Buchin, W. Meulemans, and B. Speckmann. Locally correct Fréchet matchings. In *Proc. 20th Annu. European Sympos. Algorithms*, volume 7501 of *Lecture Notes Comput. Sci.*, pages 229–240, 2012.
- [19] K. Buchin, M. Buchin, M. J. van Kreveld, M. Löffler, R. I. Silveira, C. Wenk, and L. Wiratma. Median trajectories. *Algorithmica*, pages 595–614, 2013.
- [20] K. Buchin, M. Buchin, and Y. Wang. Exact algorithms for partial curve matching via the Fréchet distance. In *Proceedings of the 20th Annual ACM-SIAM Symposium on Discrete Algorithms*, pages 645–654, 2009.
- [21] K. Buchin, M. Buchin, and C. Wenk. Computing the Fréchet distance between simple polygons. *Comput. Geom. Theory Appl.*, 41(1-2):2–20, 2008.
- [22] J.-L. D. Carufel, A. Gheibi, A. Maheshwari, J.-R. Sack, and C. Scheffer. Similarity of polygonal curves in the presence of outliers. *CoRR*, abs/1212.1617, 2012.
- [23] E. W. Chambers, É. C. de Verdière, J. Erickson, S. Lazard, F. Lazarus, and S. Thite. Homotopic Fréchet distance between curves or, walking your dog in the woods in polynomial time. *Comput. Geom. Theory Appl.*, 43(3):295–311, 2010.
- [24] D. Chen, A. Driemel, L. J. Guibas, A. Nguyen, and C. Wenk. Approximate map matching with respect to the Fréchet distance. In *ALLENEX*, pages 75–83, 2011.

- [25] D. Chen, L. J. Guibas, Q. Huang, and J. Sun. A faster algorithm for matching planar maps under the weak Fréchet distance. http://www.geomtop.org/paper_ppt/matchingpm.pdf, 2009.
- [26] Y. K. Cheung and O. Daescu. Fréchet distance problems in weighted regions. *Discrete Math., Alg. and Appl.*, 2(2):161–180, 2010.
- [27] R. Cole. Slowing down sorting networks to obtain faster sorting algorithms. *J. ACM*, 34(1):200–208, 1987.
- [28] A. F. Cook and C. Wenk. Geodesic Fréchet distance inside a simple polygon. *ACM Trans. Algorithms*, 7(1):9, 2010.
- [29] A. F. Cook, Iv and C. Wenk. Shortest path problems on a polyhedral surface. In *Proc. 11th Workshop Algorithms Data Struct.*, volume 5664 of *Lecture Notes Comput. Sci.*, pages 156–167. Springer, 2009.
- [30] M. De Berg and A. F. Cook, Iv. Go with the flow: The direction-based Fréchet distance of polygonal curves. In *Proc. 18th Internat. ICST Conf. Theory on Theory and Practice of Algorithms in (Comput.) Systems*, volume 6595 of *Lecture Notes Comput. Sci.* Springer, 2011.
- [31] A. Driemel and S. Har-Peled. Jaywalking your dog: computing the Fréchet distance with shortcuts. In *Proceedings of the 23rd Annual ACM-SIAM Symposium on Discrete Algorithms*, SODA '12, pages 318–337. SIAM, 2012.
- [32] A. Driemel, S. Har-Peled, and C. Wenk. Approximating the Fréchet distance for realistic curves in near linear time. *Discrete Comput. Geom.*, 48(1):94–127, 2012.
- [33] A. Dumitrescu and G. Rote. On the Fréchet distance of a set of curves. In *CCCG*, pages 162–165, 2004.
- [34] A. Efrat, Q. Fan, and S. Venkatasubramanian. Curve matching, time warping, and light fields: New algorithms for computing similarity between curves. *J. Math. Imaging Vis.*, 27:203–216, April 2007.
- [35] A. Efrat, L. J. Guibas, S. Har-Peled, J. S. B. Mitchell, and T. M. Murali. New similarity measures between polylines with applications to morphing and polygon sweeping. *Discrete Comput. Geom.*, 28(4):535–569, 2002.
- [36] T. Eiter and H. Mannila. Computing discrete Fréchet distance. Technical Report CD-TR 94/64, Laboratory for Expert Systems, TU Vienna, Austria, 1994.

- [37] M. Fréchet. Sur quelques points du calcul fonctionnel. In *Rendiconti del Circolo Mathematico di Palermo*, pages 1–74, 1906.
- [38] A. Gajentaan and M. H. Overmars. On a class of $O(n^2)$ problems in computational geometry. *Comput. Geom. Theory Appl.*, 45(4):140–152, 2012.
- [39] L. J. Guibas and J. Hershberger. Optimal shortest path queries in a simple polygon. *J. Comput. Syst. Sci.*, 39(2):126–152, 1989.
- [40] M. Hagedoorn. *Pattern Matching Using Similarity Measures*. PhD thesis, Utrecht University, 2000.
- [41] S. Har-Peled and B. Raichel. The Fréchet distance revisited and extended. In *Proceedings of the 27th annual ACM symposium on Computational geometry*, SoCG '11, pages 448–457. ACM, 2011.
- [42] J. Hershberger. A new data structure for shortest path queries in a simple polygon. *Inform. Process. Lett.*, 38(5):231–235, 1991.
- [43] M. Jiang, Y. Xu, and B. Zhu. Protein structure-structure alignment with discrete Fréchet distance. *J. Bioinform. Comput. Biol.*, 6(1):51–64, 2008.
- [44] M.-S. Kim, S.-W. Kim, and M. Shin. Optimization of subsequence matching under time warping in time-series databases. In *Proceedings of the 2005 ACM symposium on Applied computing*, SAC '05, pages 581–586. ACM, 2005.
- [45] S. Kwong, Q. He, K.-F. Man, C. W. Chau, and K.-S. Tang. Parallel genetic-based hybrid pattern matching algorithm for isolated word recognition. *IJPRAI*, 12(4):573–594, 1998.
- [46] A. Maheshwari, J.-R. Sack, and K. Shahbaz. Computing Fréchet distance with speed limits. In *CCCG*, pages 107–110, 2009.
- [47] A. Maheshwari, J.-R. Sack, K. Shahbaz, and H. Zarrabi-Zadeh. Speed-constrained geodesic Fréchet distance inside a simple polygon. In *CCCG*, pages 179–182, 2010.
- [48] A. Maheshwari, J.-R. Sack, K. Shahbaz, and H. Zarrabi-Zadeh. Fréchet distance with speed limits. *Comput. Geom. Theory Appl.*, 44(2):110–120, 2011.
- [49] A. Maheshwari, J.-R. Sack, K. Shahbaz, and H. Zarrabi-Zadeh. Improved algorithms for partial curve matching. In *Proc. 19th Annu. European Sympos. Algorithms*, volume 6942 of *Lecture Notes Comput. Sci.*, pages 518–529, 2011.

- [50] A. Maheshwari, J.-R. Sack, K. Shahbaz, and H. Zarrabi-Zadeh. Staying close to a curve. In *CCCG*, 2011.
- [51] A. Maheshwari, J.-R. Sack, K. Shahbaz, and H. Zarrabi-Zadeh. Improved algorithms for partial curve matching. *Algorithmica*, pages 1–17, 2013.
- [52] A. Maheshwari and J. Yi. On computing Fréchet distance of two paths on a convex polyhedron. In *Proc. 21st European Workshop Comput. Geom.*, pages 41–44, 2005.
- [53] N. Megiddo. Applying parallel computation algorithms in the design of serial algorithms. *J. ACM*, 30(4):852–865, 1983.
- [54] A. Mosig and M. Clausen. Approximately matching polygonal curves with respect to the Fréchet distance. *Comput. Geom. Theory Appl.*, 30(2):113–127, 2005.
- [55] S. Pelletier. Computing the Fréchet distance between two polygonal curves, URL: <http://www.cim.mcgill.ca/~stephane/cs507/Project.html>.
- [56] G. Rote. Computing the Fréchet distance between piecewise smooth curves. *Comput. Geom. Theory Appl.*, 37(3):162–174, 2007.
- [57] E. Sriraghavendra, K. Karthik, and C. Bhattacharyya. Fréchet distance based approach for searching online handwritten documents. In *ICDAR*, pages 461–465, 2007.
- [58] E. Sriraghavendra, K. Karthik, and C. Bhattacharyya. Fréchet distance based approach for searching online handwritten documents. In *Proc. 9th Internat. Conf. Document Anal. Recognition*, pages 461–465, 2007.
- [59] R. E. Tarjan. *Data structures and network algorithms*. Society for Industrial and Applied Mathematics, Philadelphia, PA, 1983.
- [60] T. Wylie and B. Zhu. Discretely following a curve (short abstract). In *Computational Geometry: Young Researchers Forum (CG:YRF)*, 2012.